

**Simulation of the Numerical Behavior of Stone and
Geosynthetic Encapsulated Sand Columns in
Tuzla Area**

Sajjad Mirsalehi

Submitted to the
Institute of Graduate Studies and Research
in partial fulfillment of the requirements for the Degree of

Master of Science
in
Civil Engineering

Eastern Mediterranean University
January 2013
Gazimağusa, North Cyprus

Approval of the Institute of Graduate Studies and Research

Prof. Dr. Elvan Yılmaz
Director

I certify that this thesis satisfies the requirements as a thesis for the degree of Master of Science in Civil Engineering.

Assist. Prof. Dr. Mürüde Çelikağ
Chair, Department of Civil Engineering

We certify that we have read this thesis and that in our opinion it is fully adequate in scope and quality as a thesis for the degree of Master of Science in Civil Engineering.

Asst. Prof. Dr. Huriye Bilsel
Supervisor

Examining Committee

1. Assoc. Prof. Dr. Zalihe Sezai

2. Asst. Prof. Dr. Huriye Bilsel

3. Asst. Prof. Dr. Mehmet Metin Kunt

ABSTRACT

One of the major challenges among engineers is to construct various types of structures over weak soils. Among various technologies implemented by engineers, stone or sand columns are the most beneficial methods for modification of weak soils, such as alluvial soils. These methods mitigate poor deposits, modifying their properties by the use of materials such as stone or sand. The target of present study was to determine the influence of stone or sand columns in alluvial deposits of Tuzla. For this purpose, numerical simulation was carried out to model the behavior of settlement, excess pore water pressures, stresses around columns, bulging, hoop tension force and consolidation time. The Plaxis finite element software was used to evaluate the effect of columns in undrained condition. Mohr-Coulomb model was selected for all materials. In Plaxis the axisymmetric analysis for unit cell and plain strain analysis for full-scale analysis were used. In this thesis the settlement, excess pore water pressures, stress, and consolidation time were analyzed to determine the behavior of stone column under an embankment construction in unit cell and full-scale conditions. In addition, the bulging and hoop tension force around encapsulated sand column with geotextile was analyzed. The results of this study indicate that, stone column has a remarkable influence on decreasing settlements and accelerate the consolidation time. Larger the column diameter, higher is the bearing capacity and lower is the settlement. The maximum settlement occurs at ground level and reduces by increasing depth and increasing column diameter. By using stone column due to larger stress confining around stone column, the amount of vertical settlements increased in stone column and rapidly decreased by increasing distance from column, and afterwards remained constant. The maximum bulging occurred at

1.06D of sand columns. By increasing, the diameter of columns bulging increased. Using geotextile with higher stiffness, amount of bulging reduced, also value of the hoop tension force increased. Therefore, higher stiffness has lower settlement compared to conventional sand column. Lateral settlements increased initially and then reduced with increasing depth, and distance from the embankment.

Keywords: Alluvial soil, embankment fill, Plaxis, stone column, encapsulated sand column, hoop tension.

ÖZ

İnşaat Mühendisliği'nde karşılaşılan zorluklardan biri zayıf zeminler üzerinde bina inşa etmektir. Allüvyon gibi zayıf zeminlerin özelliklerini değiştirerek güçlendiren teknikler arasında en uygun olan taş veya kum kolon kullanımınıdır. Bu çalışmanın amacı taş ve kum kolon kullanımının Tuzla bölgesindeki allüvyonlar üzerindeki etkisini belirlemektir. Bu amaçla nümerik simülasyon yöntemi ile oturma, aşırı boşluk suyu basıncı, kolon çevresindeki stresler, kolon duvarında kabarma, çevre gerilme kuvveti ve konsolidasyon zamanı modellenmiştir. Plaxis sonlu elemanlar yazılımı kullanılarak kolonların drenajsız koşulda etkileri çalışılmıştır. Tüm malzemeler için Mohr-Coulomb modeli seçilmiştir. Birim hücre modeli için axisimetrik analiz yöntemi seçilirken, düz gerilme modeli de tam ölçek analiz için kullanılmıştır. Bu tez çalışmasında oturmalar, aşırı boşluk suyu basıncı, ve stresler analiz edilerek, toprak dolgu altında taş kolonların birim hücre ve tam ölçekli koşulda davranışı çalışılmıştır. Bunun yanında kabarmalar, dairesel gerilim ve geotekstille desteklenmiş kolonların davranışları da irdelenmiştir. Sonuç olarak, taş kolonların oturmaları azaltmada ve konsolidasyon hızını artırmada çok etkili olduğu gözlemlenmiştir. Kolon çapları arttıkça taşıma gücü artıyor ve oturmalar azalıyor. Maksimum oturma yer yüzeyinde olup derinlik ve çap arttıkça azalıyor. Taş kolonun etrafında oluşan stresler taş kolon içerisindeki düşey oturmaları artırıyor, ve süratle dışa doğru azalarak sabitleniyor. Maksimum kabarma ise 1.06 D kum kolon derinliğinde oluşuyor. Kolon çapı arttıkça kabarma da artıyor. Geotekstille desteklenen kolonlarda ise geotekstilin dayanımı arttıkça, kabarma azalıyor, çevre gerilme dayanımı ise artıyor. Dolayısıyla yüksek dayanımlı geotekstille desteklenen

kolonlarda oturmalar da azalıyor. Yanal oturmalar da önce artmış, derinlik ve yanal mesafe arttıkça ise azalmıştır.

Anahtar Kelimeler: Alüvyon topraklar, toprak dolgu, Plaxis, taş kolon, sarmalanmış kum kolon, dairesel gerilme.

ACKNOWLEDGEMENTS

Foremost, I would like to convey my heartfelt gratitude to my advisor, Asst. Prof. Dr. Huriye Bilsel for the patient guidance, advice, and encouragement throughout this work. Her valuable effort and time dedicated to this research are deeply appreciated.

Besides my advisor, I would like to thank the rest of my thesis committee: Assoc. Prof. Dr. Zalihe Sezai and Asst. Prof. Dr. Mehmet Metin Kunt for taking time to review my thesis.

I would like to thank my parents and my brother and sister for their never-ending love, support and sacrifice in encouraging me to complete this research.

Finally, I would also like to thank all the members of staff at Civil Engineering institute who helped me a lot.

TABLE OF CONTENTS

ABSTRACT	iii
ÖZ	v
ACKNOWLEDGEMENTS	vii
LIST OF TABLES	xiii
LIST OF FIGURES	xiv
LIST OF SYMBOLS	xix
1 INTRODUCTION	1
1.1 Background and Problem Statement.....	1
1.2 Scope and Study Objective	2
1.3 Thesis Outline	2
2 LITERATURE REVIEW.....	4
2.1 General.....	4
2.2 Methods for Enhancement of Soft Soil.....	4
2.3 Different Systems for Columns Installation.....	5
2.3.1 Vibro-compaction	5
2.3.1.1 Vibro-Replacement Procedure or Wet Method.....	5
2.3.1.2 Vibro-displacement Procedure or Dry Method.....	6
2.3.2 Ramming Technique	7
2.4 Effect of column installation.....	8
2.5 Stress Distribution on Soil and Columns	8
2.6 Group Stone Columns	10
2.7 Mechanism of Bulging in Single and Group Columns	11
2.7.1 Single Column.....	11

2.7.2 Group Columns	13
2.8 Ultimate Bearing Capacity of Columns	14
2.8.1 Single Column.....	14
2.8.1.1 Pressure Meter Theory	15
2.8.1.2 Passive Theory	15
2.8.1.3 Vesic Theory	16
2.9 Settlement Prediction	17
2.9.1 Equilibrium Theory for Prediction Settlement.....	18
2.9.1.1 Barkslade Theory	18
2.9.1.2 Abhoshi Theory.....	20
2.9.2 Analytical Theory for Prediction Settlement	21
2.9.2.1 Priebe Theory	21
2.9.2.2 Van Impe and De Beer Theory	22
2.9.3 Empirical Method.....	24
2.9.4 Numerical Prediction	24
2.10 Previous Investigated on Columns.....	25
2.10.1 Numerical Study.....	25
2.10.2 Experimental Study	30
2.11 Geosynthetic:	34
2.11.1 Different Types and Applying Areas	34
2.11.2 Geotextile	35
2.11.3 Geogrid.....	35
3 ANALYSIS OF SOIL PARAMETERS BY NOVOSPT FOR SOILS OF TUZLA	37
3.1 Tuzla Area.....	37
3.2 NovoSPT Software	38

3.2.1 Introduction	38
3.2.2 Procedure of Software	38
3.3 Material Preparation for Finite Element Simulation Using Plaxis Software ...	39
3.3.1 Introduction	39
3.3.3 Mohr- Coulomb Model Parameters	40
3.3.3.1 Young`s modulus (E)	41
3.3.3.2 Friction Angle (Φ)	42
3.3.3.3 Undrained Shear Strength (S_u)	43
3.3.3.4 Basic Parameters for Simulating in Plaxis	44
4 STONE COLUMN BENEATH AN EMBANKMENT COSTRUCTION IN UNIT CELL IDEALIZATION.....	45
4.1 Unit Cell Conception	45
4.1.1 Area Replacement Ratio	45
4.2 Materials and Parameters for Numerical Analyses.....	47
4.3 Numerical Procedure.....	49
4.4 Analysis of Single Column as a Unit Cell	51
4.5 Analysis and Results	53
4.5.1 Group A: Different Column Materials.....	53
4.5.2 Group B: Different Column Diameters.....	55
4.5.2.1 Consolidation End Times Analysis with Respect to Time.....	55
4.5.2.2 Settlement Analysis with Respect to Time	56
4.5.2.3 Settlement Analysis versus Depth.....	57
4.5.2.4 Settlement versus Time	59
4.5.2.5 Maximum Vertical Settlement at a Distance from Column Centerline	62
4.5.2.6 Study of Settlement by Area Ratio and Improvement Factor	63

4.5.2.7 Excess Pore Water Pressure with respect to Time	64
4.5.2.8 Stress Analysis	67
4.5.3 Group C: Different Column Spacing	69
4.5.3.1 Consolidation End Time Analysis with Respect to Time	69
4.5.3.2 Settlement Analysis versus Time	70
4.5.3.3 Excess Pore Water Pressure Analysis versus Time	71
5 BULGING AND HOOP TENSION ANALYSES IN UNIT CELL IDEALIZATION.....	73
5.1 Introduction.....	73
5.2 Column Bulging.....	73
5.3 Hoop Tension Force.....	75
5.4 Unit Cell Idealization of Sand Column in Different Models.....	77
5.5 In-situ Soil Parameters	78
5.6 Mesh Analyses	80
5.7 Results of Finite Element Analyses	81
5.7.1 Group A: Effect of Different Load Size on Bulging.....	81
5.7.2 Group B: Effect of Different Diameters of Sand Column on Bulging and Vertical Displacement.....	82
5.7.4 Group D: Effect of Different Areas of Load on Bulging	85
5.7.5 Group E: Effect of Different Stiffnesses of Geosynthetic Material	86
5.7.5.1 Influence of Stiffness on Bulging	86
5.7.5.2 Effect of Stiffness on Hoop Tension.....	87
5.7.5.3 Influence of Stiffness on Vertical Displacement	88
5.7.5.4 Influence of Stiffness on Maximum Bulging.....	89
5.7.6 Group F: Effect of Diameter on Hoop Tension Force	90

6 Full-SCALE ANALYSIS OF STONE COLUMNBENEATH AN EMBANKMENT STRUCTURE.....	92
6.1 Introduction.....	92
6.2 Study Area.....	92
6.3 Materials and Parameters	92
6.4 Numerical Procedure.....	93
6.5 Results of Analyses	96
6.5.2 Settlement versus Depth.....	98
6.5.3 Lateral Settlement versus Depth	100
6.5.5 Consolidation End Time Analyses	104
7 CONCLUSIONS.....	109
REFERENCES.....	112

LIST OF TABLES

Table 1: Different types of geosynthetic and application areas	35
Table 2: Three kinds of geotextile and geogrid material and application area	36
Table 3: Correction factors for standard penetration test.....	38
Table 4: Estimation of undrained shear strength by N value.....	41
Table 5: Classification of soils based on stiffness versus SPT N value.....	41
Table 6: Fill and stone column materials	48
Table 7: Gravel and sand materials	48
Table 8: Properties of clay bed (Borehole 36)	49
Table 9: Various model analysis	52
Table 10: Various models of analysis	77
Table 11: Properties of Sand and clay bed.....	79
Table 12: Material properties of geotextile.....	79
Table 13: Properties of soil strata beneath the embankment.....	93
Table 14: Material properties of stone and embankment fill.	93

LIST OF FIGURES

Figure 1: Procedure of vibro-replacement	6
Figure 2: Procedure of vibro-displacement.....	7
Figure 3: Stress distribution on column and soil.....	9
Figure 4: Stress distribution on column and soil.....	9
Figure 5: Relationship between stress ratio and distance from column.....	10
Figure 6: Relationships between bearing capacity and number of column	11
Figure 7: Bulging occurs in single column in homogeneous layer a) bulging failure, b) shear failure, c) punching failure	12
Figure 8: Types of bulging occurs in single column in heterogeneous layer.....	13
Figure 9: Types of failures in-group columns.....	13
Figure 10: Factors for cavity theory.....	17
Figure 11: Measured settlement versus estimated settlement	20
Figure 12: Relationships between area ratio and improvement factor to determine settlement	21
Figure 13: Procedure of stone walls replaced by stone column.....	22
Figure 14: Relationships of settlement repletion coefficient (B) against area ratio (as)	23
Figure 15: Empirical theory of.....	24
Figure 16: Lateral bulging reduced due to geogrid stiffness.....	25
Figure 17: Lateral bulging versus depth	27
Figure 18: Settlement versus pressure affected by geosynthetic	28
Figure 19: Hoop tension force versus depth	29

Figure 20: Different analyses of stone columns on a) settlement, b) hoop tension, c) bulging failure	32
Figure 21: Experimental set up of stone column	34
Figure 22: Woven and nonwoven type of geotextile	35
Figure 23: Location of island of Cyprus in the Mediterranean Sea	37
Figure 24: Location of Tuzla on the map of Cyprus	38
Figure 25: Input parameters page of NovoSPT software.....	39
Figure 26: Bore hole locations in Tuzla area	40
Figure 27: Estimation of Young's modulus according to plasticity index and SPT N value	41
Figure 28: Estimation of Young's Modulus according to SPT blow count and Poisson's ratio.....	42
Figure 29: Various patterns of unit cell: (a) Triangular, (b) Square, and (c) Hexagonal	47
Figure 30: Axisymmetric model for single stone column in both reinforced and unreinforced conditions.....	49
Figure 31: Calculation steps of embankment construction	50
Figure 32: Mesh analyses for different steps of embankment construction	51
Figure 33: Influence of different materials of column on the settlement versus time	54
Figure 34: Influence of different materials of column on the settlement versus depth	54
Figure 35: Influence of different materials of column on the consolidation end times	55
Figure 36: Effect of various diameters of column on the consolidation end times....	56
Figure 37: Effect of various diameters of column on settlement versus time.....	57

Figure 38: Effect of various diameters of column on settlement versus depth.....	58
Figure 39: Analysis of settlement with respect to time after the first construction stage.....	60
Figure 40: Analysis of settlement with respect to time after the second construction stage.....	60
Figure 41: Analysis of settlement with respect to time after 2 years	61
Figure 42: Analysis of settlement with respect to time after the consolidation end time.....	61
Figure 43: Effect of various diameters of column on vertical settlements from column centerline	62
Figure 44: Maximum settlement versus area ratio	63
Figure 45: Improvement factor versus area ratio	63
Figure 46: Dissipation of excess pore water pressure of (a) unreinforced and (b) reinforced unit cell	64
Figure 47: Effect of various diameters of column on Excess pore water pressure versus time for $D=0.5$, $D=0.85$, $D=1$	65
Figure 48: Effect of various diameters of column on Excess pore water pressure versus time for $D=1.2$, $D=1.5$	65
Figure 49: Effect of various diameters of column on Excess pore water pressure versus time	66
Figure 50: Effect of various diameters of column on excess pore water pressure versus time for first and second stages of construction.....	66
Figure 51: Effective vertical stress versus time at point D and E in reinforced compare to unreinforced	68
Figure 52: Stress versus distance from column centerline line.....	68

Figure 53: Effect of column spacing on the consolidation end times	70
Figure 54: Effect of column spacing on settlement versus time	71
Figure 55: Effect of column spacing on excess pore water pressure versus time.....	72
Figure 56: Bulging failure in sand columns in different steps of loading	74
Figure 57: Bulging under various types of loading	75
Figure 58: Hoop tension force around column	76
Figure 59: Fine mesh analysis.....	80
Figure 60: Bulging versus depth under different loads	81
Figure 61: Bulging versus depth in for different diameters of sand column	83
Figure 62: Vertical settlement versus depth in soil for different column diameters..	83
Figure 63: Bulging versus depth under different areas of rigid footing.....	84
Figure 64: Distance from column centerline versus stress under different areas of rigid footing.....	85
Figure 65: Bulging versus depth under of different areas of load.....	86
Figure 66: Bulging versus depth for different stiffnesses of geotextile	87
Figure 67: Hoop tension versus depth for different stiffnesses of geotextile	88
Figure 68: Effect of various stiffnesses of geotextile on vertical settlements at varying distances from the centerline	89
Figure 69: Maximum bulging versus geotextile stiffness under different magnitudes of load.....	90
Figure 70: Hoop tension versus depth for different diameters of column	91
Figure 71: Point location in FEM analyses	95
Figure 72: Mesh analyses of full-scale model.....	95
Figure 73: Settlement versus time at point A for different columns heights	97
Figure 74: Settlement versus time at point B for different columns heights	97

Figure 75: Settlement versus time at point D for different columns heights	98
Figure 76: Settlement versus depth for different height of columns at point E	99
Figure 77: Settlement versus depth for different height of columns at point C.....	99
Figure 78: Settlement versus depth for different height of columns at point D.....	100
Figure 79: Lateral Settlement versus depth for different height of columns at point C	101
Figure 80: Lateral Settlement versus depth for different height of columns at point D	101
Figure 81: Settlements from embankment centerline	102
Figure 82: Settlements from embankment centerline	103
Figure 83: Settlements from embankment centerline	103
Figure 84: Consolidation end time	104
Figure 85: Excess pore water pressure versus time for different height of columns at point E.....	106
Figure 86: Excess pore water pressure versus time for different height of columns at point F	106
Figure 87: Excess pore water pressure versus time for different height of columns at point G.....	107
Figure 88: Excess pore water pressure versus time for of different height of columns at point H.....	107
Figure 89: Excess pore water pressure versus time for of different height of columns at point I	108

LIST OF SYMBOLS

Symbol	Meaning
A	Total area of unit cell
a_s	Area ratio
A_s	Total area of column
C	Cohesion
C_u	Undrained shear strength
C_c	Compression index
C_e	Energy level correction
C_n	Overburden factor
C_b	Borehole diameter
C_r	Rod length
D	Diameter of column
E	Young's modulus
E_c	Modular elasticity of clay
e_0	Initial void ratio
e	Void ratio
F'_c, F'_q	Factors for cavity theory
G_s	Specific gravity
K_p	The coefficient of passive earth pressure

Symbol	Meaning
K_h	Horizontal Permeability
K_v	Vertical Permeability
m_v	Volume coefficient of compressibility
N	Concentration factor of stress
PI	Plasticity index
q_{ult}	Carrying capacity of column
Q	Total stress equivalent to failure depth
W	Water content
Z	Footing depth from ground add depth of column bulge
σ_3	Ultimate lateral resistance
σ_0	Original effective stress
σ_c	Stress over column
σ_s	Stress over soil
σ_{rl}	The ultimate horizontal pressure
σ_{r0}	The entire preliminary horizontal stress
σ	Average stress
μ_c	Stress ratio
γ_w	Wet unit weight
γ_{dry}	Dry unit weight
Γ	The bulk density of soft soil
Y	Poisson's ratio
Φ	Friction angle
Ψ	Dilatancy angle

Chapter 1

INTRODUCTION

1.1 Background and Problem Statement

The past decade has seen the quick development of many structures, which are near the sea or river. However, the major problem with these rapid alterations is lack of the appropriate soil in these regions due to poor shear strength and greater compressibility of the soil. Therefore, the methods for resolving of these problems were revealed. Various methods have been determined to modification of soil that consists of saturated clay or alluvial deposit, such as geosynthetic reinforcement, mini piles, lime columns, stone and sand columns, dynamic compaction, and others. Among the competitive processes of improvement technology, the stone or sand columns, due to easier installation, are beneficial. This method is set up in replacement method, displacement method, and ramming. In addition, in all of methods the columns can be installed as conventional columns or as geosynthetic stone or sand columns (GSC).

The strategy of these columns is to reduce the amount of settlement and increment of bearing capacity. Stone or sand columns also speed up the consolidation time and dissipate the excess pore water pressures.

In the last sixty years, there has been an increasing interest in using stone columns in different countries. Recently the New Airbus in Germany utilized 60000 encased sand columns by various kinds of geosynthetic materials.

This research has intended to assess the performance of stone and sand columns on Tuzla region, in Northern Cyprus situated in the delta of Pedios River, comprised of weak soil deposits. Numerical analyses either in axisymmetric or plain strain model have been selected to represent the behavior of columns in different areas of Tuzla.

1.2 Scope and Study Objective

Based on numerical simulation by Plaxis version 8.6 the essential features of stone and sand columns in three-bore holes of Tuzla area was evaluated in undrain position. The Mohr-Coulomb model was adopted for both of plain strain and axisymmetric model. In addition, the requirement parameters were extracted from Novo SPT Software.

This paper attempts to address the following parameters:

1. Different space and column diameters,
2. Different geosynthetic material stiffnesses,
3. Different types of load on column and different rigid plate areas,
4. Unit cell and full-scale analyses.

1.3 Thesis Outline

This investigation provides the following chapter:

Chapter 1 includes general description of thesis and dissertation objectives and scopes.

Chapter 2 provides the literature review. It involves the experimental and numerical simulation of columns in unit cell and plain strain analysis on weak soil deposits.

Chapter 3 includes the study area of Tuzla region and provides required parameters by Novo SPT software.

Chapter 4, the unit cell conceptions of columns beneath an embankment construction in various models were evaluated by FEM analysis using Plaxis version 8.6.0 software.

Chapter 5 assesses the hoop tension and bulging of ordinary and geotextile encapsulated sand column in unit cell using axisymmetric analysis.

Chapter 6 includes the design of the full-scale simulation of embankment over sand columns in Tuzla.

Chapter 7 represents the numerical conclusions of this thesis.

Chapter 2

LITERATURE REVIEW

2.1 General

One of the most significant issues in ground development is the modification of foundation structure under particular loading condition. Soft soils because of excessive settlements and low shear strength need further improvement. The use of encased stone and sand columns can be effective as a new methodology for improving clay or silt foundation under different structures such as buildings, road embankments, dike structures, and others.

2.2 Methods for Enhancement of Soft Soil

Because of construction industry developing in soft soil areas next to sea, river, and harbor, different approaches have been applied to modificate the weak structures of soft soil as follows:

1. Fiber reinforced,
2. Dynamic compaction,
3. Lime columns,
4. Geosynthetic reinforcement,
5. Stone and sand columns,
6. Vacuum preloading process,
7. Mini piles,
8. Preloing by vertical drain.

Some of the advantages of using stone or sand columns are as follows:

1. Due to easier installation of stone and sand columns, modification of soft soils by this method can be economical,
2. Stone column increase bearing capacity because of high permeability of the material, which is used in column,
3. The material of the column act likes the drain hole and causes to decrease the consolidation time.

2.3 Different Systems for Columns Installation

There are two schemes for installation of columns in different soils, which are vibro-compaction and ramming method.

2.3.1 Vibro-compaction

The vibratory compaction technique do not accepted in soils with considerable amount of clay and silt. For design of structure on these types of soils, the new method should be applied. The stone column technique, as a vibro replacement or vibro displacement can be suitable instead of vibro-compaction process in soft soils.

2.3.1.1 Vibro-Replacement Procedure or Wet Method

In this method, in-situ soil is removed to a required depth and replaced by column material. The hole is made by water jetting using probe, and then column material added in uncased hole. Wet method is suitable for cohesive soil and soil with high level of water table. Specific advantages of wet method are as follows:

1. Water jetting has an important role in stabilizing the hole and removing the soil from inside the hole,

2. Due to sustained hole during the construction, the percentage of collapse is reduced,
3. Proceeding the wet method, water used in system cools motor which is acceptable for electric saving.

Likewise, a large quantity of water may cause pollution, delay in work, and increase time of construction. Figure 1 shows the procedure of vibro-replacement consideration.

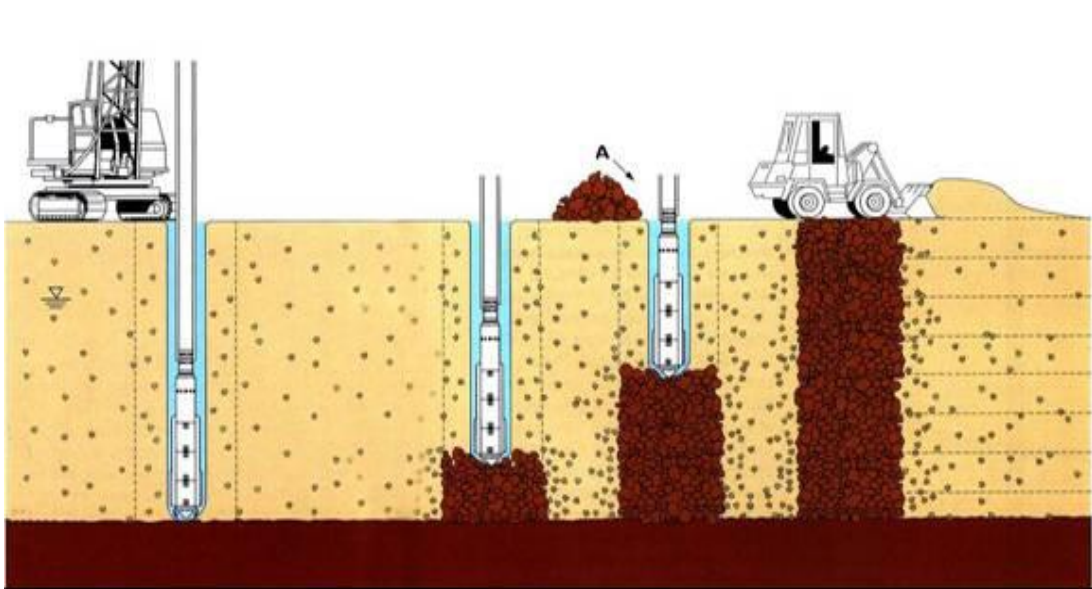


Figure 1: Procedure of vibro-replacement (Keller, 2002)

2.3.1.2 Vibro-displacement Procedure or Dry Method

In dry method, a steel pipe by using a vibratory probe is vibrated beneath soil layers and displaced the soft soil. The compressed air is used for penetrate the vibratory probe. In this case, for sand column with geotextile, after the replacing of soft soil the geotextile is installed and filled with sand, then pipe reclamation under vibration and GEC filled with different materials by various densities. Vibro-displacement method is usually proper for lower water table, soil with undrained shear strength

about 40 to 60 kN/m² and cohesionless soil. The major difference between vibro-displacement and vibro-replacement is the omission of jetting water in making the hole. Procedure of vibro-displacement is shown in Figure 2.

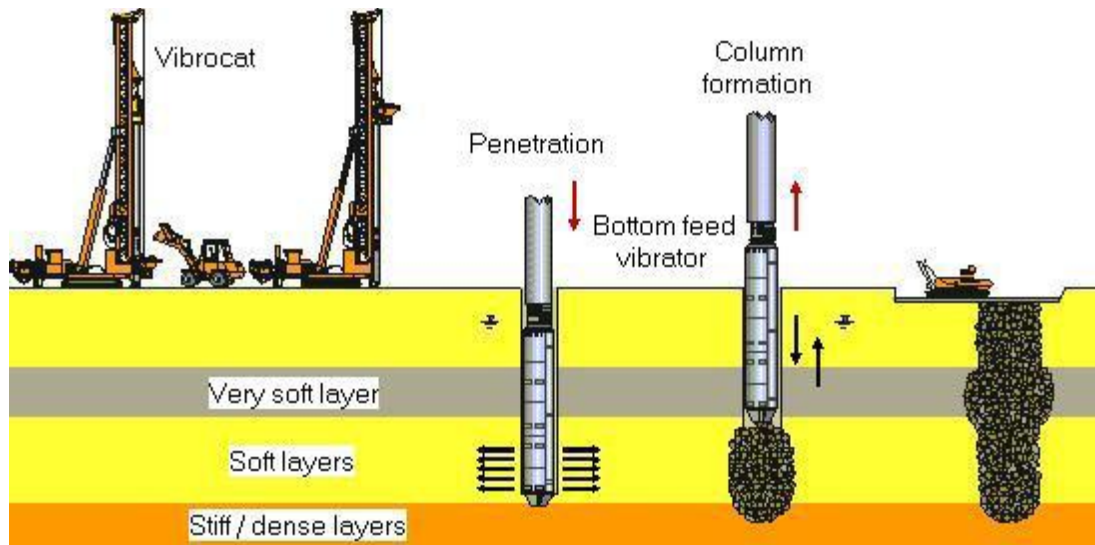


Figure 2: Procedure of vibro-displacement (Keller, 2002)

2.3.2 Ramming Technique

In the ramming method, first boreholes are made using steel pipe. Then soil in the boreholes is excavated out by auger. After that, using a weight of 125 kg dropping from a height of 750 cm, stones are compacted in the hole with. The best advantage of this technique is that it does not need labor skill.

2.4 Effect of column installation

The spacing between columns, installation method, and type of soil are important features for the alteration of horizontal earth pressures. The earth coefficient and excess pore water pressure in the surrounding soils increase notably throughout the installation of columns.

Kirsch (2008) deliberated the effect of installation of 25 group stone columns in soft soil deposits. The model was evaluated by numerical analysis using expansion theory. The result showed that, after putting columns in soil, the magnitude of stresses increase in column and in surrounding soil.

2.5 Stress Distribution on Soil and Columns

The stress concentration on column and soil are shown in Figure 3 and Figure 4 (Bergado et al., 1996; Barksdale & Bachus, 1983). Because of higher stiffness of stone columns than the surrounding soil, the stress area of stone columns is dominated by confining soil around columns. However, the vertical settlement of column and soil is similar. Stress concentration factor (SCF) can be represented as Equation 1.

$$SCF = \sigma_c / \sigma_s \quad (1)$$

where,

σ_c = Stress over column

σ_s = Stress over soil

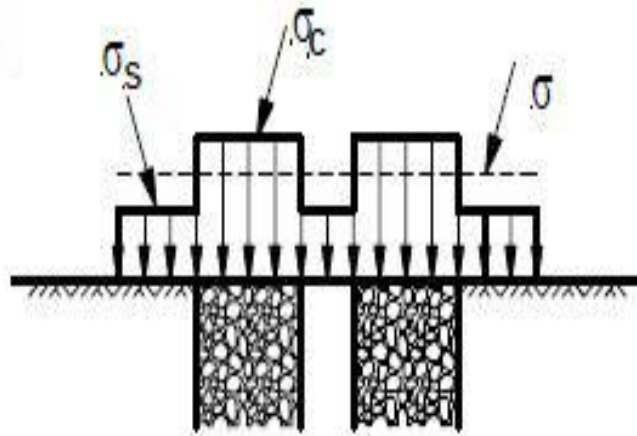


Figure 3: Stress distribution on column and soil (Bergado et al., 1996)

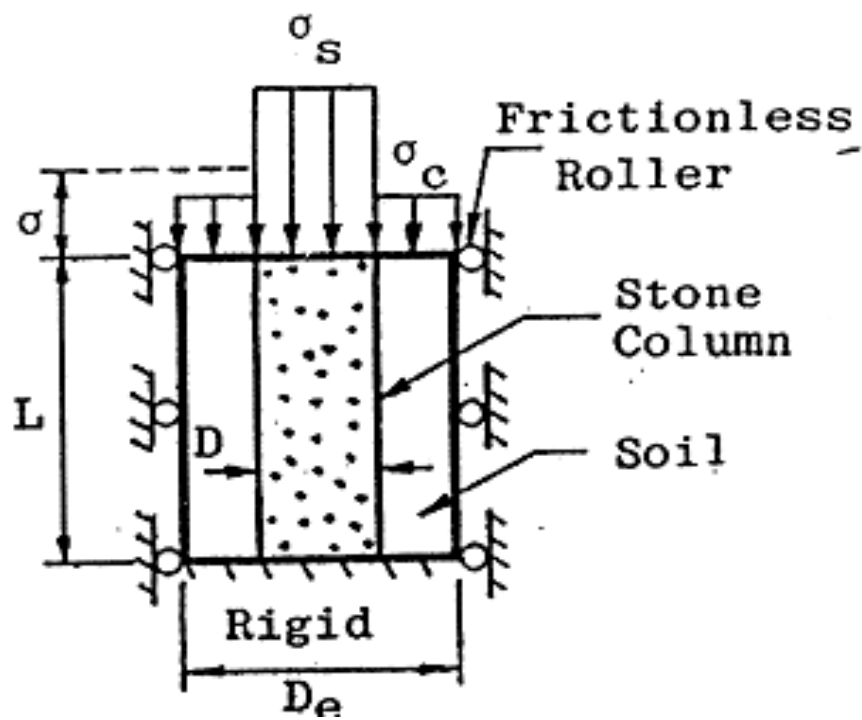


Figure 4: Stress distribution on column and soil (Barksdale & Bachus, 1983)

Also, Choobbasti et al. (2011) assessed the alteration of stresses in soil after construction of column as a function of ratio between horizontal and vertical stress (σ_h/σ_v). Figure 5 shows the relationships between stress ratio and distance from column. It can be observed that, the ratio of stress decreases markedly by increasing distance from column centerline.

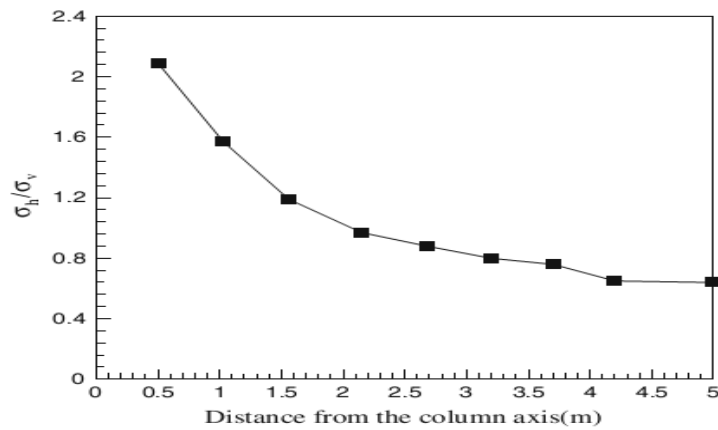


Figure 5: Relationship between stress ratio and distance from column (Choobbasti et al., 2011)

2.6 Group Stone Columns

When single stone column is compared to group stone columns slightly difference in amount of bearing capacity can be observed. This alteration occurs at group stone columns among inner columns. The amount of bearing capacity increases in group arrangements rather than single column due to restricting of interior column by surrounding column at group arrangements. Figure 6 represents increasing in amount of bearing capacity accordance to number of column.

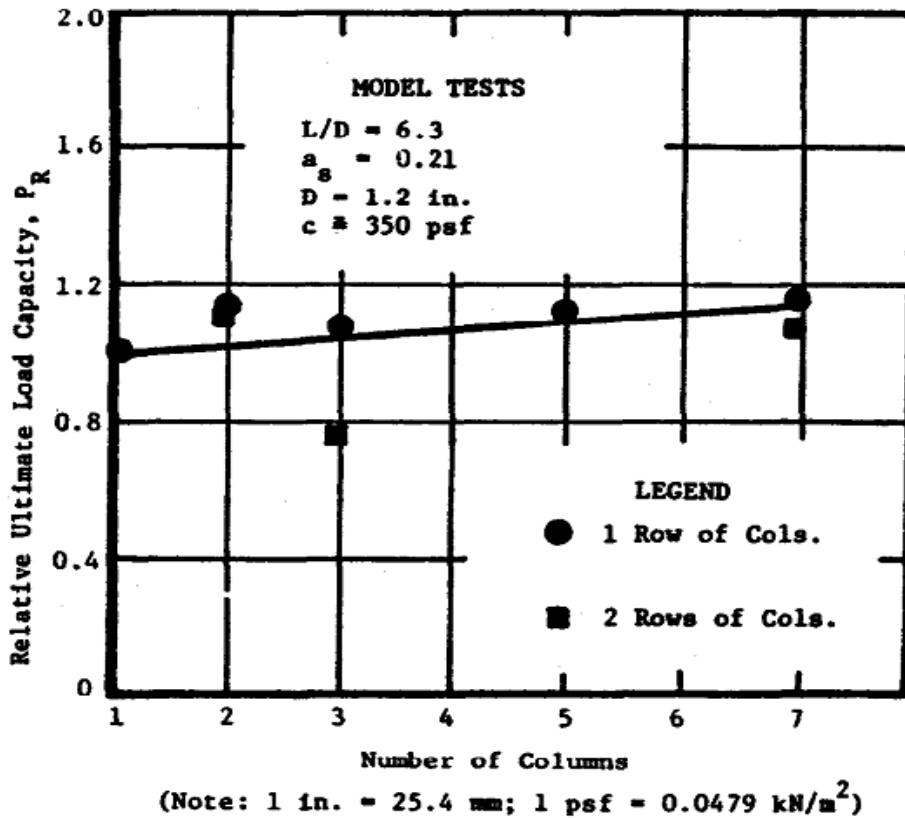


Figure 6: Relationships between bearing capacity and number of column (Barksdale & Bachus, 1983)

2.7 Mechanism of Bulging in Single and Group Columns

2.7.1 Single Column

Construction of stone column can be observed in both floating and unfloating (end of column in firm strata) condition. Three types of failure condition for both of them detected by Barksdale & Bachus (1983). These are:

- 1-Bulging failure,
- 2- Shear failure,
- 3-Punching failure.

The three types of failure can be seen in Figure 7.

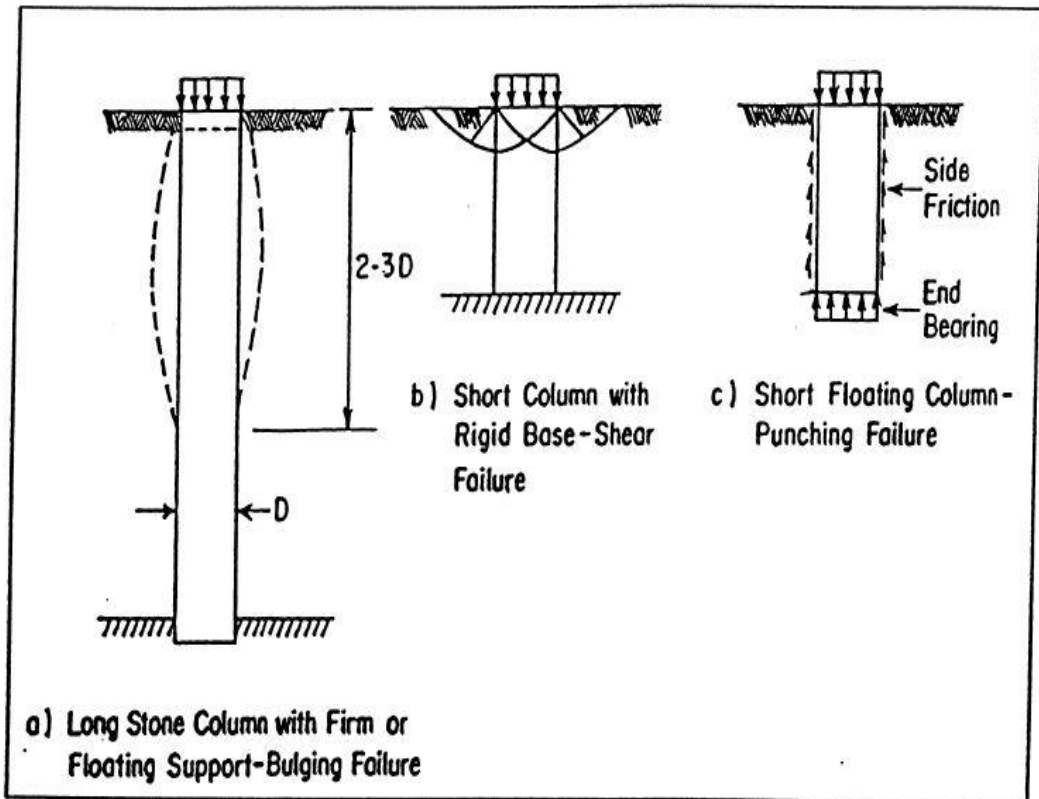


Figure 7: Bulging occurs in single column in homogeneous layer a) bulging failure, b) shear failure, c) punching failure (Barksdale & Bachus, 1983)

It can be seen from Figure 8 the failure mechanism in homogeneous layer while Figure 8 shows the types of bulging in a heterogeneous layer. It is clear that, weak soil strata have great influence on column bulging.

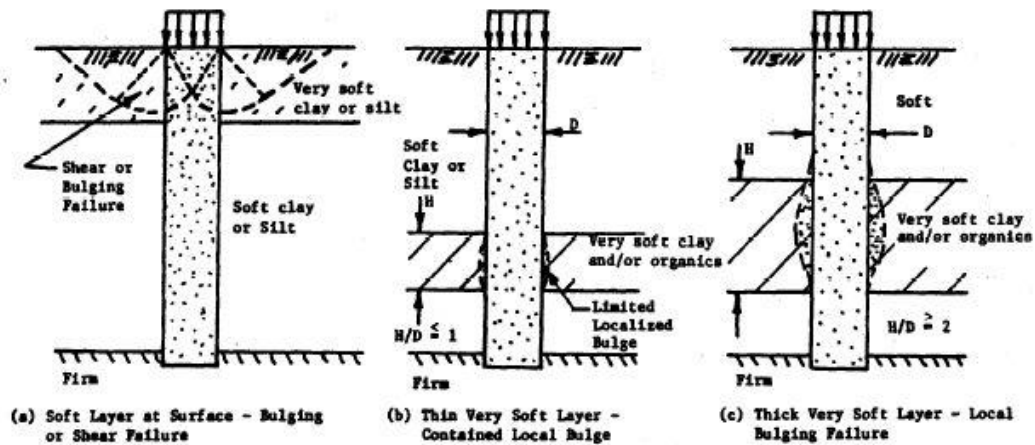


Figure 8: Types of bulging occurs in single column in heterogeneous layer (Barksdale & Bachus, 1983)

2.7.2 Group Columns

Figure 9 illustrates the failure mechanism on group columns. It can be observed that, there are different types of failure, which occurs, in columns. Spreading failure is the phenomenon that it is occurred in construction of an embankment over weak deposits. In addition, bulging failure and punching can be observed.

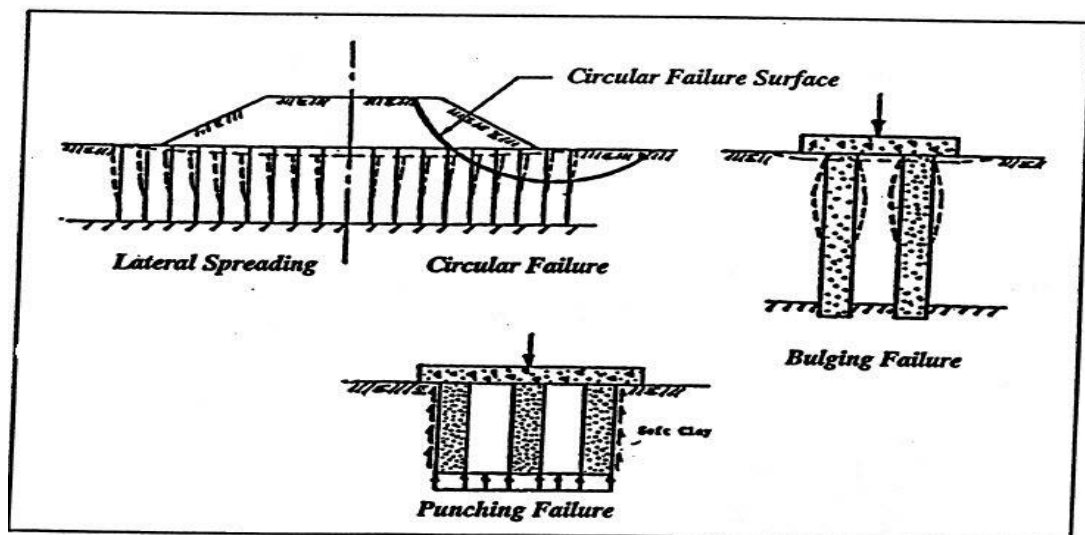


Figure 9: Types of failures in-group columns (Barksdale & Bachus, 1983)

2.8 Ultimate Bearing Capacity of Columns

2.8.1 Single Column

A several studies have been done for estimation of ultimate bearing capacity in single column. Most of the theories assumed the same situation for columns and surrounding soil as follows:

1. Stress on stone column behaved based on triaxial manner,
2. Failure happens in both stone column and surrounding soil,
3. The lateral stress σ_3 replace as the ultimate passive resistance.

According to plastic theory, the lateral stress can be shown as Equation 2.

$$\sigma_1 / \sigma_3 = \frac{1 + \sin \phi_s}{1 - \sin \phi_s} \quad (2)$$

where,

σ_1 / σ_3 (Stress ratio) = K_p = the coefficient of passive earth pressure,

ϕ_s = Friction angle of stone column.

Currently, three different methods present the ultimate capacity of single column:

1. Pressure meter theory,
2. Passive theory,
3. Vesic theory.

2.8.1.1 Pressure Meter Theory

According to elastic plastic theory and long expanding cylindrical cavity the ultimate lateral stress around stone column are shown in Equation 3 (Gibson & Anderson, 1961).

$$\sigma_{rl} = \sigma_{r0} + c_u [1 + \ln\{\frac{E_c}{2c_u (1+\nu_c)}\}] \quad (3)$$

where,

σ_{rl} = The ultimate horizontal pressure,

σ_{r0} = The entire preliminary horizontal stress,

c_u = Undraiend shear strength,

E_c = Modular elasticity of clay,

ν_c = Poisson's ratio of clay.

2.8.1.2 Passive Theory

Base on earth pressure method, the Equation 4 carried out to determine the behavior of carrying capacity by (Greenwod, 1970).

$$\gamma Z K_p + 2c_u \overline{K_p} \quad (4)$$

where,

q_{ult} = Carrying capacity of column,

γ = The bulk density of soft soil,

c_u = Undraiend shear strength.

Z = Footing depth from ground add depth of column bulge

Equation 5 expresses as below due to applying load area on soil, that q is equal to load per unit area.

$$q_{ult} = \gamma Z K_p + 2c_u \overline{K_p} + q K_p \quad (5)$$

2.8.1.3 Vesic Theory

Vesic (1972) according to plastic and elastic theory and cavity theory represents the ultimate horizontal resistance around soil as presented in Equation 6.

$$\sigma_3 = c F'_c + q F'_q \quad (6)$$

where,

σ_3 = Ultimate lateral resistance,

c = Cohesion,

q = Total stress tantamount to failure depth,

F'_c, F'_q = Factors for cavity theory.

The factors for cavity theory can be estimated by rigidity index and internal friction angle as shown in Figure 10. Equation 7 can calculate the rigidity index.

$$I_r = \frac{E_c}{2(1+\nu)(c+q \tan \phi_c)} \quad (7)$$

Now, by changing the Equation 6 to Equation 2 and assumed q_{ult} instead of σ_1 , the bearing capacity of column can be expressed by Equation 8.

$$q_{ult} = [c F'_c + q F'_q] \left(\frac{1+\sin \phi_s}{1+\sin \phi_s} \right) \quad (8)$$

Note: $F'_c = \ln I_r + 1$ for case of $\phi_c = 0$

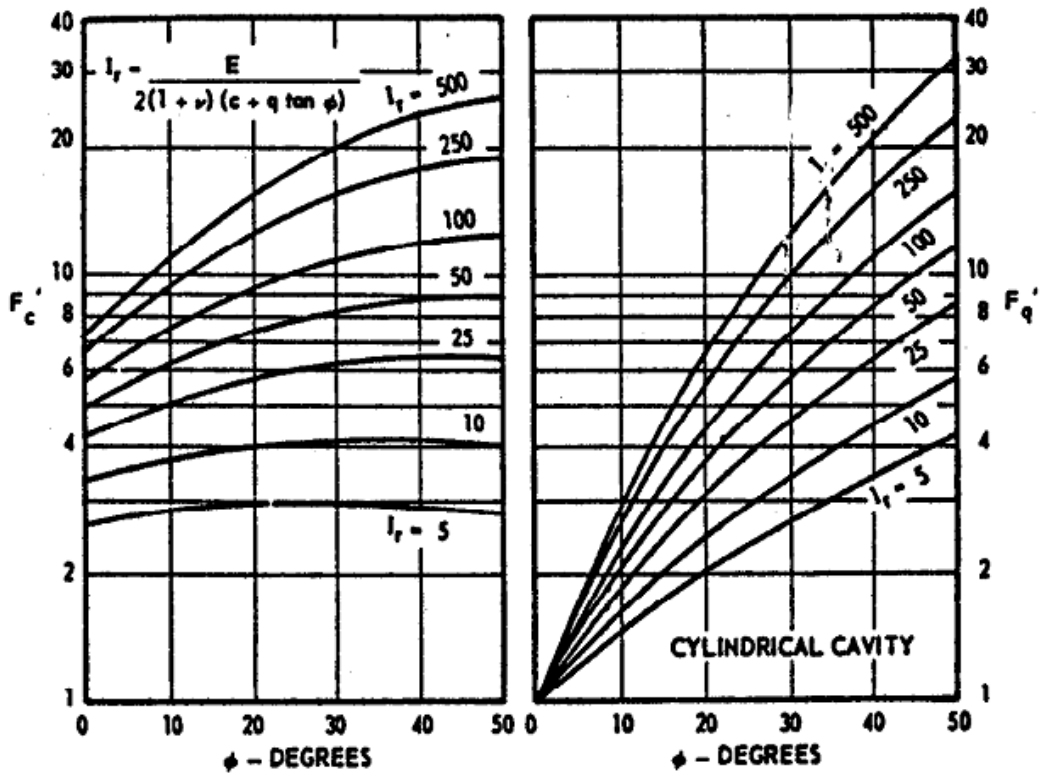


Figure 10: Factors for cavity theory (Vesic, 1972)

2.9 Settlement Prediction

For prediction of the settlement in composite soil considerable amount of literature has been published by various researchers using approximate method that use shortening assumptions or sophisticate method according to elastic and plastic theory. The majority of studied used the same assumptions to calculate the settlement, a) predict base on unit cell idealization, b) infinite area of loading.

2.9.1 Equilibrium Theory for Prediction Settlement

Equilibrium theory proposed base on Barkslade (1981) and Abhoshi et al. (1979). These approaches are useful for prediction of sand compacting piles and stone column as a ground development method. Equilibrium method design base on following assumptions:

1. Unit cell conception is usable,
2. The force that carried by stone column and surrounding soil is equals to vertical load in unit cell idealization,
3. Vertical settlement of stone column and surrounding soil are equal,
4. Similar vertical stress, because of exterior loading occurs through the stone column length.

2.9.1.1 Barkslade Theory

Barkslade (1981) conducted that the settlement under the stone column should be calculated in distinct process and generally, this amount of settlement is low, so it can be leaving out. Because of applied stress on soft soil, the vertical stress changed as follows:

$$\sigma_c = \mu_c \cdot \sigma \quad (9)$$

$$q_{ult} = \left(\frac{1}{1 + n-1 \text{ as}} \right) \quad (10)$$

Thus, presented the settlement equation for reinforced and none reinforced method according to one consolidation theory as shown in Equation 11, and Equation 12.

For reinforced method is equal to:

$$S_t = \frac{C_c}{1+e_0} + H \text{Log}_{10}\left\{\frac{\sigma_0+\sigma_c}{\sigma_0}\right\} \quad (11)$$

For unreinforced method is equal to:

$$S_t = \frac{C_c}{1+e_0} + H \text{Log}_{10}\left\{\frac{\sigma_0+\sigma}{\sigma_0}\right\} \quad (12)$$

where,

σ_c = Switch in stress in soft soil due to external load,

μ_c = Stress ratio,

n = Concentration factor of stress,

a_s = Area ratio,

σ = Average stress,

C_c = Compression index,

e_0 = Initial void ratio,

H = Vertical column height,

σ_0 = Original effective stress.

2.9.1.2 Abhoshi Theory

Aboshi et al. (1979) represented the settlement reduction factor for improving ground by stone column.

$$\beta = \frac{S_t}{S_0} = \frac{m_v \mu_c \sigma H}{m_v \sigma H} \quad (13)$$

m_v = volume coefficient of compressibility

However, Abhoshi compare the settlement versus field data as shown in Figure 11 to determine the suitability of this method. In addition, He never uses the data for in-situ soil to estimating of settlement.

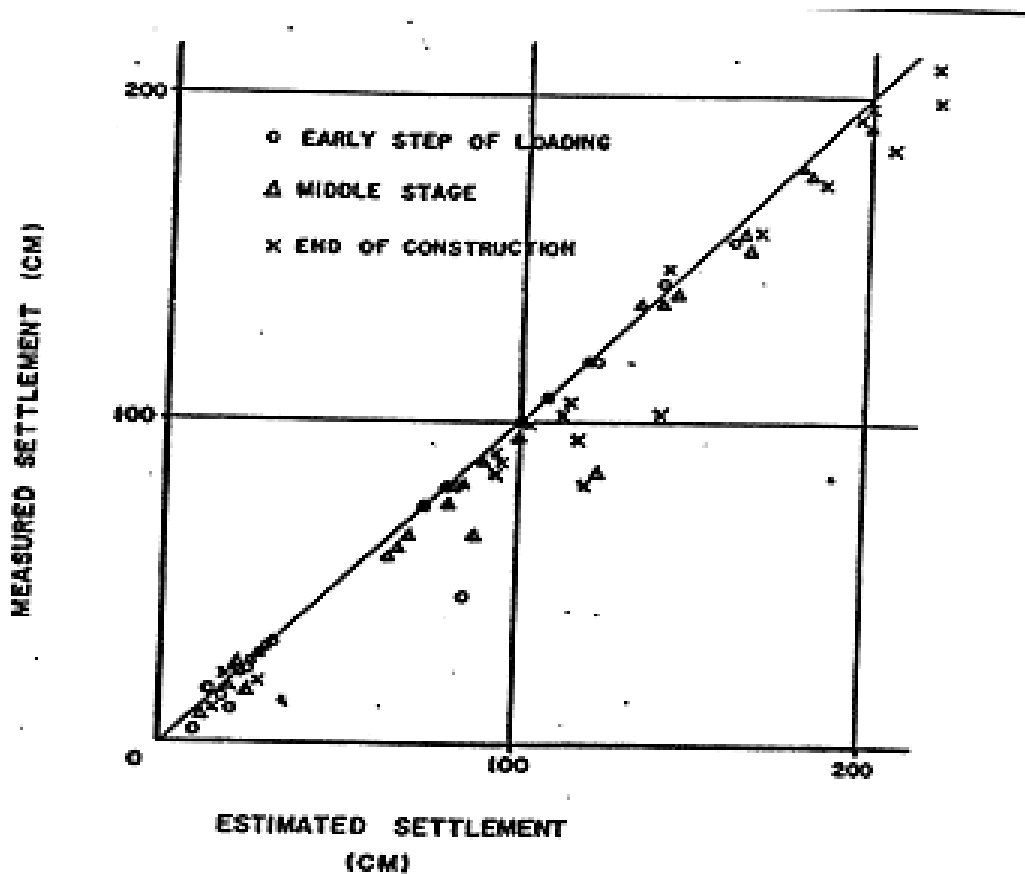


Figure 11: Measured settlement versus estimated settlement (Aboshi et al. 1979)

2.9.2 Analytical Theory for Prediction Settlement

2.9.2.1 Priebe Theory

According to unit cell, rankine earth pressure, and elastic theory, a new method for determination the settlement recommended by Priebe (1976). He proposed this theory by improvement factor versus the area ratio. Improvement factor is a rate for settlement between none reinforced ground and reinforced ground stabilized by stone column. Furthermore, Priebe modified a new version that is contained column compressibility, resolution for single and strip footing, captivity of overburden and modular ratio for soil and stone column. Figure 12 illustrates the method demonstrated by (Priebe, 1995).

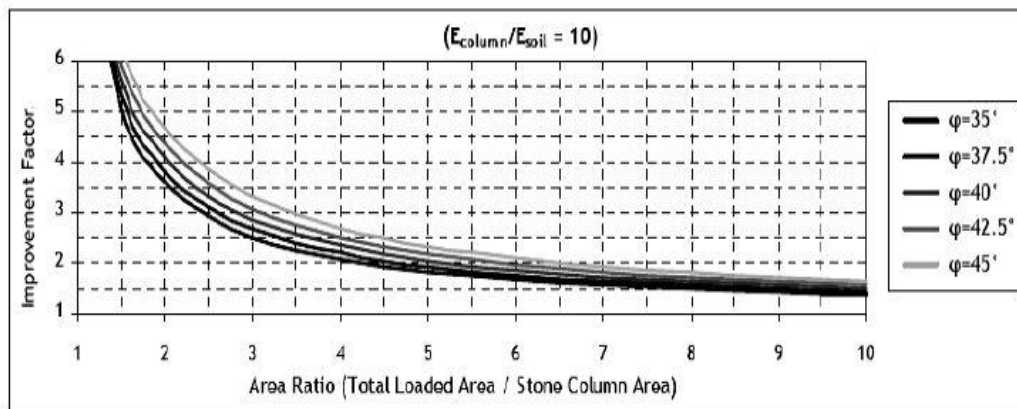


Figure 12: Relationships between area ratio and improvement factor to determine settlement (Priebe, 1995)

2.9.2.2 Van Impe and De Beer Theory

Van Impe and De Beer (1983) suggested a method for soft soil improving by stone column to estimate the reduction of settlement. The method represents base on inflection of the granular strip at stable volume beneath restriction of equilibrium estate. The stone walls were switched by stone columns with the same plan area as shown in Figure 13. In addition, Figure 14 determines the relationships between stress ratios of stone columns and settlement repletion coefficient (B) against area ratio (a_s).

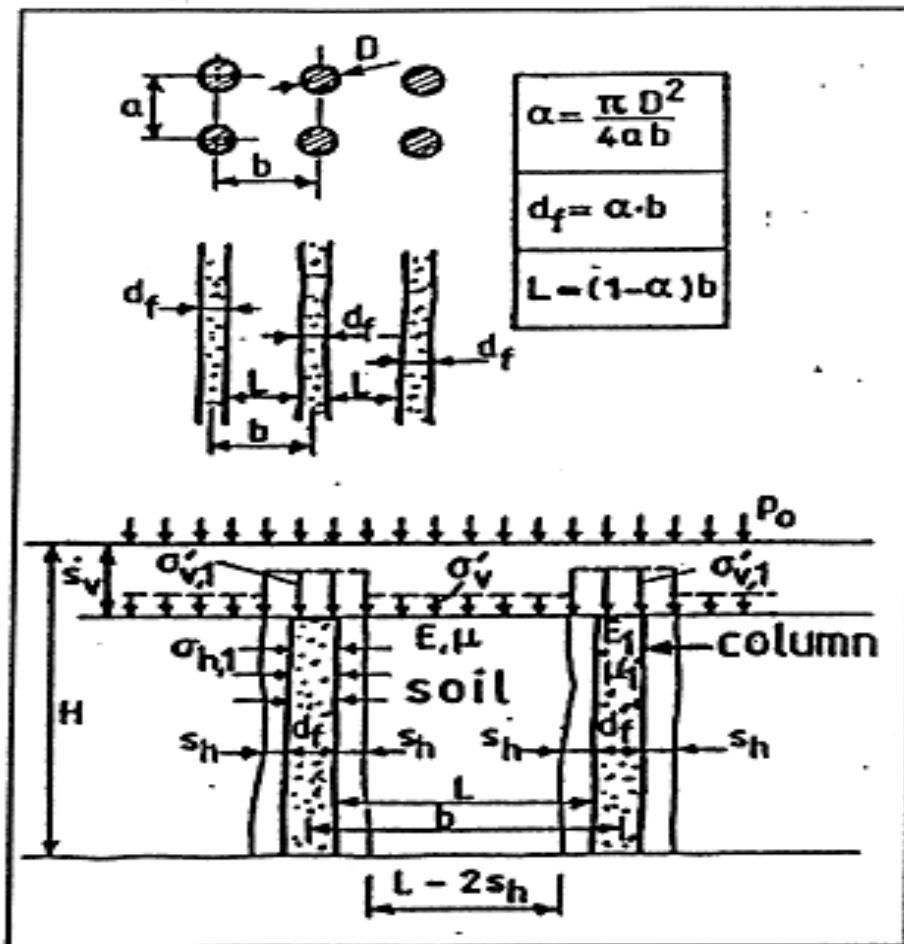


Figure 13: Procedure of stone walls replaced by stone column (Van Impe & De Beer, 1983)

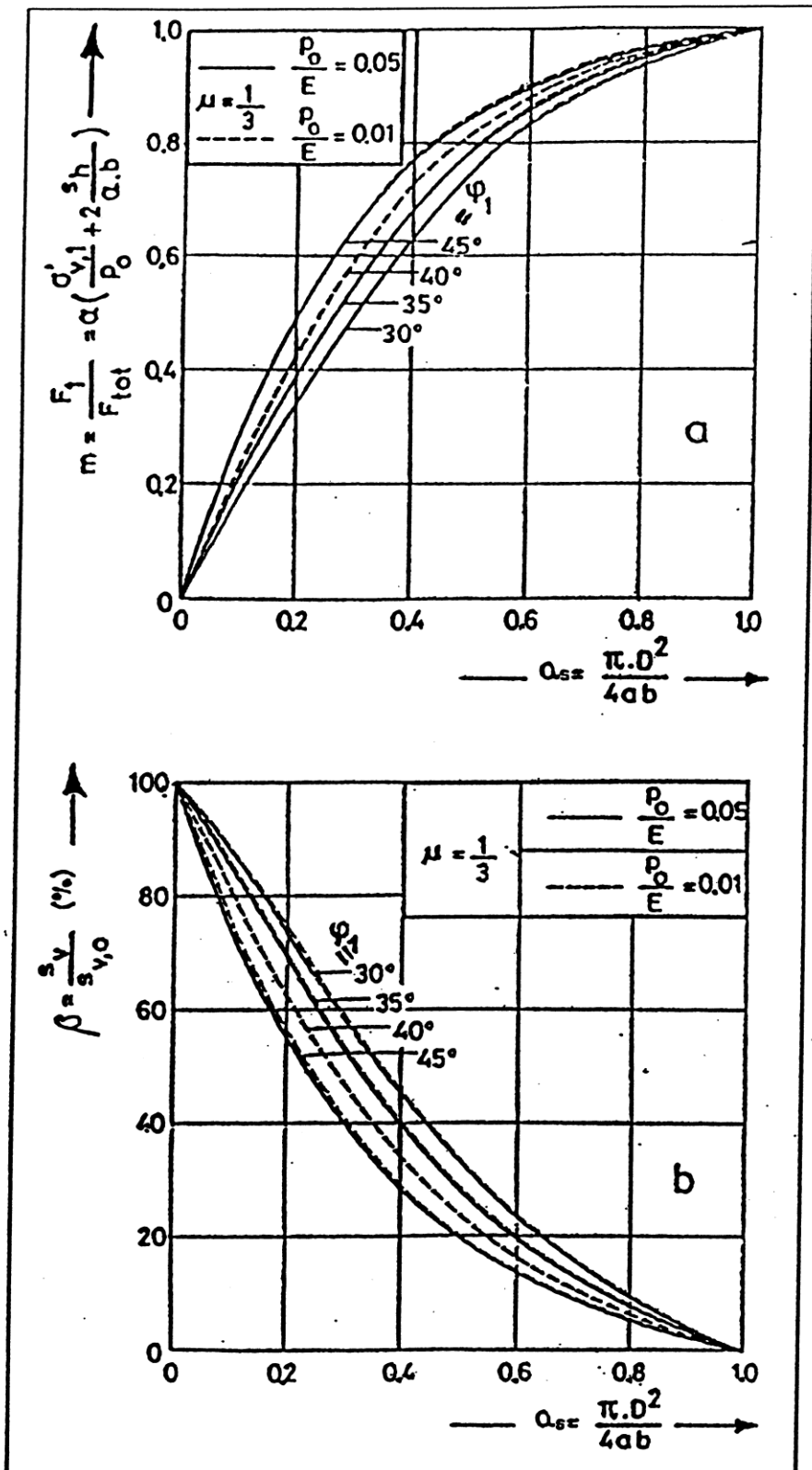


Figure 14: Relationships of settlement reduction coefficient (B) against area ratio (as)

2.9.3 Empirical Method

This method estimated base on undrained shear strength of original soil and spacing distance among stone columns. Firstly, one curve determined to calculate the settlement of reinforced soil utilize stone column by Greenwood (1970) then These curves were updated and designed accordance area ratio as shown in Figure 15 (Greenwood & Kirsch, 1983).

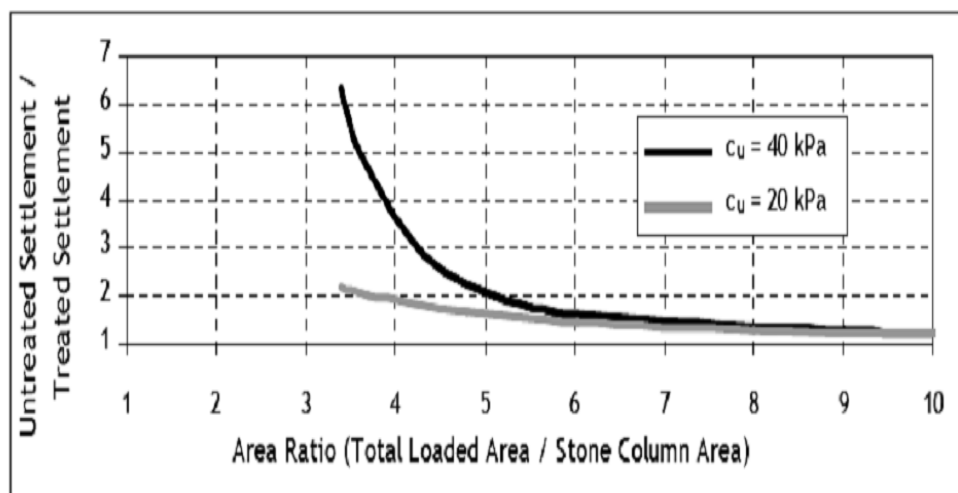


Figure 15: Empirical theory of (Greenwood & Kirsch, 1983)

2.9.4 Numerical Prediction

Another acceptable method for calculating the settlement and consolidation analysis of soft soil stabilize by stone column is numerical method. There are large volumes of published studies describing the role of numerical simulation of column for improving the weak soils beneath different structures.

2.10 Previous Investigated on Columns

2.10.1 Numerical Study

Balaam et al. (1977) evaluated the granular column beneath a rigid footing. They realized that by reduction quantity in spacing among stone columns a substantial decreasing in settlement observed.

Elsawy et al. (2010) reviewed the performance of full-scale analyses of stone column in Bremerhaven clay. The FEM analyses using Plaxis program was carried out to evaluation the effect of geogrid stiffness and geogrid depth in stone columns. drained and undrained condition has been used for clay. Geogrid encased stone column restricted the independence behave of columns in clay and make radial tension force. Due to this ability of geogrid materials the bearing capacity of the soil increased by increasing stiffness of geogrid. In addition, the amount of lateral bulging decreased by increasing in geogrid stiffness, Figure 16 represents the effect of geogrid stiffness in lateral bulging of columns.

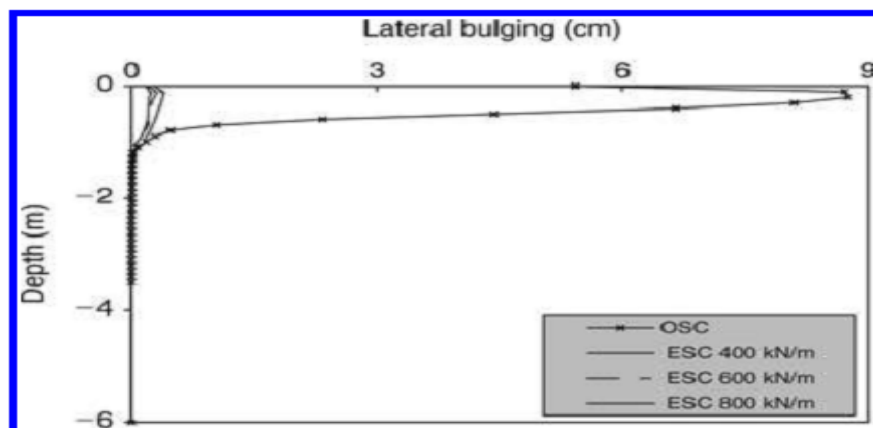


Figure 16: Lateral bulging reduced due to geogrid stiffness (Elsawy et al. 2010)

Additionally, the lateral bulging of stone column occurs in depth of two times larger than the diameter of column in undrained condition but in drained situation the lateral bulging happened along stone columns because of stress transfer. In addition, the bearing capacity increased and lateral bulging reduced by increasing in depth of geogrid encasement.

Elshazly et al. (2006) presented new relationships between various stresses in soil and different spacing of inner columns because of vibro-installation of stone columns. They deduced a new coefficient, K^* , coefficient of horizontal to vertical stress ratio. Subsequently, they understood, the decreasing trend of value of K^* observed enhancing of inner-column spacing.

Lo et al. (2009) reported the numerical performance of encapsulate stone columns with geosynthetic material under an embankment construction. Behavior of ordinary stone columns was not sufficiently effective in decreasing settlement because the stress concentration in stone columns was not confining as well as the encased stone columns. A unit cell concept was carried out in this study. Coupled analysis by following assumptions was used:

1. Sand blanket above stone columns in 4 days,
2. Embankment designed layer by layer at rate 25 m/day,
3. Beneath the ground level initial stress determined,
4. Stone columns material replaced by soft soil, and then geosynthetic properties activated.

Geosynthetic material with lateral stiffness of 2000 kN/m and axial stiffness of 3% of horizontal stiffness was taken to evaluation of geosynthetic stone columns. The relationship of settlement versus time was taken to appraise the amount of settlement at ground level. In 10 years, the settlement above stone columns was 0.87 m whereas geosynthetic encased column decreased this amount to 0.27 m. the settlement situates as a bumping near the stone column. Finally, calculated settlement is considerable affected by the confining stress in geosynthetic.

A relationship exists between the behavior of geosynthetic stone columns under an embankment construction, influence of encasement in lateral bulging of stone columns were analyzed and results reveals that the lateral bulging of stone columns reduced, related to presence of geogrig material around stone columns as shown in Figure17 (Murugesan & Rajagopal, 2006).

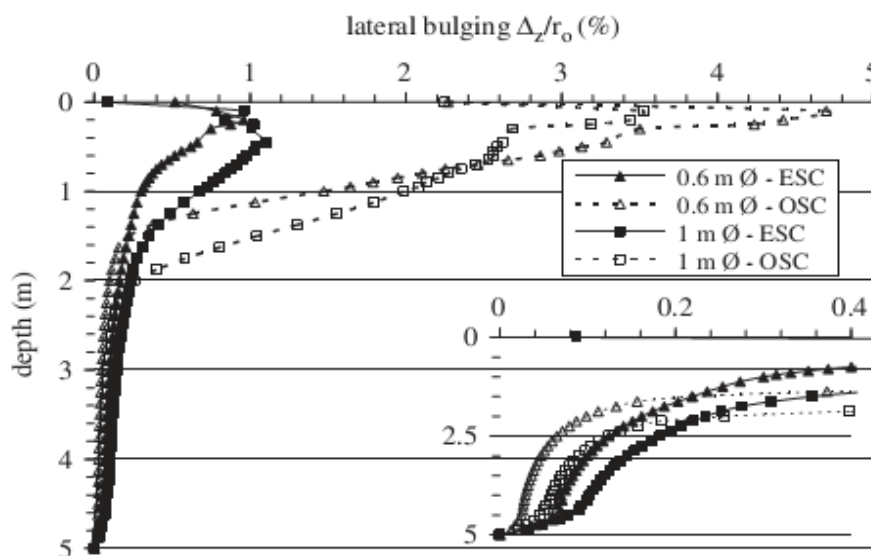


Figure 17: Lateral bulging versus depth (Murugesan & Rajagopal, 2006)

Further, the influence of varied geogrids stiffness evaluated by settlement and pressure as are shown in Figure 18.

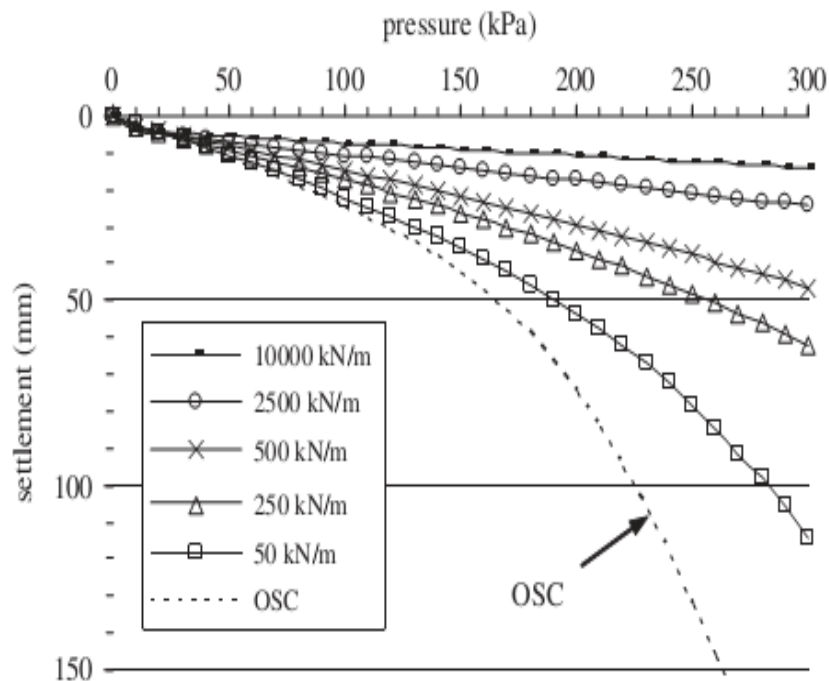


Figure 18: Settlement versus pressure affected by geosynthetic (Murugesan & Rajagopal, 2006)

It can be shown that, the amount of settlement reduced by increasing in stiffness of geogrid materials rather than regular column. In addition, Figure 19 depicts the performance of different diameter of stone columns and different stiffness of geogrid on hoop tension. The hoop tension force improved by increasing in stiffness of geogrid and in presence of geogrid material around stone columns, the performance of smaller diameter is better than larger diameter.

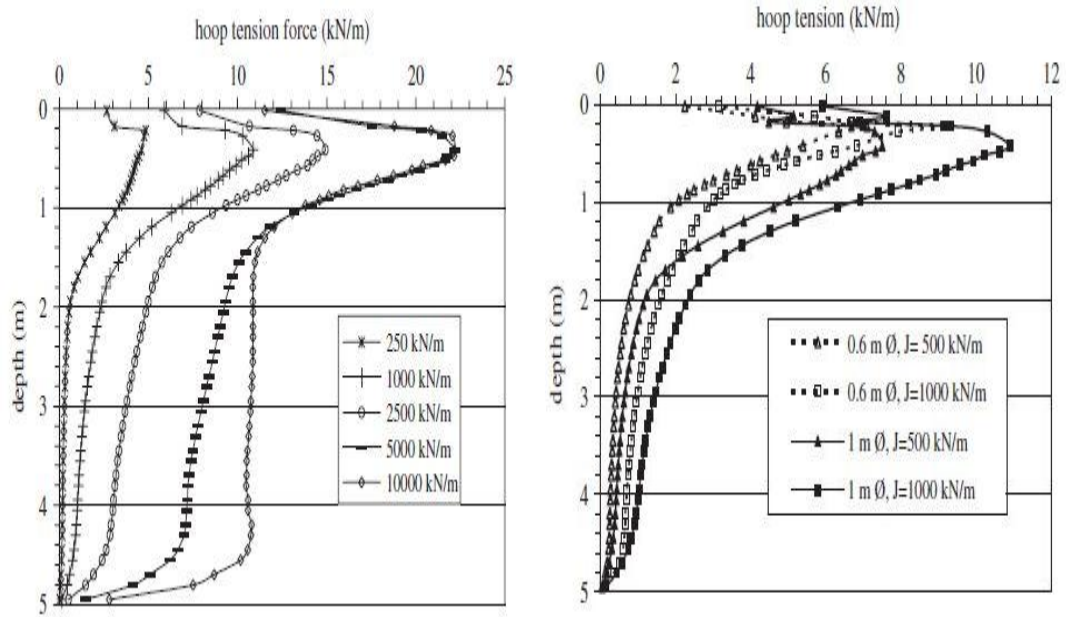


Figure 19: Hoop tension force versus depth (Murugesan & Rajagopal, 2006)

The influence on different spacing on stone columns under 2 meter height embankment over a soft soil by depth 5.5 m were performed by Domingues et al. (2007). The replacement area ratio and improvement factor was taken to assess the effect of columns in settlement and value of bulging. Unit cell analyses using axisymmetric model have been used. The results reveal that, when area replacement ratio reduced the amount of settlement and stone column bulging reduced, but the improvement factor (fraction of un-reinforcement to reinforcement soil area by stone columns) increased.

Abusharar et al. (2009) presented a series of numerical modeling on full-scale analyses of multi-column under an embankment construction, the settlement; excess pore water pressure and axial force on column effective have been calculated. Multi-column incorporate as a ground improvement method has considerable effect on reducing the total and differential settlement, and confines the horizontal movement of the embankment. In addition, in multi-column construction, the long columns

have better performance to accelerate the consolidation time rather than short columns.

Oliveira & Lemos (2010) studied on numerical estimating of settlement, lateral displacement, and excess water pressure of Portuguese soft soil beneath an embankment construction. The embankment structure consists of six layers in 420 days. Evaluation consist of large displacement accompanied reduce in settlement and speeds up to excess pore water dissipation.

Zahmatkesh et al. (2010) also implemented numerical analyses of stone columns in soft clay. Numerical study contained that, after installation of stone columns the amount of stress is remarkable decreased with distance from the column.

2.10.2 Experimental Study

Bae et al. (2002) performed a series of laboratory test and finite element analyses in single and group stone column to realize the behavior of failure in columns. The main failure happened as bulging failure in single stone column at depth of 1.6 to 2.8 times of diameter of stone column and for group stone columns appeared as conical failure.

The performance of encapsulate stone columns by different types of geogrid on carrying bearing capacity were done by (Malarvizhi & Ilamparuthi, 2004). They compared the treat part to untreated part and found that the bearing capacity of treated part by ordinary and encased stone columns was 2 or 3 times more than the untreated condition.

Sharma et al. (2004) conducted a series of experimental tests to specify the effect of geogrid on bearing capacity and value of bulging. Meanwhile the load applied either in same diameter of stone column or total area of stone column and surrounding soil. It was detected geogrid has significantly developed the bearing capacity and decrease the bulging of columns. The bulging occurred in 1.33 diameter of stone column.

Malarvizhi & Ilamparuthi (2006) have researched on performance of geogrid stone column in clay with high plasticity (CH) both in numerical and experimental method. The experimental test were accompanied in cylindrical tank with 400 mm diameter and 300 mm height and the numerical method were analyzed by Finite element method using plaxis 2D. Three different diameter of encased and ordinary stone column were applied to representation of settlement under different magnitude of load, hoop tension, and value of bulging in column as shown in Figure 20. Therefore, the column load increased by the increasing in diameter of column. The maximum hoop tension of geogrid material increased from 1.03 kN/m to 1.55 kN/m based on reduction on column diameter. Moreover, area of loading in stone column played an important role in value of bulging and stress on stone column. A significant increase in stress on stone column occurs in 3D load area rather than 1D load area. Encased material of stone column increases the amount of stress on stone column rather than the ordinary column.

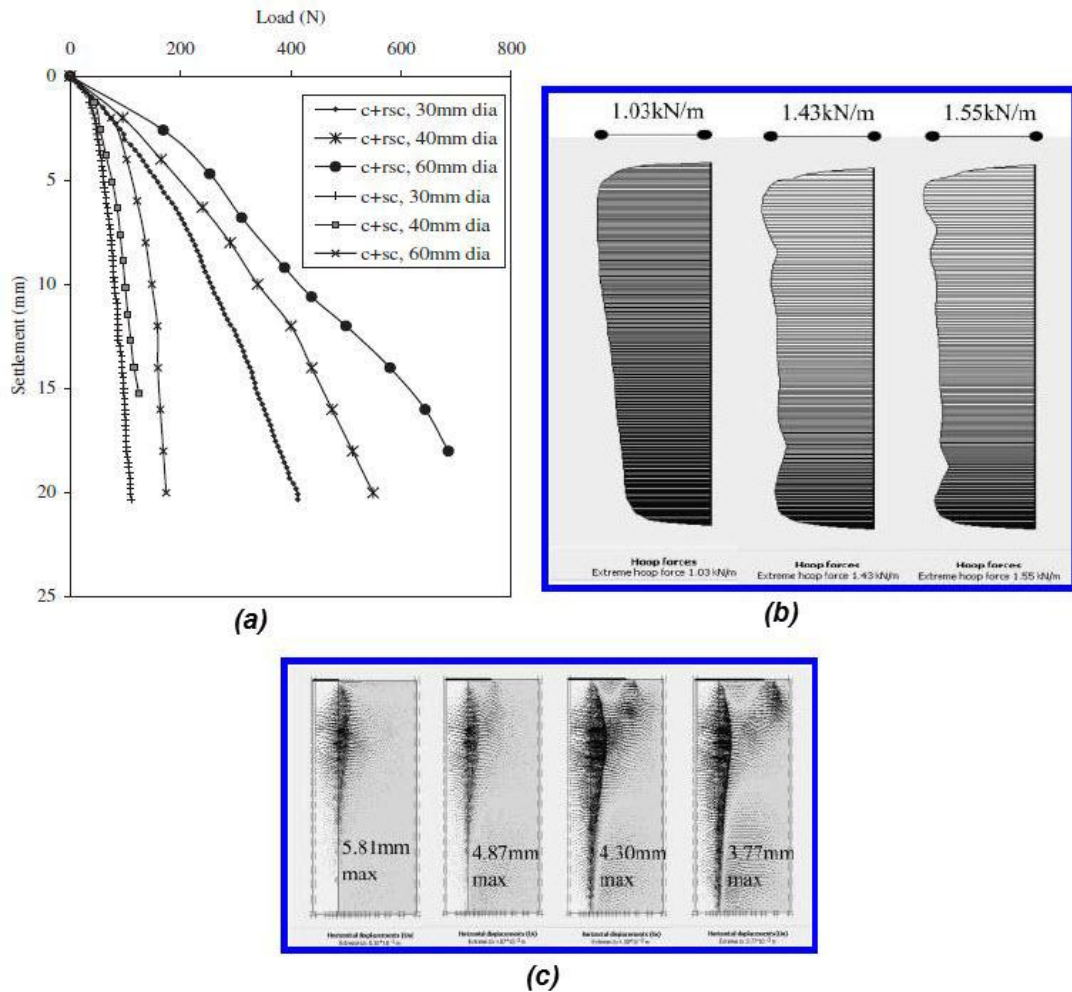


Figure 20: Different analyses of stone columns on a) settlement, b) hoop tension, c) bulging failure (Malarvizhi & Ilamparuthi, 2006)

Ambily and Gandhi (2007) studied a series of laboratory tests on performance of single stone column and seven group stone columns by various parameters like loading type, angle of friction of stone columns, undrained shear strength, and column spacing. Column with 100 cm in diameters were selected. Moreover, the finite element analyses were carried out to compare with experimental results. The following results were achieved:

1. The bulging occurs at a depth of 0.5 times of diameters of stone column when the loading applied in stone column,

2. The amount of settlement increased as a result of increase in space of column,
3. Stiffness improvement depends on stone column friction angle and space.

Malarvizhi et al. (2008) studied the effect of encapsulated stone columns using both numerical method and triaxial test on encapsulated columns. The stress versus strain behavior of two stone column diameters at three pressures have been compared between triaxial test and finite element Plaxis software. Due to encased material, the strength of stone columns increased rather than non-encapsulated stone columns.

Genil & Bouazza (2009) perused the effect of stone columns on stress reduction and bulging failure. It was found that geogrid can considerably reduce the stress up to 80% in comparison with untreated soil. Meanwhile bulging in single stone column occurs at depth of 2 diameter of column and bulging in group stone columns happen throughout length of stone column.

Deb et al. (2010) described the performance of geogrid sand layer on stone column by experimental method. The following details were selected to describe the laboratory model:

1. Single stone column with 50 mm diameter in square tank (525 mm size and 400 mm height),
2. Clay deposit prepared by compaction method,
3. Replacement method used for stone column installation,
4. Geogrid material put on the stone column beneath 50 mm sand layer ,
5. A rigid footing with diameter equal to 10 mm used to apply the load.

Set up procedure of experimental methods illustrates in Figure 21.

The results showed that in the presence of geogrid under sand layer above stone column, the load carrying capacity has substantially increased and the bulging decreased, meanwhile the bulging happened in deeper depth than unreinforced column.

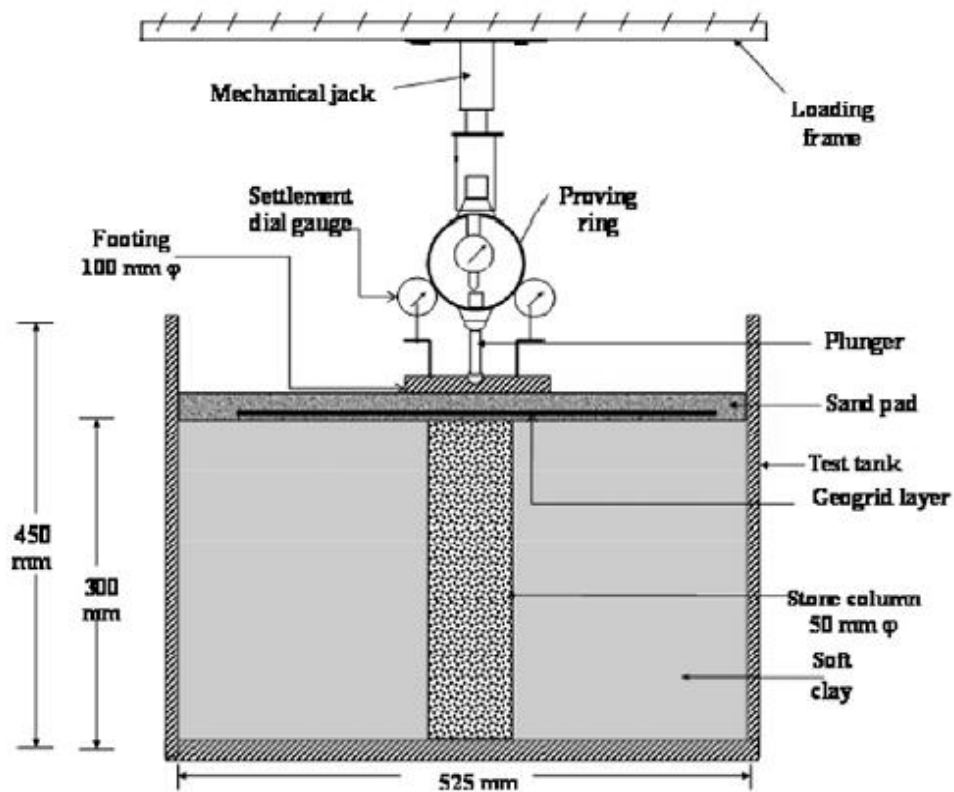


Figure 21: Experimental set up of stone column (Deb et al. 2010)

2.11 Geosynthetic:

2.11.1 Different Types and Applying Areas

In recent years, the terms geosynthetic was popular to use in different structures.

Table 1 shows the different types of gesynthetics for different application areas.

Table 1: Different types of geosynthetic and application areas (Jacques, 1999)

	Geotextile	Geo-membrane	Geogrid	GCL	Geocomposite sheet drain	Geocomposite strip (wick) drain	Geocell	Erosion control product	HDPE vertical barrier
Separation	X	X			X				
Reinforcement	X		X				X		
Filtration	X				X				
Drainage	X				X	X			
Barrier	X ^a	X		X					X
Protection	X			X	X		X	X	

2.11.2 Geotextile

This kind of geosynthetic material consists of woven and nonwoven products. The woven product was built by outmoded weaving system and varied kind of weave. Furthermore, nonwoven product was built by using filaments texture method. The woven and nonwoven types of geotextile are shown in Figure 22.

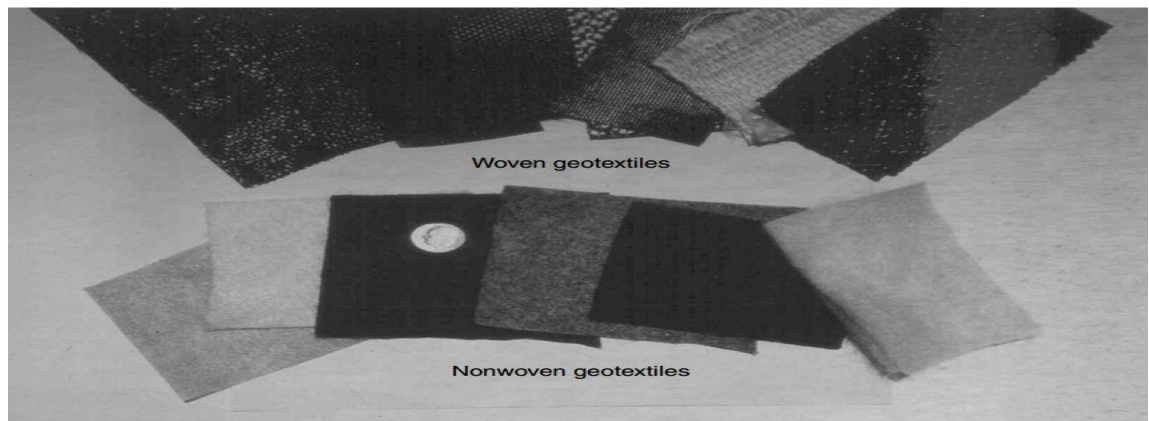





Figure 22: Woven and nonwoven type of geotextile (Jacques, 1999)

2.11.3 Geogrid

The geogrid consists of three-polymer materials (polyester or coated polyester, polypropylene, polyethylene) which are the coated form either found in woven type or knitted.

Table 2 represents some types of geogrid and geotextile that are used recently in research projects in Germany and Netherlands.

Table 2: Three kinds of geotextile and geogrid material and application area (Huesker company)

Name	Application area	stiffness	picture
<p>Fortrac® Geogrid</p>	<p>Slob stabilization Retaining wall Landfill ...</p>	<p>Between 20 to 400 special as up to 1000</p>	
<p>Stabilenka® Geotextile</p>	<p>Embankment on soft ground Earth structure</p>		
<p>Ringtrac® Geotextile</p>	<p>Encased sand column</p>	<p>Up to 400</p>	

Chapter 3

ANALYSIS OF SOIL PARAMETERS BY NOVOSPT FOR SOILS OF TUZLA

3.1 Tuzla Area

The objective of this research is to establish whether stone or sand columns can be effective in improving the soils of Tuzla area. Tuzla is on the eastern coast of Northern Cyprus, in Famagusta Bay, which, consists of alluvial soil deposits of the Delta of River Pedios. The region consists of saturated clays, sands, and silts of low to high plasticity intermittently distributed within the alluvial deposits of 50-60 m depth. Figures 23 and Figure 24 illustrate the geographic map of Cyprus and Tuzla area.



Figure 23: Location of island of Cyprus in the Mediterranean Sea



Figure 24: Location of Tuzla on the map of Cyprus

3.2 NovoSPT Software

3.2.1 Introduction

One of the popular softwares, which determine different parameters of soil profiles, is Novo SPT. This software involves approximately 270 correlations found by various researchers to determine soil parameters such as elasticity modulus, shear strength, friction angle, shear wave velocity, California bearing ratio, bearing capacity of shallow foundation and other soil parameters.

3.2.2 Procedure of Software

In order to assess different parameters of soil by NovoSPT, the software requires standard penetration test blow count (N) as input parameter. The field value is modified to N_{60} by the software using the correction factors as defined in Table 3.

Table 3: Correction factors for standard penetration test

C_e	C_b	C_s	C_r	C_n
Energy level correction	Borehole diameter	Sampling method	Rod length	Overburden factor

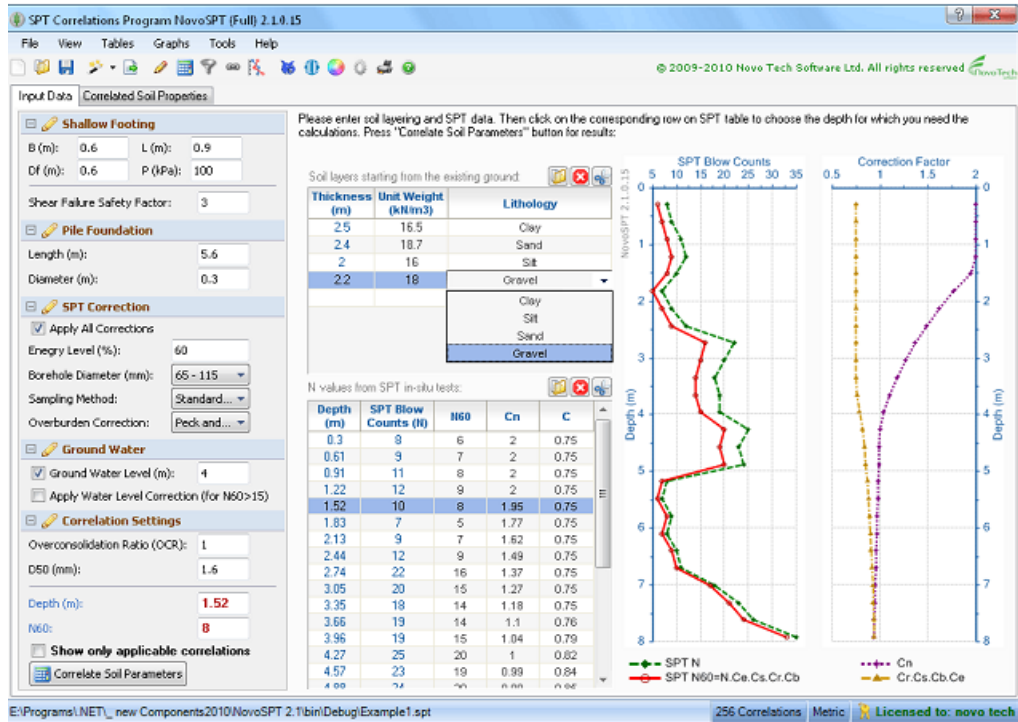


Figure 25: Input parameters page of NovoSPT software

Figure 25 shows the input parameters required for NovoSPT software.

Finally, the Novo SPT software estimated the N_{60} values and then correlated to different soil parameters using empirical relationships suggested by various researchers.

3.3 Material Preparation for Finite Element Simulation Using Plaxis Software

3.3.1 Introduction

Numerical analyses by Plaxis software for saturated clays were used in either Mohr-Coulomb model or Soft Soil Creep model. Both of models needs to some parameters that are related to structure of the models. In this study, all of the models are based on Mohr-Coulomb model. Therefore, by data extracted from Nov SPT and initial test

on soil profiles in site for each borehole we can determine the valuable information to proceeding of analyses by Plaxis.

3.3.2 Material preparation

The SPT data used in this thesis were adopted from Erhan (2009), and Lakayan (2012) and imported to NovoSPT software to retrieve the desired parameters for Plaxis modeling. The locations of all the Bore holes from the subject area are shown in Figure 26.



Figure 26: Bore hole locations in Tuzla area

3.3.3 Mohr- Coulomb Model Parameters

The Mohr-Coulomb model is the elastic perfectly plastic model for soil behavior. This model involves five basic parameters, Young`s modulus, friction angle, Poisson`s ratio, cohesion, and dilatancy angle.

3.3.3.1 Young's modulus (E)

Young's modulus is the stiffness parameters which is used either in Elastic model or Mohr-Coulomb model. This value can be obtained by using a tentative correlation, related to laboratory test result on soil samples. For determining the Young's modulus by Novo SPT, there are some correlations between N value and Young's modulus which are listed in Table 4.

Table 4: Classification of soils based on stiffness versus SPT N value

Cohesionless soil type	E_s/N
Silty sand or silt and mixture	4
Clean, fine or medium sand	7
Coarse sand	10
Sandy gravel	12

Figure 27 shows the correlation between Young's modulus, plasticity index and SPT N value for sand and gravel (Hemsely, 2000).

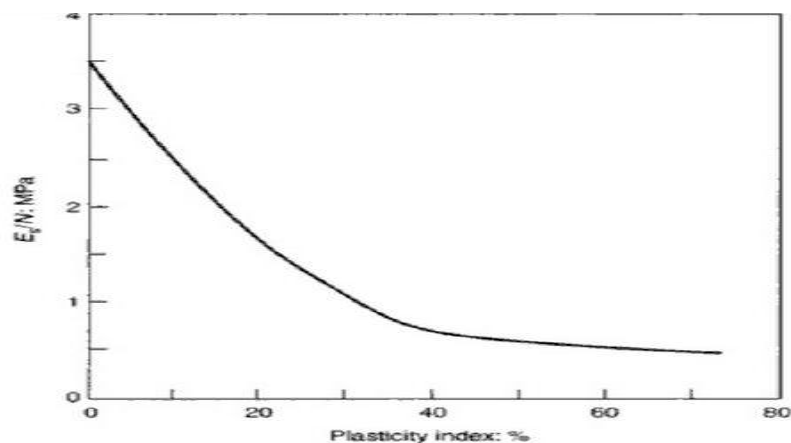


Figure 27: Estimation of Young's modulus according to plasticity index and SPT N value (Hemsely, 2000)

Correlation between SPT blow count and Young's modulus and Poisson's ratio of soil is shown in Figure 28.

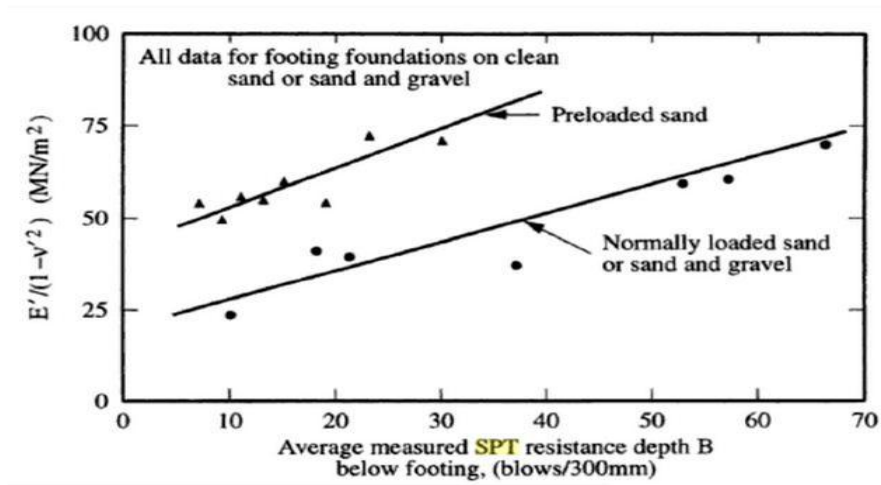


Figure 28: Estimation of Young's Modulus according to SPT blow count and Poisson's ratio (D'Appolonia et al. 1970)

Young's modulus of cohesive soil mainly CL and CL-ML has been estimated by as follows (Behpoor & Gahramani, 1989).

$$E_s = 0.17 N_{60} \text{ (MPa) while } N_{60} < 25 \quad (14)$$

3.3.3.2 Friction Angle (Φ)

The angle of internal is one of the important factors to describe the shear strength of the soil. Friction angle can be determined as shown in Equation 15 (Das, 2011).

$$\Phi = 27.1 + 0.3 N_{60} - 0.00054 [N_{60}]^2 \quad (15)$$

Other correlations of angle of internal friction and SPT-N value are given in Equations 16 and 17 (Robertson 2006; Ruwan 2008).

$$\Phi = 15.4[N_{60}]^{0.5} + 20 \quad (16)$$

$$\Phi = 3.5N^{0.5} + 22.3 \quad (17)$$

3.3.3.3 Undrained Shear Strength (S_u)

Various formulas are proposed by various researchers to determine the amount of undrained shear strength for different types of the soils base on N value as presented in Table 5.

Table 5: Estimation of undrained shear strength by N value (Afkhami, 2009)

Scientist name	Description	Undrained Shear Strength (kPa)
Sanglerat (1972)	Clay Silty clay	12.5N 10N
Terzaghi & Peck (1967)	Fine-grained soil	6.25N
Hara et al. (1974)	Fine-grained soil	29N 0.72
	Highly plastic soil	12.5N
Sowers (1979)	Medium plastic clay Low plastic soil	7.5N 3.75N
Nixon (1982)	Clay	12N
Sivrikaya & Toğrol (2002)	Highly plastic soil	4.85N field 6.82N60
	Low plastic soil	3.35N field 4.93N60
	Fine-grained soil	4.32N field 6.18N60
Stroud (1974)	PI<20	(6-7)N
	20<PI<30	(4-5)N
	PI>30	4.2N
Décourt (1990)	Clay	12.5N 15N60
Ajayi & Balogun (1988)	Fine-grained soil	1.39N+74.2
Hettiarachchi & Brown (2009)	Fine-grained soil	4.1N60
Sirvikaya (2009)	UU Test	3.33N – 0.75wn+ 0.20LL + 1.67PI
	UU Test	4.43N60 – 1.29wn + 1.06LL + 1.02PI
	UCS Test	2.41N – 0.82wn + 0.14LL + 1.44PI
	UCS Test	3.24N60 – 0.53wn – 0.43LL + 2.14PI

3.3.3.4 Basic Parameters for Simulating in Plaxis

Furthermore, according to NovoSPT output results for soil profiles for Bore hole 36 (Chapter 4), Bore hole 21 (Chapter 5), and Bore hole 38 (Chapter 6) the Young's modulus (E) values were adopted from Ghahramani and Behpoor (1989), shear strength values were adopted from Bowles (1988) and for friction angle due to undrained condition it assumed becomes zero. Other parameters base on SPT test results provided by (Erhan, 2009) are given in Equations 18-21. Bulk unit weight, dry unit and saturated, and Poisson's ratio regards to Equation 18-20 (Das, 2011) and Equation 21 (Das, 2008).

$$\gamma = \frac{(1+w)\gamma_w G_s}{1+e} \quad (18)$$

$$\gamma_d = \frac{\gamma_w G_s}{1+e} \quad (19)$$

$$\gamma_{sat} = \frac{(e\gamma_w)\gamma_w G_s}{1+e} \quad (20)$$

$$v = 0.25 + 0.00225 (PI) \quad (21)$$

where,

w = Water content,

γ_w = Water unit weight,

G_s = Specific gravity,

e = Void ratio,

PI = Plasticity index.

Permeability is assumed to be 10^{-7} cm/sec for all clays.

Chapter 4

STONE COLUMN BENEATH AN EMBANKMENT CONSTRUCTION IN UNIT CELL IDEALIZATION

4.1 Unit Cell Conception

Most studies in the field of ground improvement by stone columns have focused on unit cell and full-scale analyses. The unit cell pattern is convenient for single stone column, and full-scale analyses are appropriate for group stone columns. The unit cell conception has been widely investigated by many researchers. According to research of Ballam & Booker (1981), there are three various patterns of preparation of single stone column in unit cell condition as follows:

1. Square pattern,
2. Triangular pattern,
3. Hexagonal pattern.

Figure 29 provides the unit cell idealization in three patterns.

4.1.1 Area Replacement Ratio

Area replacement ratio means the area of the soil that is replaced by stone column and is given in Equation 22.

$$a_s = A_s/A \quad (22)$$

where,

A = Total area of unit cell

A_s = Total area of columns

a_s = Area ratio

Equation 23 gives the relationship of total area of column with respect to diameter and spacing of columns.

$$A_s = C_1 (D/S)^2 \quad (23)$$

where,

D = Diameter of column

S = Spacing of columns

C = A constant corresponding to the pattern of column

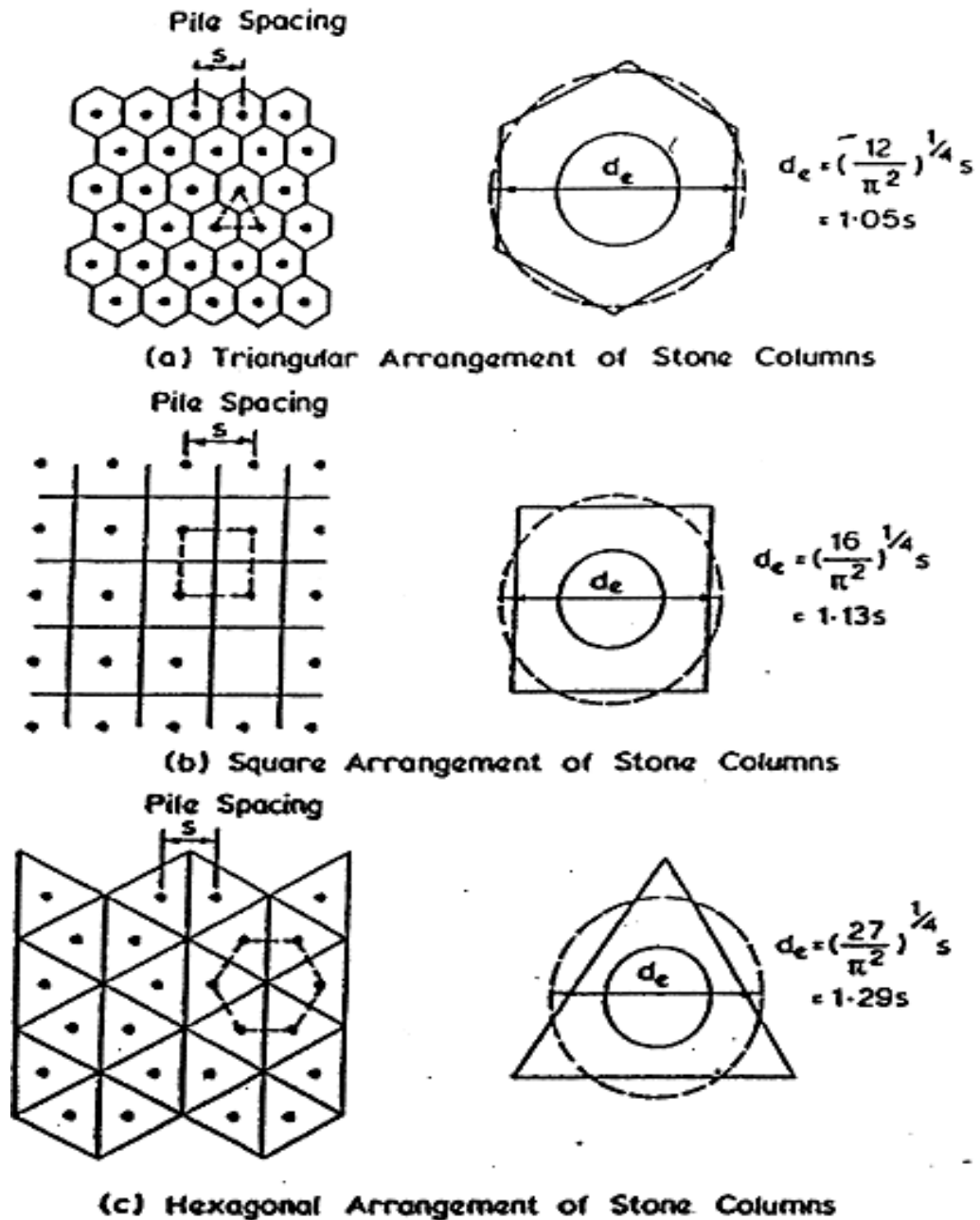


Figure 29: Various patterns of unit cell: (a) Triangular, (b) Square, and (c) Hexagonal (Ballam & Booker, 1981)

4.2 Materials and Parameters for Numerical Analyses

In order to identify the unit cell conception of single column beneath an embankment construction, details of Borehole 36 were adopted for clay bed of 8 m thickness underlain by a firm stratum. The data for embankment fill were chosen from the investigation of Abusharar et al. (2009), stone column, and sand column were

gathered from research work of Ambily & Gandhi (2007) and gravel was taken from Issac & Girish (2009). Tables 6-8 show the required materials and necessary parameters for numerical analysis.

Table 6: Fill and stone column materials

Parameter	Symbol	Stone Column	Fill
Material model	Type	Mohr-Coulomb	Mohr-Coulomb
Loading	Condition	Drained	Drained
Wet unit weight (kN/m ³)	γ_{wet}	19	20
Horizontal Permeability (m/day)	k_h	12	0.009
Vertical Permeability (m/day)	k_v	6	0.009
Young's modulus (kN/m ²)	E	55000	8000
Poisson's ratio	ν	0.3	0.3
Cohesion (kN/m ²)	c	0	1
Friction angle (°)	ϕ	43	30
Dilatancy angle (°)	ψ	10	0

Table 7: Gravel and sand materials

Parameter	Symbol	Gravel	Fill
Material model	Type	Mohr-Coulomb	Mohr-Coulomb
Loading	Condition	Drained	Drained
Wet unit weight (kN/m ³)	γ_{wet}	19.4	18
Horizontal Permeability (m/day)	k_h	6	1
Vertical Permeability (m/day)	k_v	6	0.5
Young's modulus (kN/m ²)	E	45000	20000
Poisson's ratio	ν	0.3	0.3
Cohesion (kN/m ²)	c	0	0
Friction angle (°)	ϕ	42	30
Dilatancy angle (°)	ψ	0	4

Table 8: Properties of clay bed (Borehole 36)

Depth (m)	Type	γ_{dry} (kN/m ³)	γ_{Sat} (kN/m ³)	E_s (kN/m ²)	Φ (°)	S_u (kPa)	K (m/day)
0-8	CL	15.5	19.8	2700	0	66	8.64×10^{-5}

4.3 Numerical Procedure

For the purpose of numerical analysis by Plaxis, Mohr-Coulomb model has been chosen for all materials, however drained condition was selected for fill embankment and column, and undrained condition was selected for clay deposit. This analysis was done on half of a model due to symmetry. The axisymmetric analysis has been used for single column. Axisymmetric analyses using Plaxis 2D software in both reinforced and unreinforced stone column are presented in Figure 30.

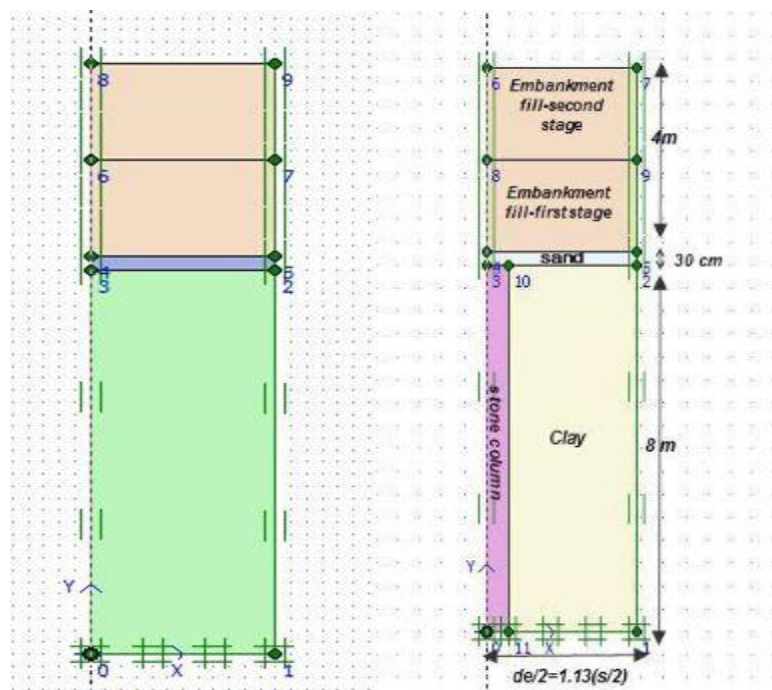


Figure 30: Axisymmetric model for single stone column in both reinforced and unreinforced conditions

Embankment fills were constructed in two equal layers of 2 m each, above a sand layer with 30 cm thickness. First stage is constructed in 5 days, and then is allowed to consolidate for 30 days. Second construction stage was built in 5 days and finally by utilizing minimum pore water pressure option allowed to evaluate the consolidation end time. Figure 31 illustrates the calculation steps of construction embankment over soft soil in Plaxis.

The screenshot shows the 'Plaxis 8.6 Calculations - M unreinforcement.PLX' window. The 'General' tab is selected, displaying the following settings:

- Phase:** Number / ID.: 4 <Phase 4>, Start from phase: 3 - <Phase 3>
- Calculation type:** Consolidation analysis
- Log info:** Prescribed minimum pore pressure reached 9.18751E-01 < 1.00000E+00
- Comments:** (Empty text area)

At the bottom, a table lists the calculation phases:

Identification	Phase no.	Start from	Calculation	Loading input	Time	Wa...	First	Last
Initial phase	0	0	N/A	N/A	0.00 ...	0	0	0
✓ <Phase 1>	1	0	Consolidation ana...	Staged construction	5.00 ...	1	1	6
✓ <Phase 2>	2	1	Consolidation ana...	Staged construction	30.0...	2	7	15
✓ <Phase 3>	3	2	Consolidation ana...	Staged construction	5.00 ...	3	16	21
✓ <Phase 4>	4	3	Consolidation ana...	Minimum pore pressure	690....	3	22	35

Figure 31: Calculation steps of embankment construction

For the evaluation of mesh analysis, fine mesh conditions were adopted in this research as shown in Figure 32 for different stages of construction.

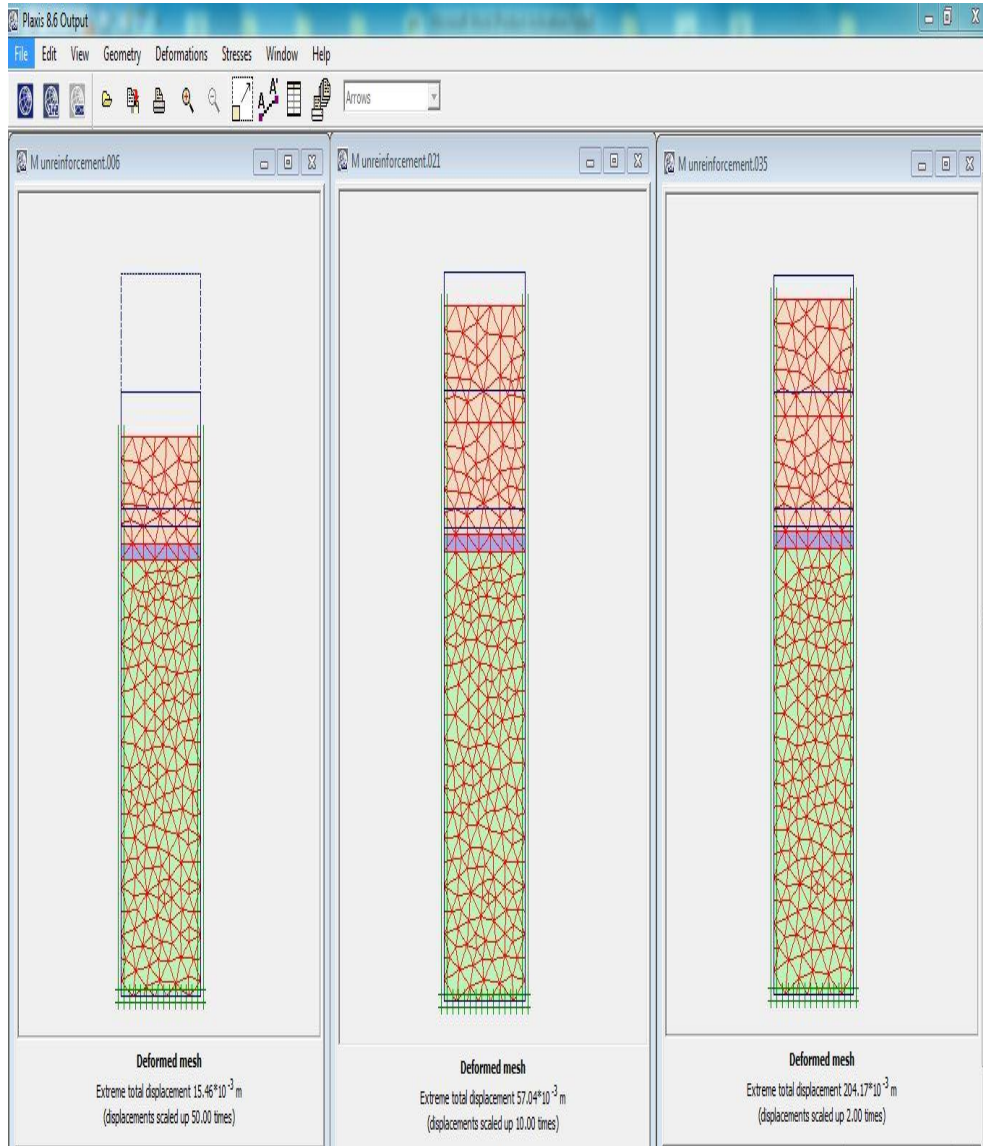


Figure 32: Mesh analyses for different steps of embankment construction
First stage, second stage, and consolidation end times

4.4 Analysis of Single Column as a Unit Cell

In this section, firstly, the influence of different types of material (stone, sand, gravel) in encapsulated column with geotextile was analyzed and then the effect of various diameters and spacing of stone columns were selected to study the behavior

of settlement, stress distribution, excess pore water pressures, and consolidation time in soil reinforced by columns under an embankment construction. From Table 9 can be seen the models studied to assess the performance of a single column.

Table 9: Various model analysis

Model name	Diameter of column (m)	D_e (width of unit cell)	Material type	Geotextile Stiffness (kN/m)	$M=(D_e/D)$
A	1	7	Stone Sand Gravel	400	-
B	0.5 0.85 1 1.2 1.5	6	stone	-	-
C	1	4 5 6	stone	-	M1=4 M2=5 M3=6

4.5 Analysis and Results

4.5.1 Group A: Different Column Materials

To compare the effect of different column materials in soft clay, three kinds of materials stone, sand and gravel were selected to evaluate the settlements with respect to time and depth. As shown in Figure 33, the effect of material in settlement versus time is evaluated. It is apparent in this figure that stone column has higher performance to reduce the amount of settlements compared to other materials. The unreinforced model has the maximum amount of settlement, which is 189 mm. Stone, sand, and gravel columns reduced this amount of settlement by 12.2%, 17.5%, 18.5% respectively. Because of the modulus of elasticity of stone and gravel being larger than sand, settlement reduction percentages of stone and gravel are approximately the same. Figure 34 shows the relationship between settlement and depth. From this data, we can see that, the maximum settlement occurred on ground surface and reduced gradually with depth to the extent that it becomes zero at depth of 8 m. According to Figure 35, the consolidation end time for untreated soil is 2145 days, while it decreased to 666 days in the presence of stone columns. Thus, stone columns have considerable effect on accelerating the consolidation time. Finally, it was decided that the stone material for this investigation is the best for columns to stabilize the soft clay under an embankment construction.

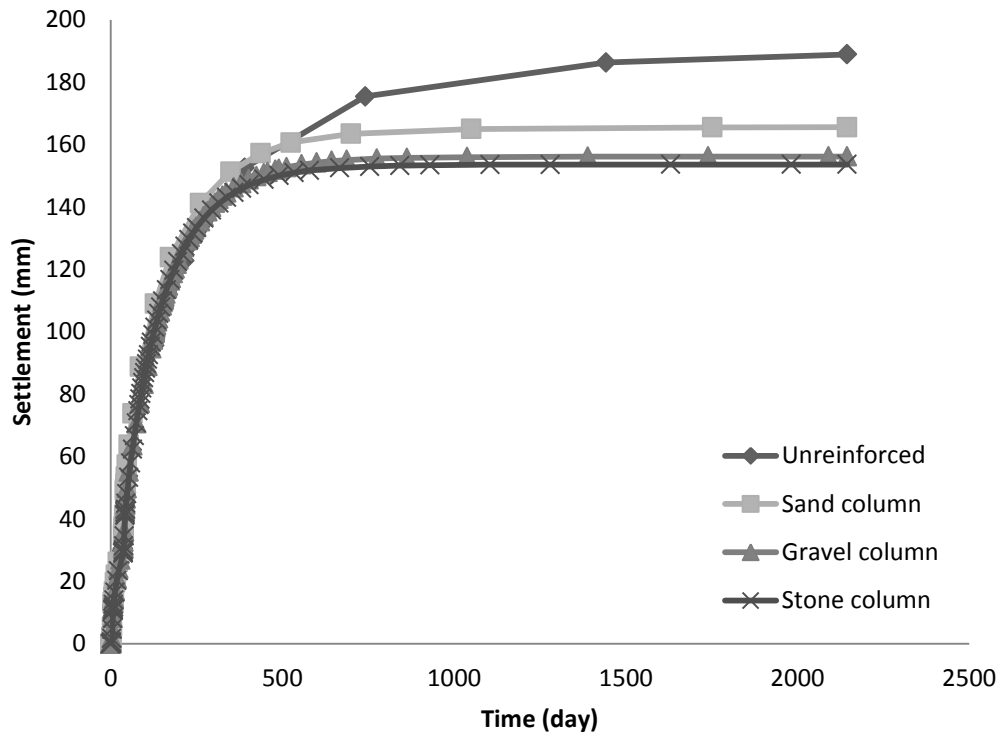


Figure 33: Influence of different materials of column on the settlement versus time

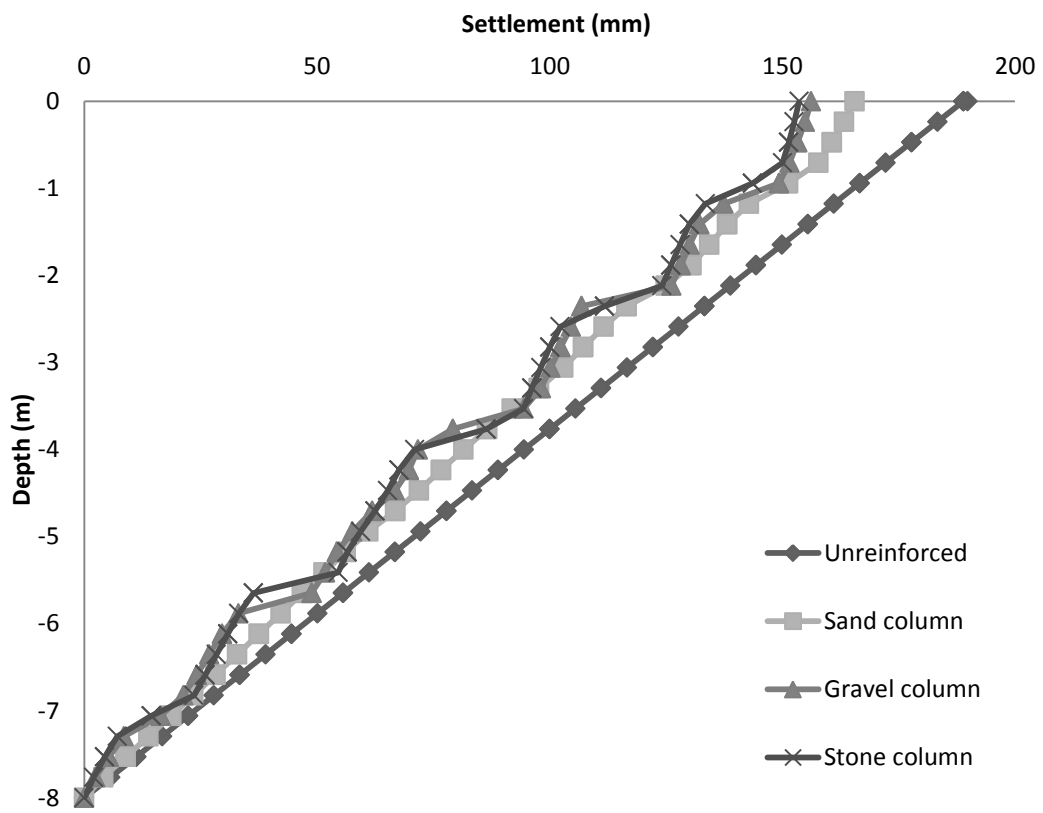


Figure 34: Influence of different materials of column on the settlement versus depth

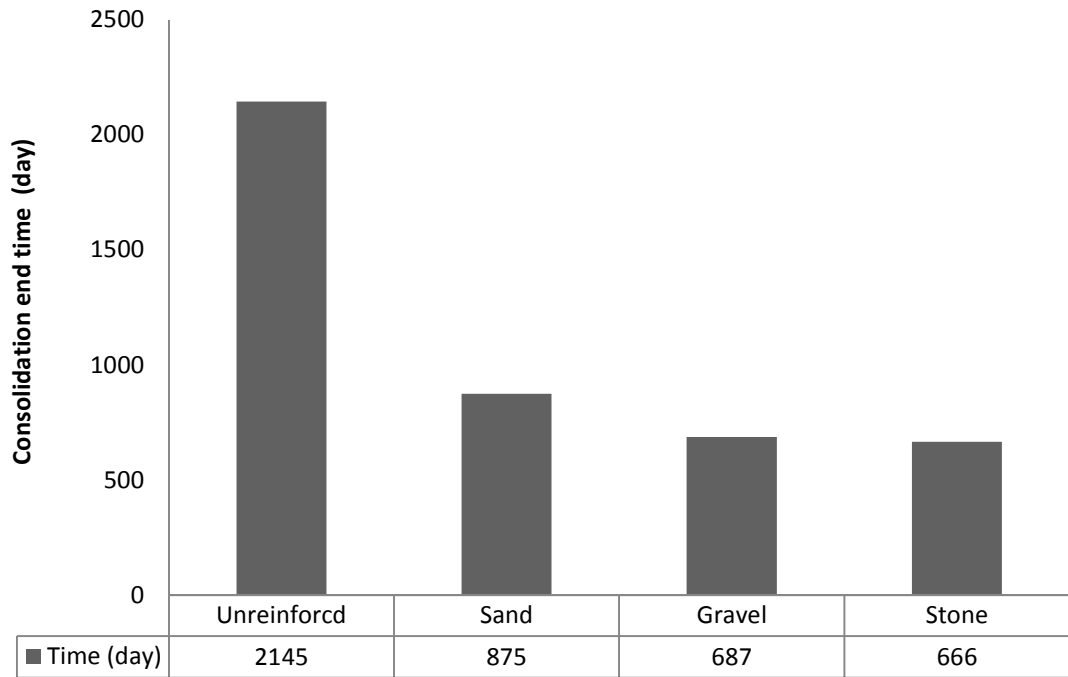


Figure 35: Influence of different materials of column on the consolidation end times

4.5.2 Group B: Different Column Diameters

In order to assess settlement, excess pore water pressure, consolidation time, and stresses in soil, different diameters of stone column (0.5, 0.85, 1, 1.2, 1.5 m) were used. For the purpose of settlement analysis, relationship between settlement versus time, settlement in various depths, maximum settlement versus area ratio, settlement analysis in different periods of time, settlement with respect to distance from embankment centerline, and improvement factor versus area ratio were studied.

4.5.2.1 Consolidation End Times Analysis with Respect to Time

As can be seen from Figure 36, the stone column with a diameter of 1.5 m speeds up the consolidation time compared to untreated condition, from 1844 days to 423 days. Thus, among various diameters of stone columns, the stone column with larger diameter has significantly influenced the dissipation of excess pore water pressure and reduced the consolidation time.

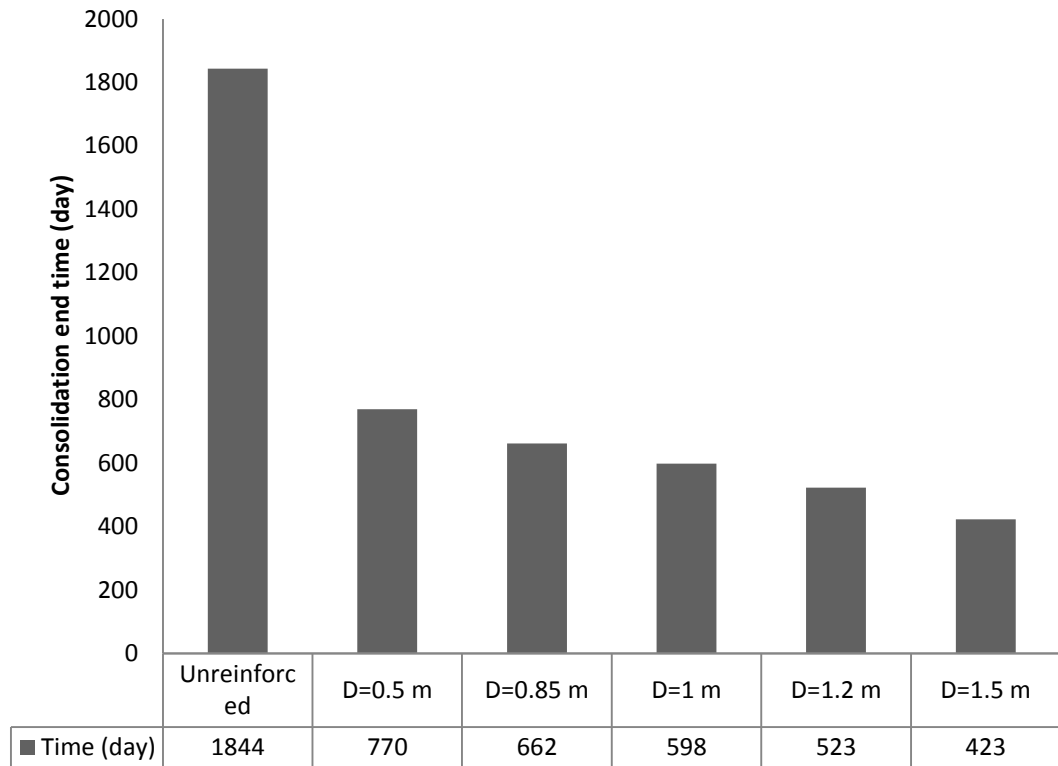


Figure 36: Effect of various diameters of column on the consolidation end times

4.5.2.2 Settlement Analysis with Respect to Time

The settlement analysis for untreated and treated soils by the use of stone columns with different diameters was done in a period of 1844 days. The results obtained from Figure 37 indicates that, maximum settlement belongs to untreated part, which is 188 mm and this amount decreased by increasing column diameters. The settlement of column with 1.5 m diameter is observed to decrease by 36%. Therefore, by increasing the column diameters, the bearing capacity and settlement characteristics of soil are enhanced.

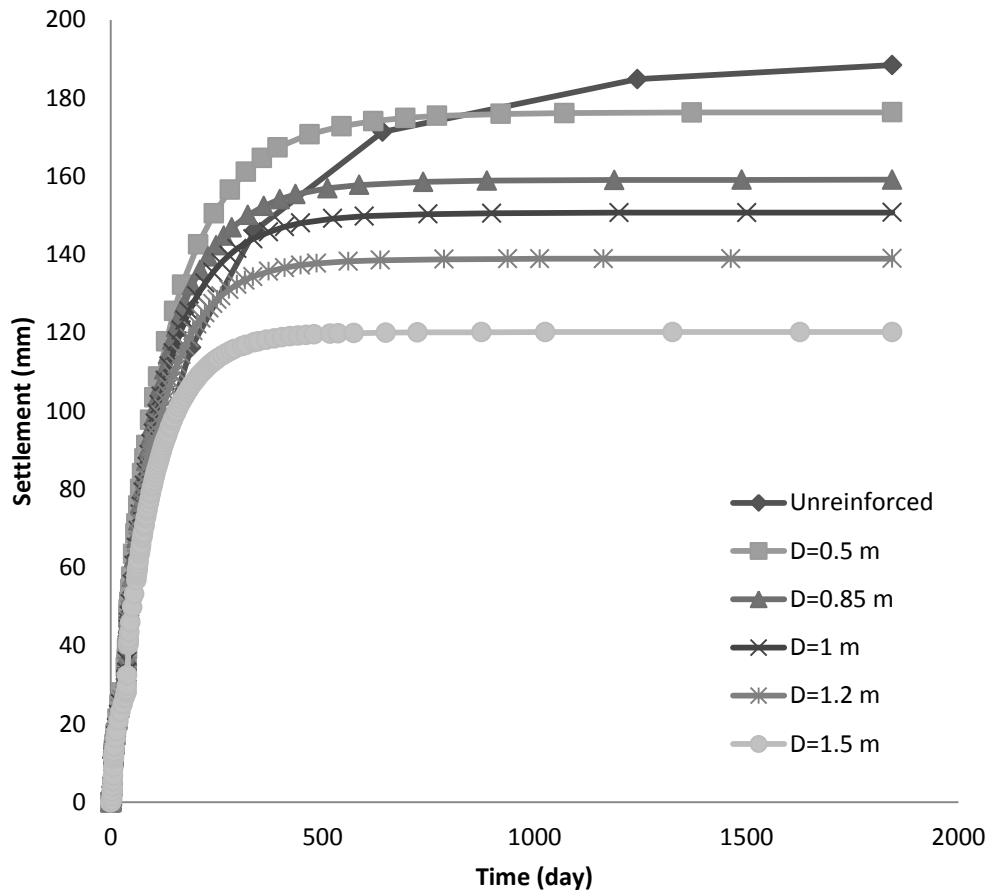


Figure 37: Effect of various diameters of column on settlement versus time

4.5.2.3 Settlement Analysis versus Depth

As it illustrates in Figures 38 there is reduction for settlement as the depth decreases. The maximum settlement occurs at ground level and reduces by decreasing depth and increasing column diameter. The biggest reduction in settlement can be seen in the upper layer, especially at ground surface, whereas, at lower depths, there is no significant difference in settlement between treated and untreated soil.

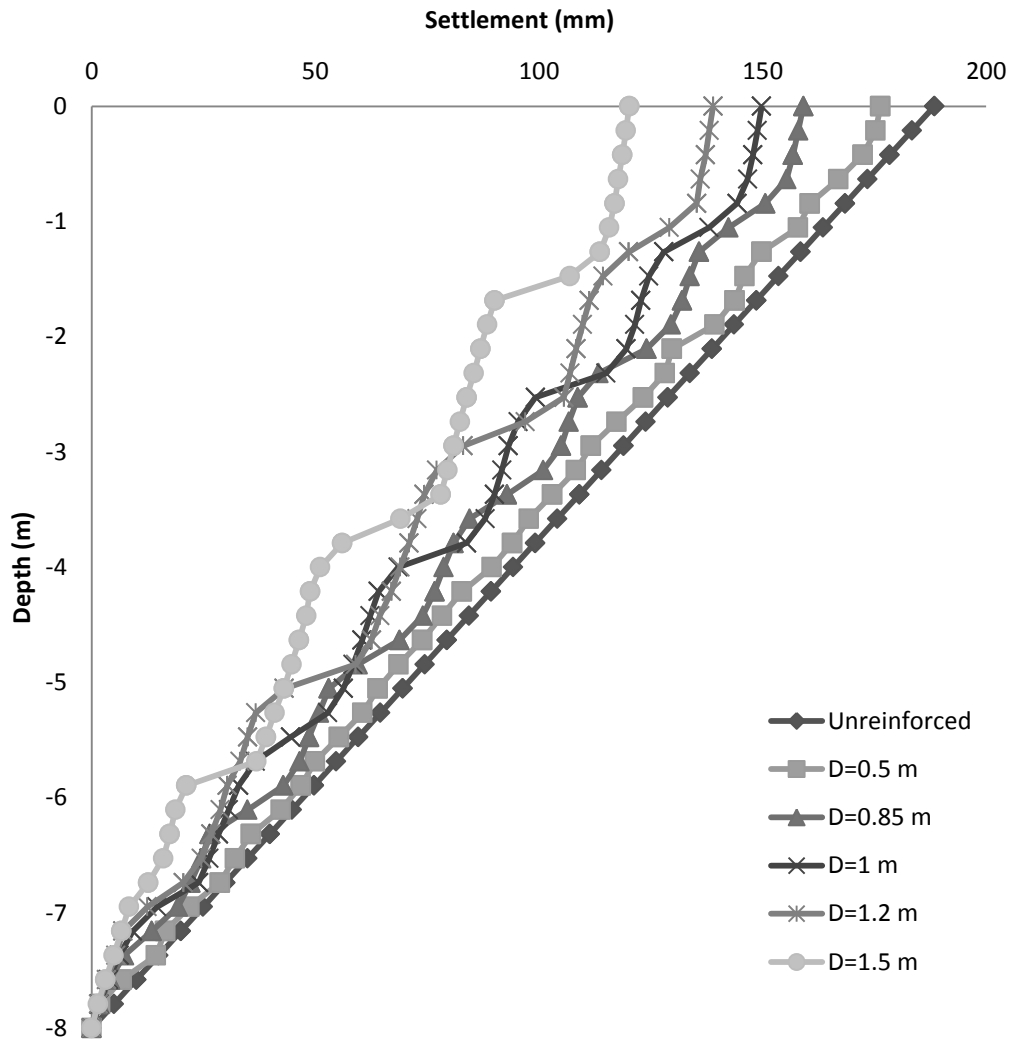


Figure 38: Effect of various diameters of column on settlement versus depth

4.5.2.4 Settlement versus Time

In order to understand the effect of time on stone column performance in soft soils under an embankment, the settlement analysis at different time intervals has been carried out at the first stage of embankment construction, second stage of embankment construction, 2 year after second stage of construction, and at the end of consolidation time. The analysis compared untreated part and treated part by stone column with 1.5 m diameter that has given the best performance. It can be seen that in Figures 39 and 40 that in the first and second construction stages of the embankment, no significant reduction in settlement was observed with neither treated nor untreated condition, due to remaining excess pore water pressures in the system. However, this difference can be seen clearly in a larger amount after 2 years of second stage of embankment construction as shown in Figure 41. In addition, the amount of settlements in unreinforced part increased by increasing time until it becomes constant at 1844 days (approximately 5 years) while in the treated part with 1.5 m stone column diameter after 423 days the amount of settlement changes into a constant value of 120 mm. Finally, an obvious benefit of reduction in settlement between treated and untreated soil can be seen at the end of consolidation with 37% reduced settlement is shown in Figure 42.

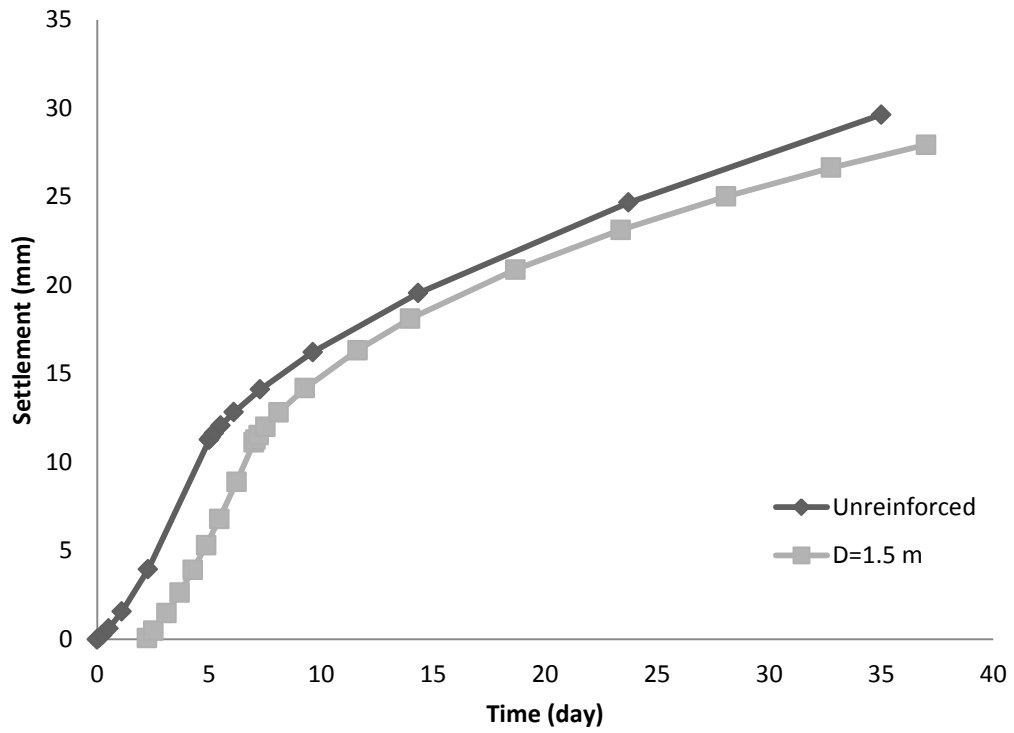


Figure 39: Analysis of settlement with respect to time after the first construction stage

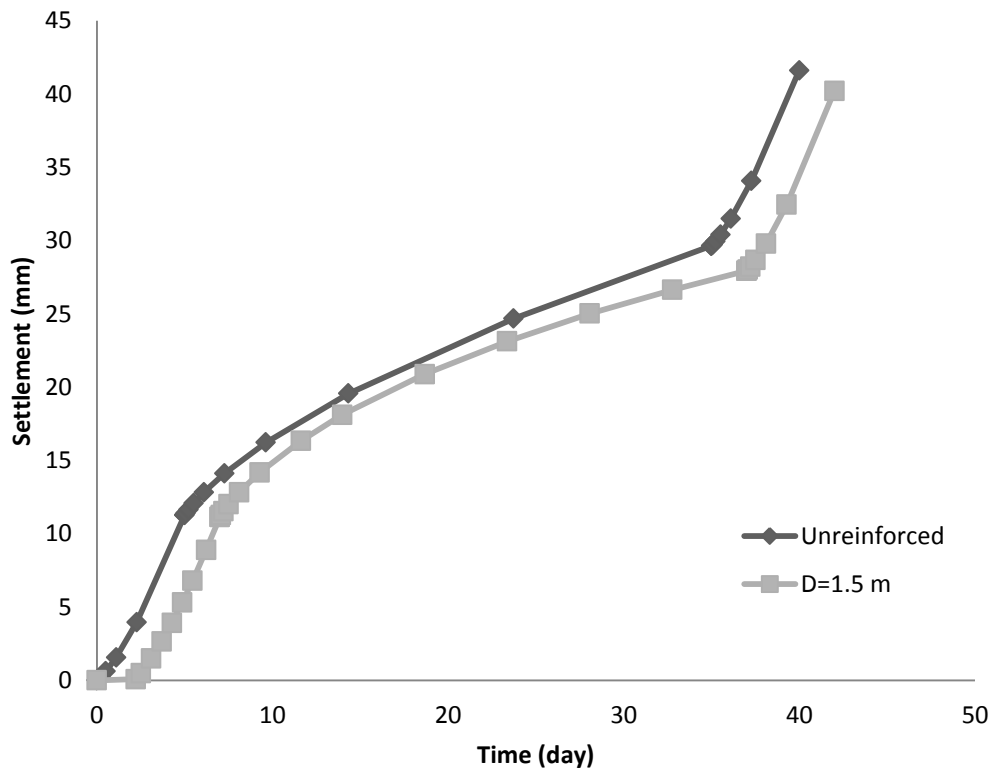


Figure 40: Analysis of settlement with respect to time after the second construction stage

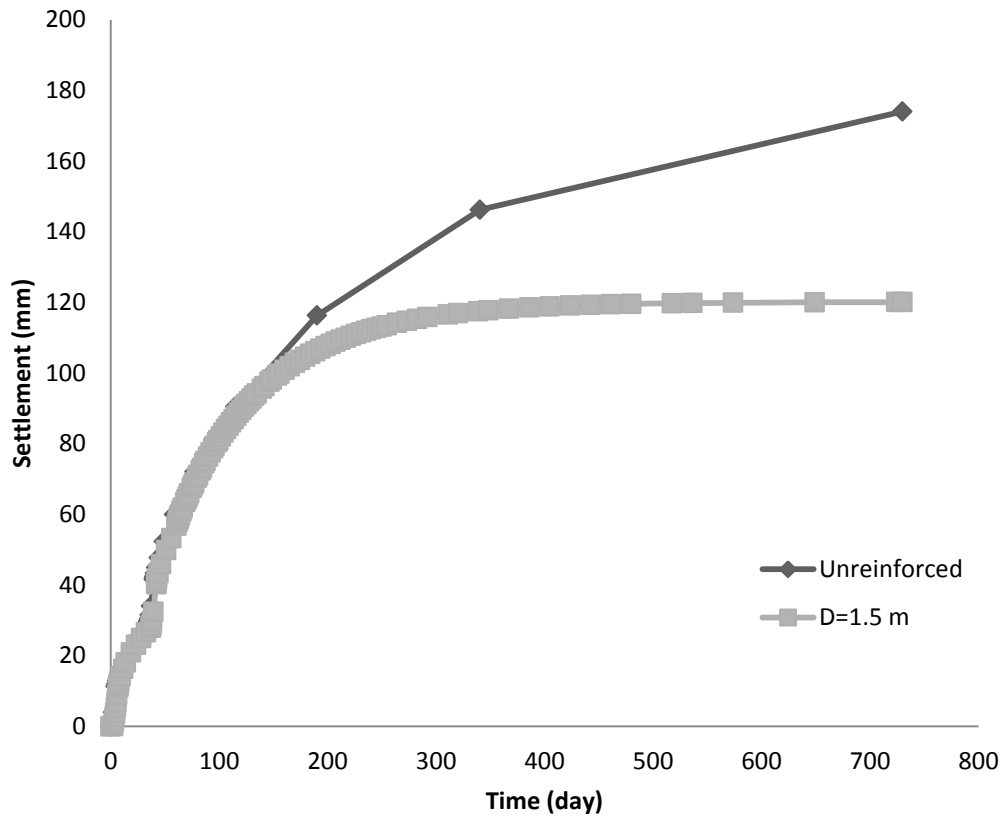


Figure 41: Analysis of settlement with respect to time after 2 years

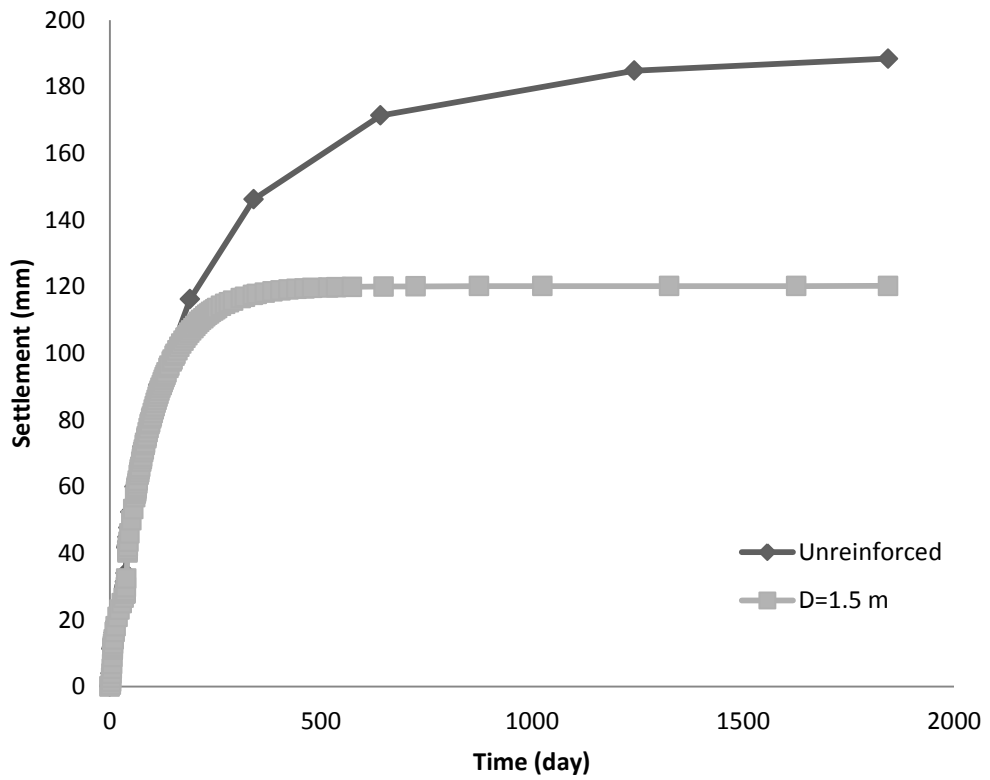


Figure 42: Analysis of settlement with respect to time after the consolidation end time

4.5.2.5 Maximum Vertical Settlement at a Distance from Column Centerline

Comparisons between the three condition (Unreinforced, D=0.5 m, D=1 m) were made using the analysis of the amount of vertical settlements with respect to distance from column centerline. Figure 43 provides relationship between the vertical settlement at the surface of soil and distance from column centerline. From this data, we can see that in unreinforced position, the amount of settlements in soil is constant. By using stone column due to larger stress confining around stone column, the amount of vertical settlements increased in stone column, then suddenly decreased by increasing distance from column, and afterwards remained constant in surrounding soil. Furthermore, by increasing the diameter of stone column the amount of settlements increased. Therefore, higher differential settlements occur when column diameter becomes larger.

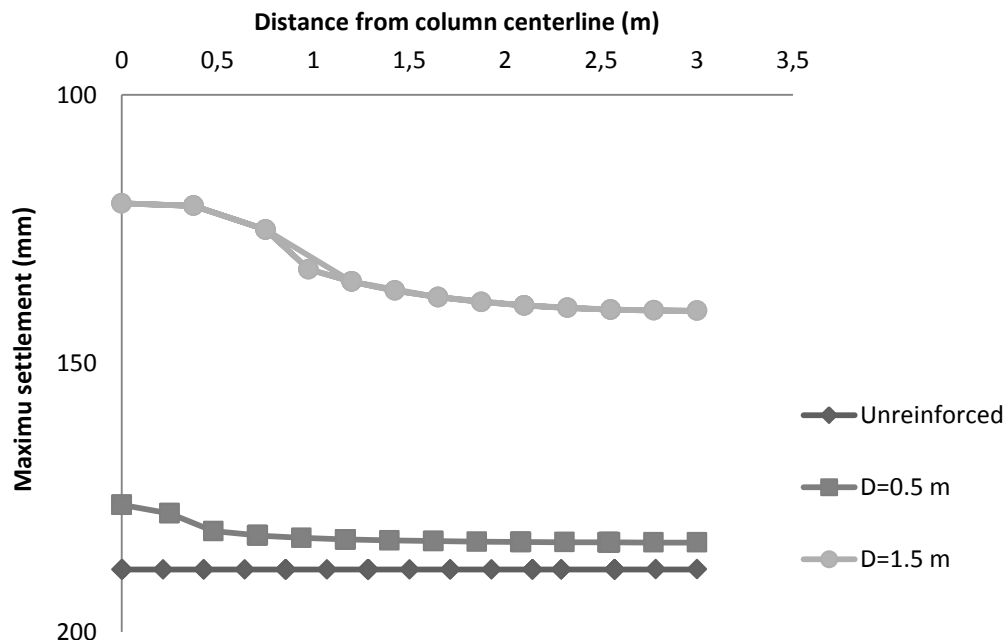


Figure 43: Effect of various diameters of column on vertical settlements from column centerline

4.5.2.6 Study of Settlement by Area Ratio and Improvement Factor

To distinguish the relationships among settlement, area ratio, and improvement factor, which is the fraction of untreated settlement over treated. Different diameters of stone columns were used. As can be seen from the Figure 44, by increasing the area ratio the maximum settlement reduced and Figure 45 shows that by increasing the area ratio the improvement factor increased.

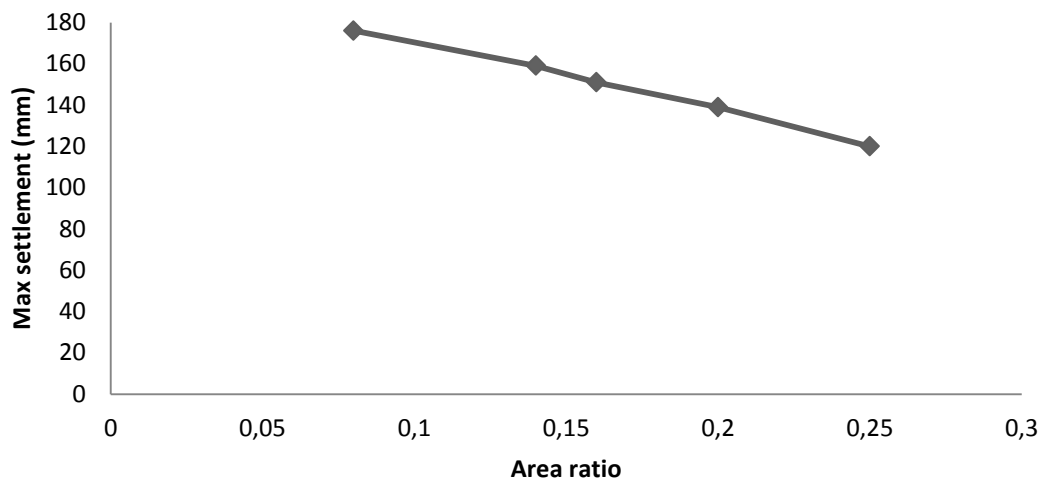


Figure 44: Maximum settlement versus area ratio

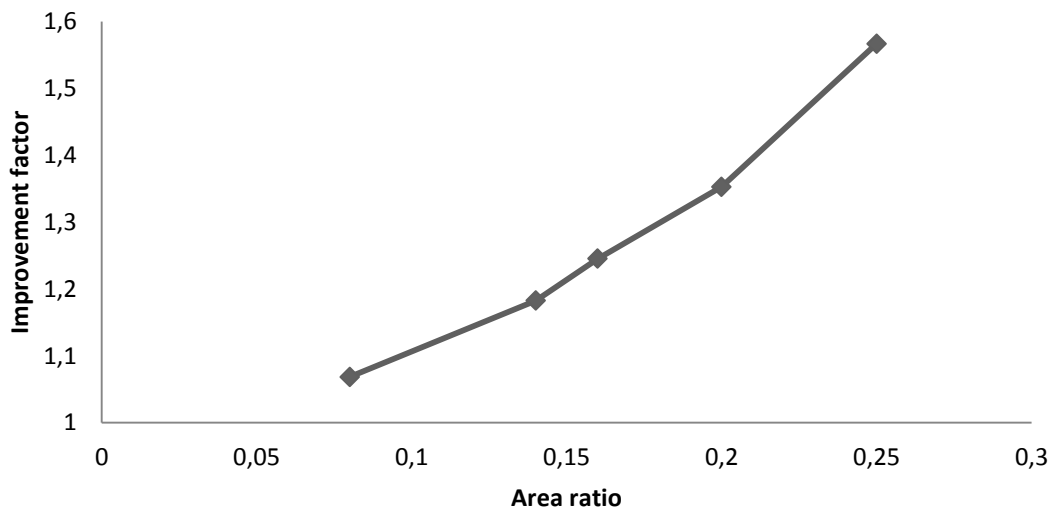


Figure 45: Improvement factor versus area ratio

4.5.2.7 Excess Pore Water Pressure with respect to Time

In this section, effect of different diameters of columns on excess pore water pressure 4 m beneath the ground surface at point B was studied. When the untreated part is improved by stone column drainage system is aggravated by adding lateral drainage to the vertical as shown in Figure 46. Figures 47-50 compare numerical data in treated and untreated soil using various stone column diameters. From this data, can be seen that the amount of excess pore water pressure arrived at the maximum amount after completion of each step of embankment construction which decreased progressively with time until becomes zero at consolidation end time. Thus, among various diameters, the column with larger diameter speeds up the consolidation time.

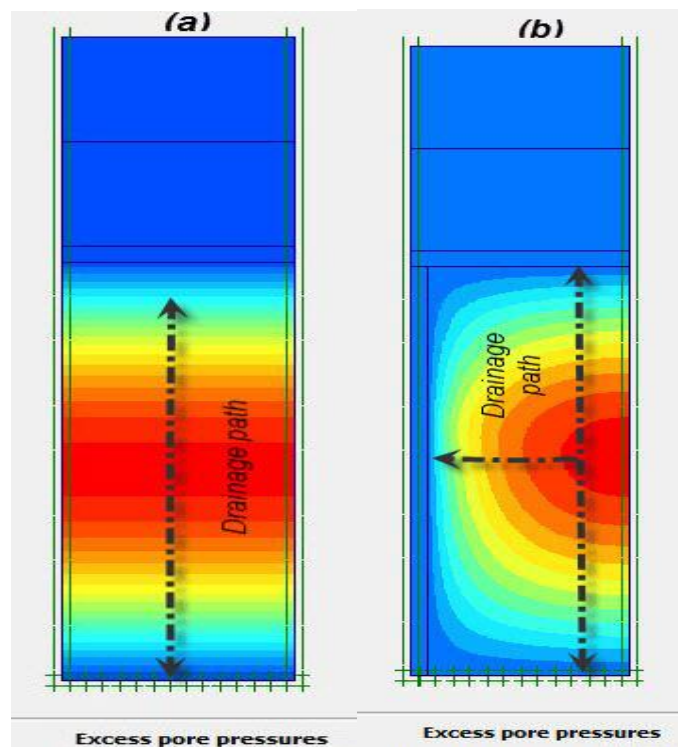


Figure 46: Dissipation of excess pore water pressure of (a) unreinforced and (b) reinforced unit cell

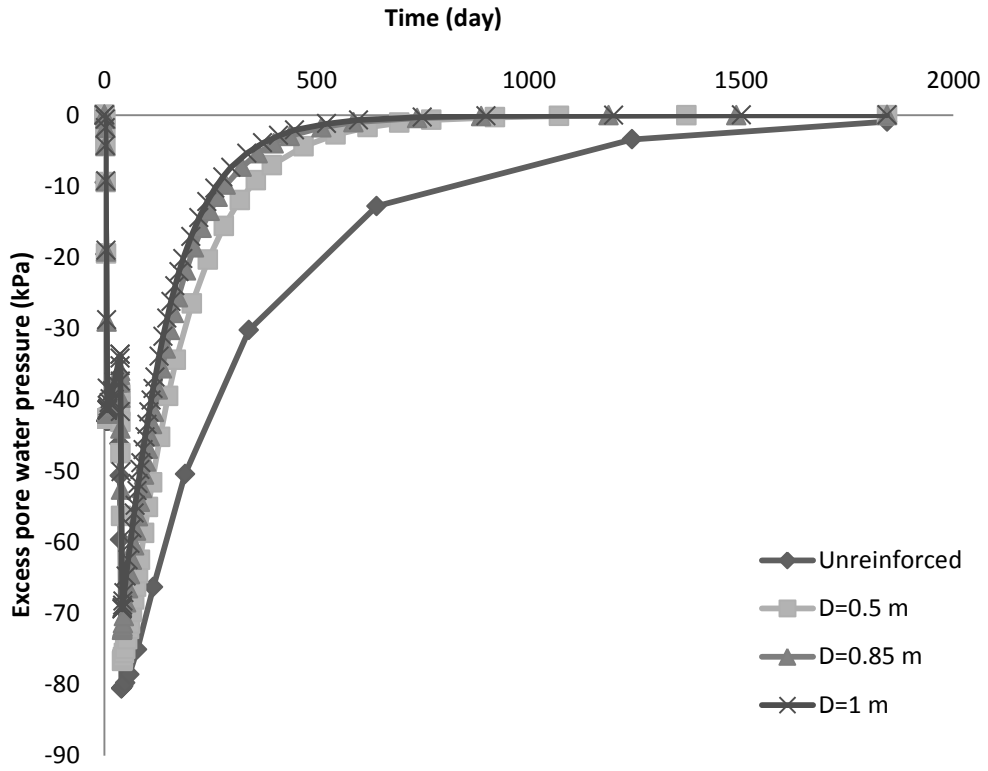


Figure 47: Effect of various diameters of column on Excess pore water pressure versus time for D=0.5, D=0.85, D=1

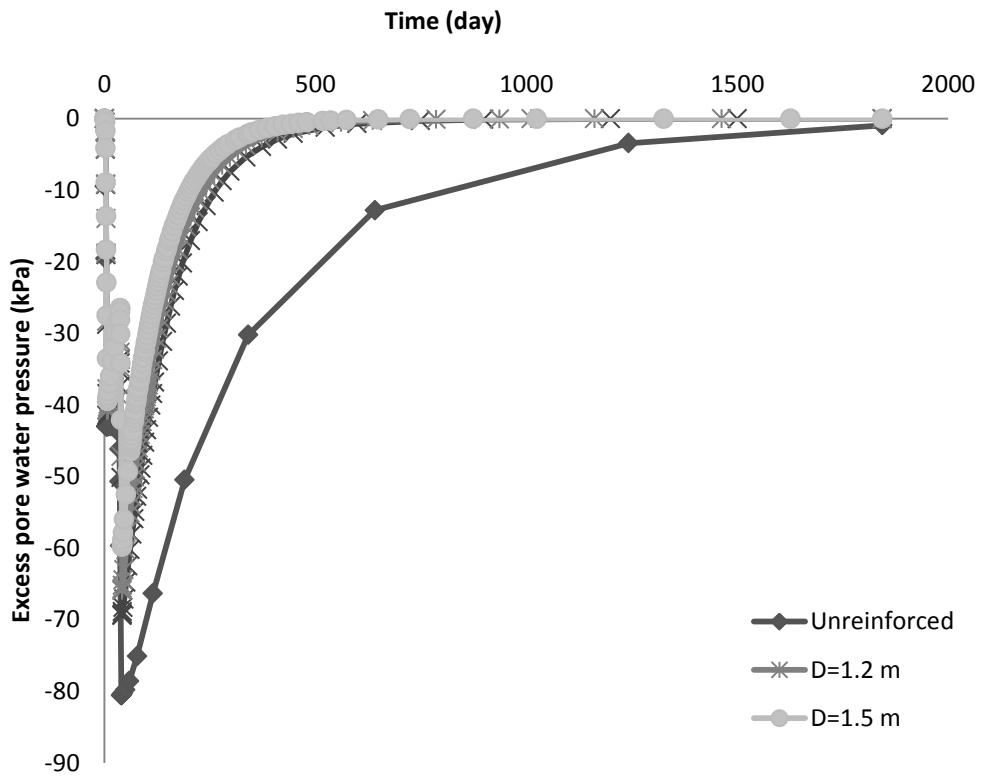


Figure 48: Effect of various diameters of column on Excess pore water pressure versus time for D=1.2, D=1.5

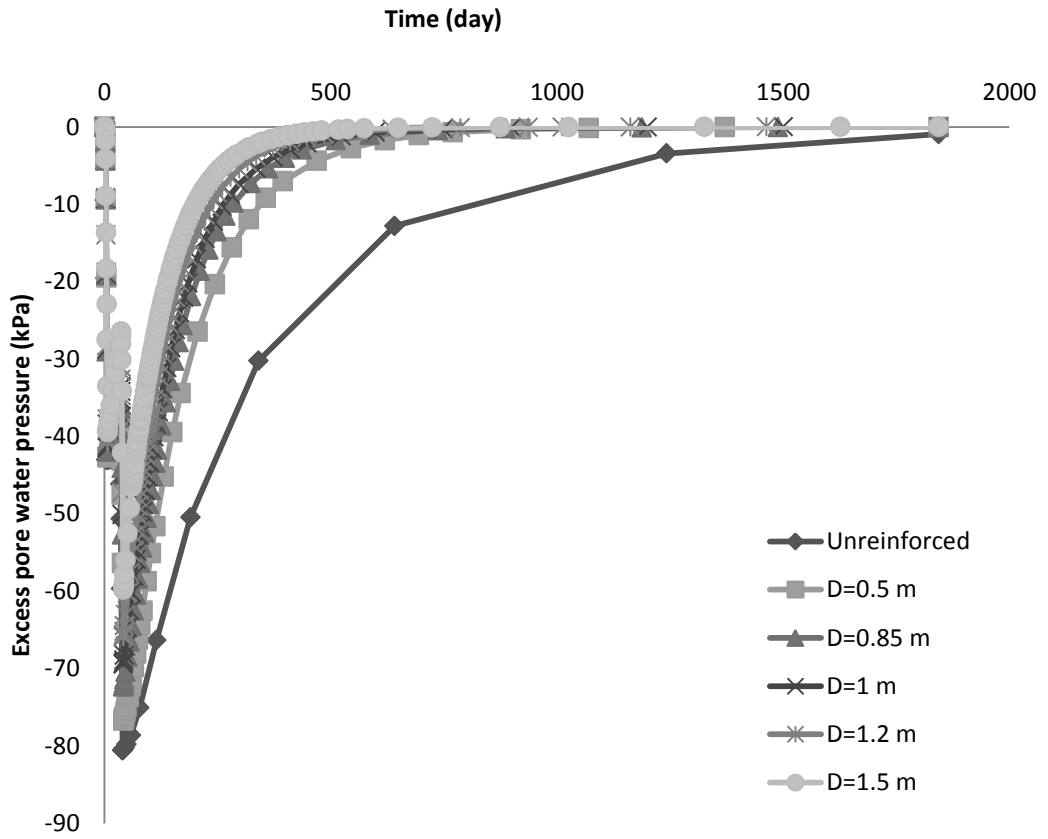


Figure 49: Effect of various diameters of column on Excess pore water pressure versus time

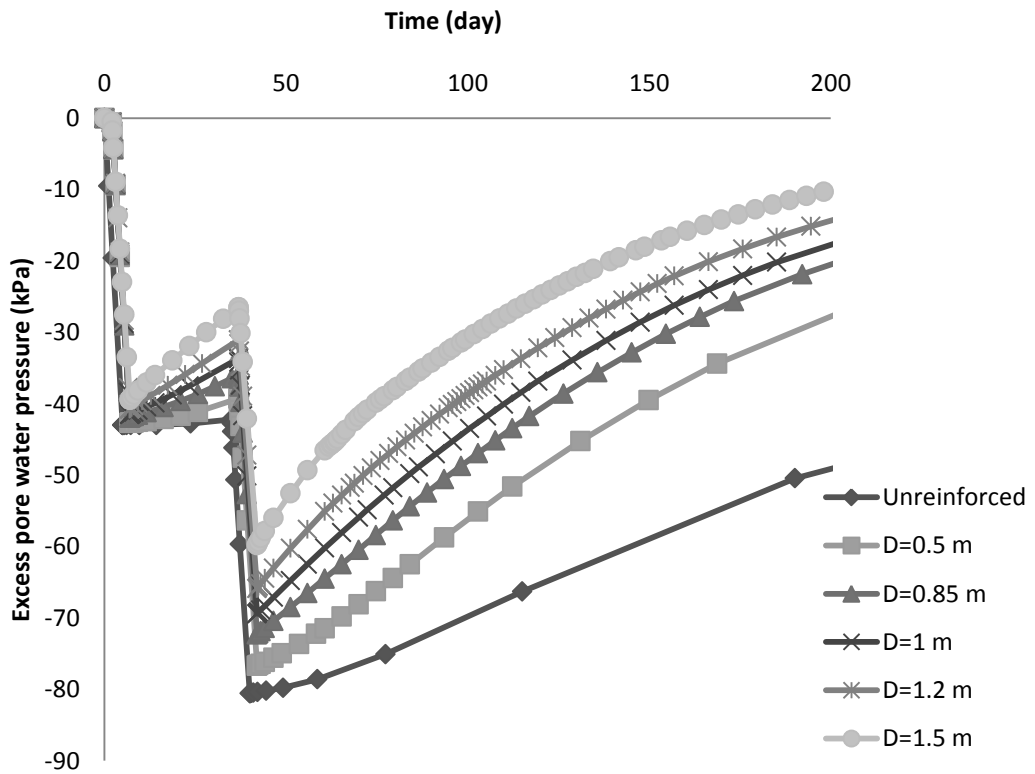


Figure 50: Effect of various diameters of column on excess pore water pressure versus time for first and second stages of construction

4.5.2.8 Stress Analysis

Two types of relationships, effective vertical stress versus time and stress versus distance from column centerline are designed to assess the stress conception in stone column and surrounding soil. For the evaluation of stress in stone column, point D at the top of the stone column and for evaluating of stress in soil point E at the top in the middle of surface of soil has been provided. The result obtained from vertical effective stress versus time is presented in Figure 51 and Figure 52. It is obvious from a Figure 51 that, after installation of stone column, the stress concentration can be observed in stone column more than surrounding soil. In addition, in reinforce situation stress concentration in soil is slightly smaller than unreinforced condition. Effective vertical stress has moderated increase into construction stage of embankment and reached to maximum value in the end of the embankment construction, then remained constant.

Figure 52 shows the effect of stress versus distance from column centerline. There was a significant difference in stress concentration in untreated and treated for different diameter of stone columns. By increasing of stone column diameter, the amount of stress will be increased around stone column. The more surprising result is, due to greater stiffness of stone column rather than adjusting soil The distribution of stress will be higher in stone column compared with surrounding soil.

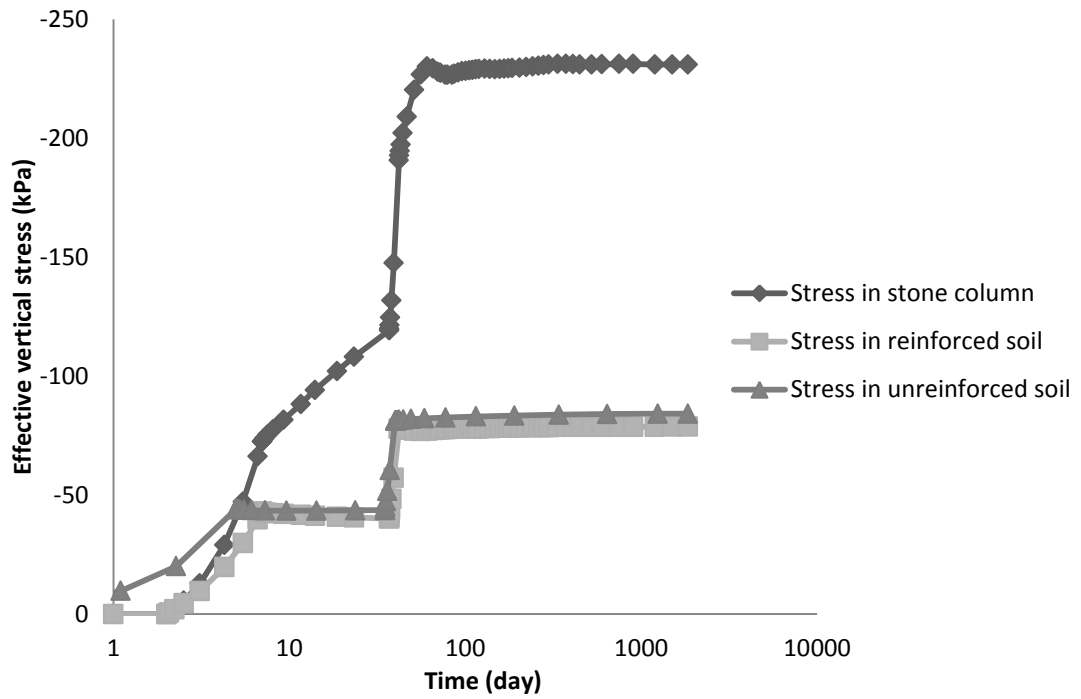


Figure 51: Effective vertical stress versus time at point D and E in reinforced compare to unreinforced

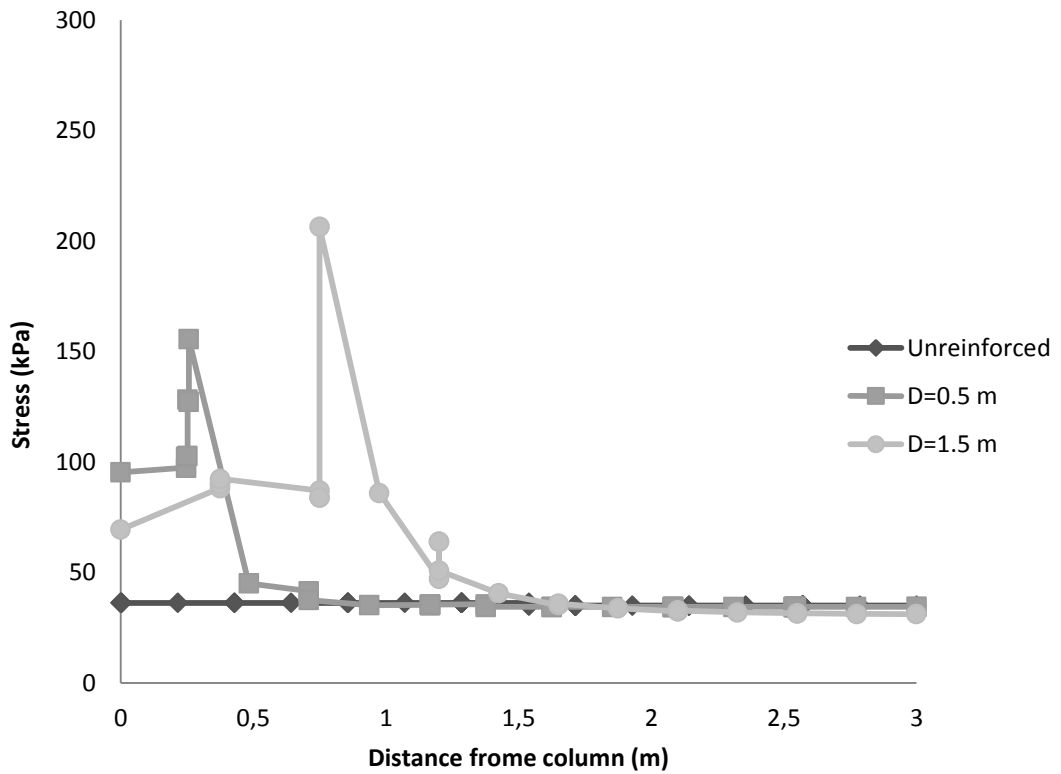


Figure 52: Stress versus distance from column centerline line

4.5.3 Group C: Different Column Spacing

For the estimation of settlement, excess pore water pressure, and consolidation end time in this section, different spacing of stone columns as a function of M ratio were prepared. Different value of d_e was prepared according to the procedure of unit cell in square pattern used by (Ballam & Booker, 1981). Thus, the different ratio of M ($M_1=4$, $M_2=5$, $M_3=6$) for stone column with 1 m diameter determined as follows:

$$M = d_e/D$$

where,

$$d_e = 1.13 S$$

D = Diameter of stone column

4.5.3.1 Consolidation End Time Analysis with Respect to Time

As can be seen from Figure 53, the stone column with the ratio of M_1 accelerates the consolidation time compared to unreinforced condition from 1844 days to 233 days. Therefore, among several different M ratios of stone columns, M_1 with smaller space has considerably an impact to dissipate the excess water pressure and reduce the consolidation time. It can be concluded that, by reducing the space of columns the amount of consolidation end time will be decreased significantly.

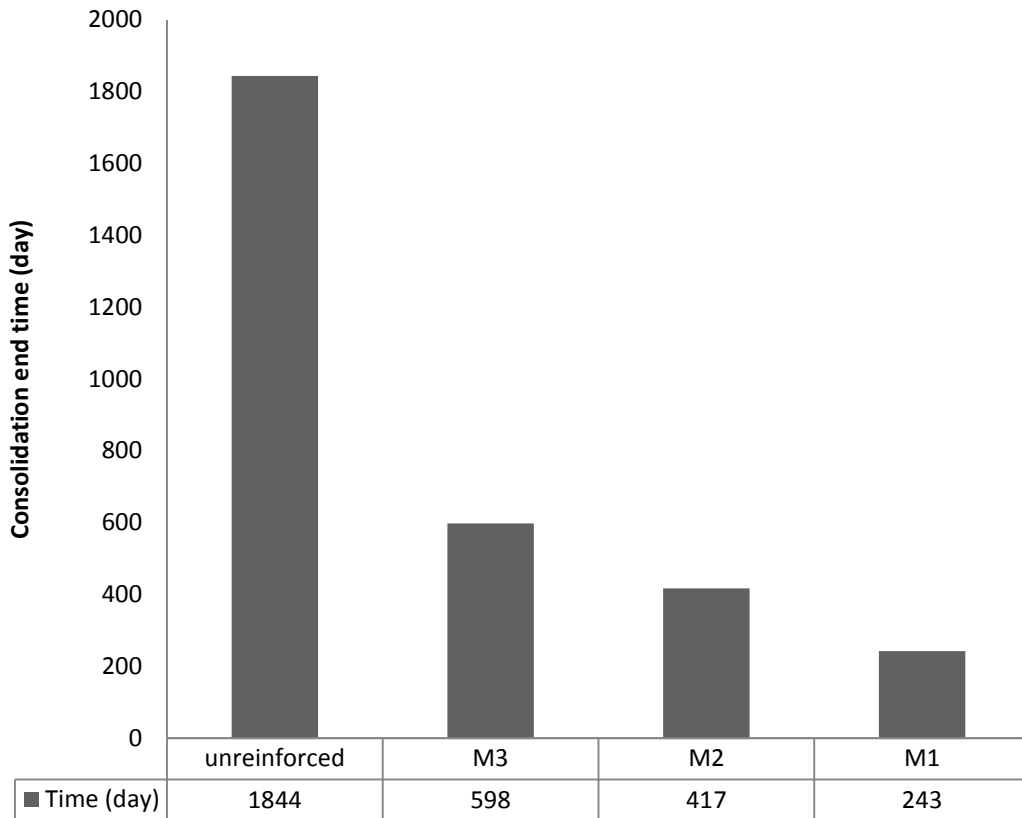


Figure 53: Effect of column spacing on the consolidation end times

4.5.3.2 Settlement Analysis versus Time

The settlement analysis for reinforced and unreinforced soil different ratios of M was assessed over a period of 1844 days. The results achieved in Figure 54 revealed that, maximum settlement occurred in unreinforced part, which is 188 mm and this amount decreased by reducing column spacing. The settlement of M1 was decreased by 32%. Consequently, by increasing the column spacing, settlement reduced.

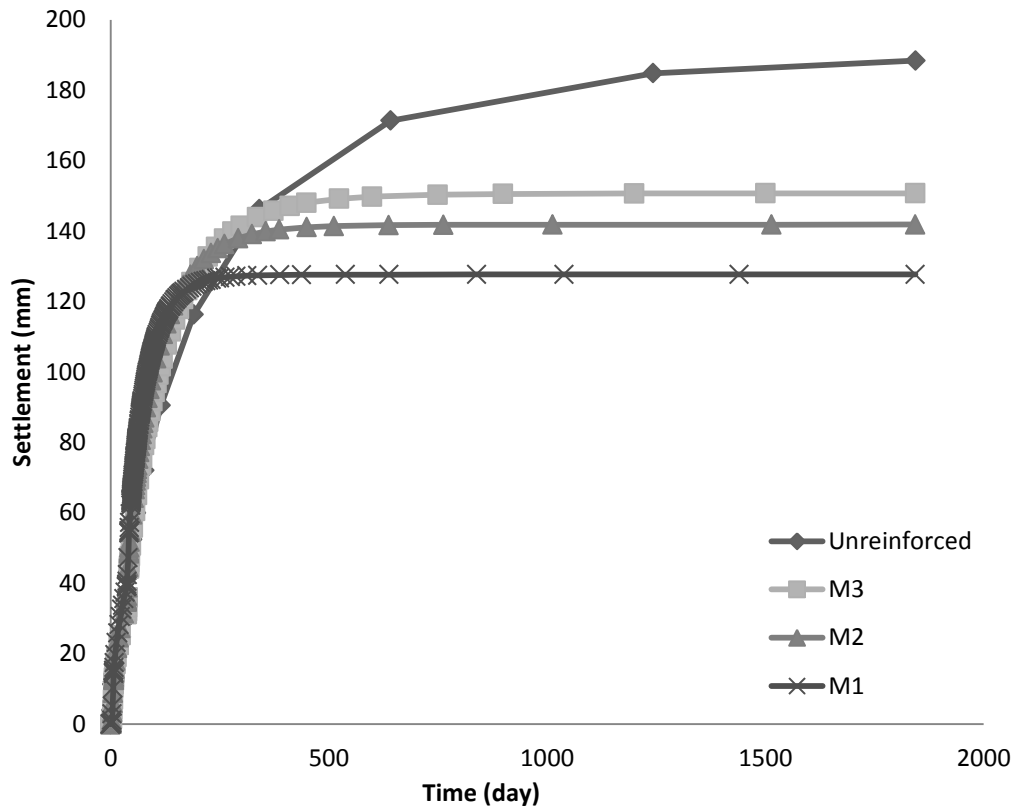


Figure 54: Effect of column spacing on settlement versus time

4.5.3.3 Excess Pore Water Pressure Analysis versus Time

The effect of different spacing of columns on excess pore water pressure, at point B at 4 m below ground surface was determined. Figure 55 compares numerical data both in reinforced with several stone column spacing and unreinforced condition. From this data, we can see that the quantity of excess water pressure accelerated by reducing the column spacing. Therefore, M1 has best performance in reducing the consolidation time and settlement. In addition, it can be seen that in unreinforced condition, the excess water pressure dissipation time is longer, while this amount gradually decreased and becomes constant after consolidation end times in reinforced by stone column.

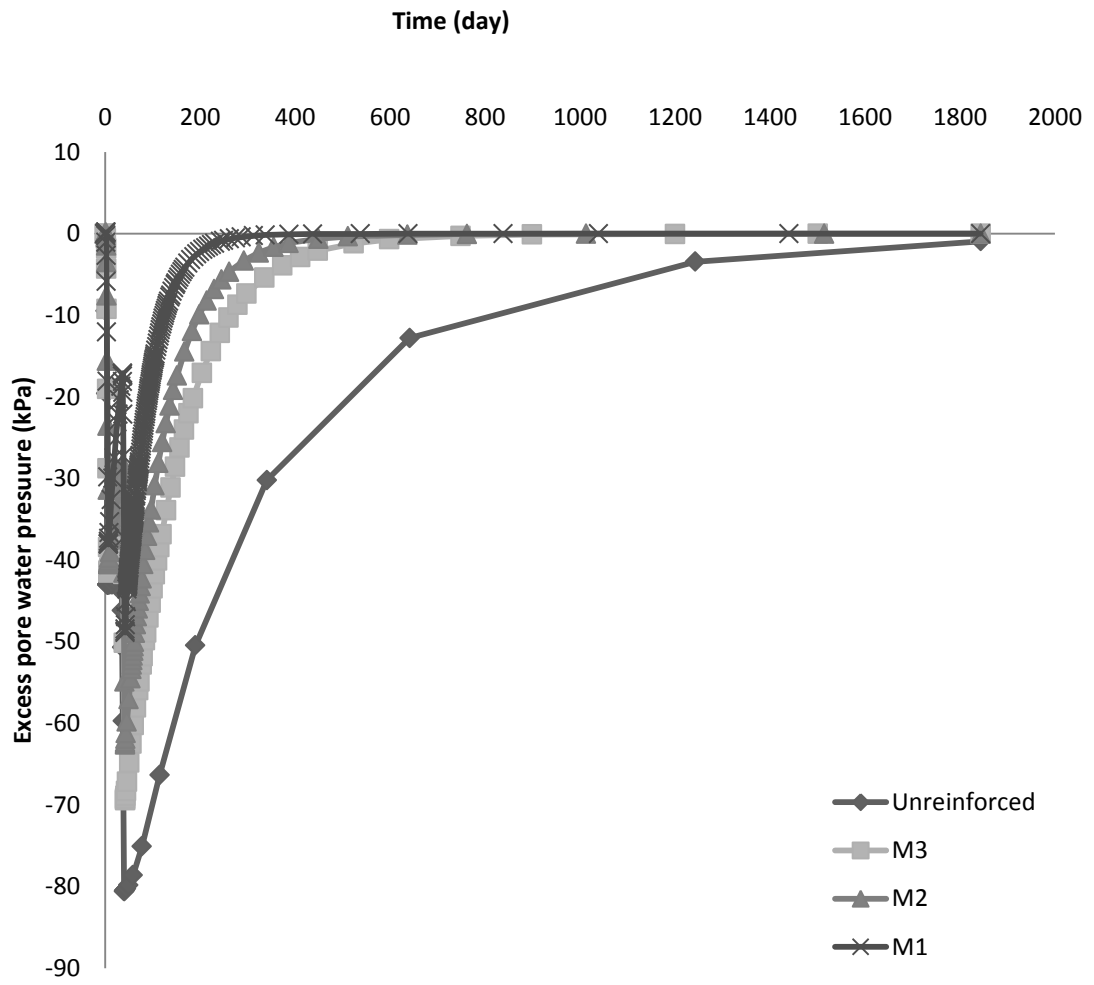


Figure 55: Effect of column spacing on excess pore water pressure versus time

Chapter 5

BULGING AND HOOP TENSION ANALYSES IN UNIT CELL IDEALIZATION

5.1 Introduction

Sand or stone columns are generally installed as conventional columns or encased columns. The behavior of both in soil is very important. Therefore, settlement, consolidation, bulging, bearing capacity, and hoop tension of geosynthetic materials used should be assessed. The geosynthetic materials such as geogrid or geotextile are very effective in providing better performance of columns in soil. In this Chapter, analysis and results of bulging, vertical settlement in ordinary sand columns and hoop tension in encased sand columns will be presented and discussed.

5.2 Column Bulging

When a load over an area equal or larger than the diameter of sand column fails it by causing a bulge along the length of column, it is called bulging failure. This type of failure depends on different parameters of columns like diameter, spacing of columns, and length, and may occur at different depths of columns. According to Mckelvey et al. (2004), bulging usually occurs in long sand columns. Figure 56 shows the bulging of sand columns after load application at mid and end of the loading time.

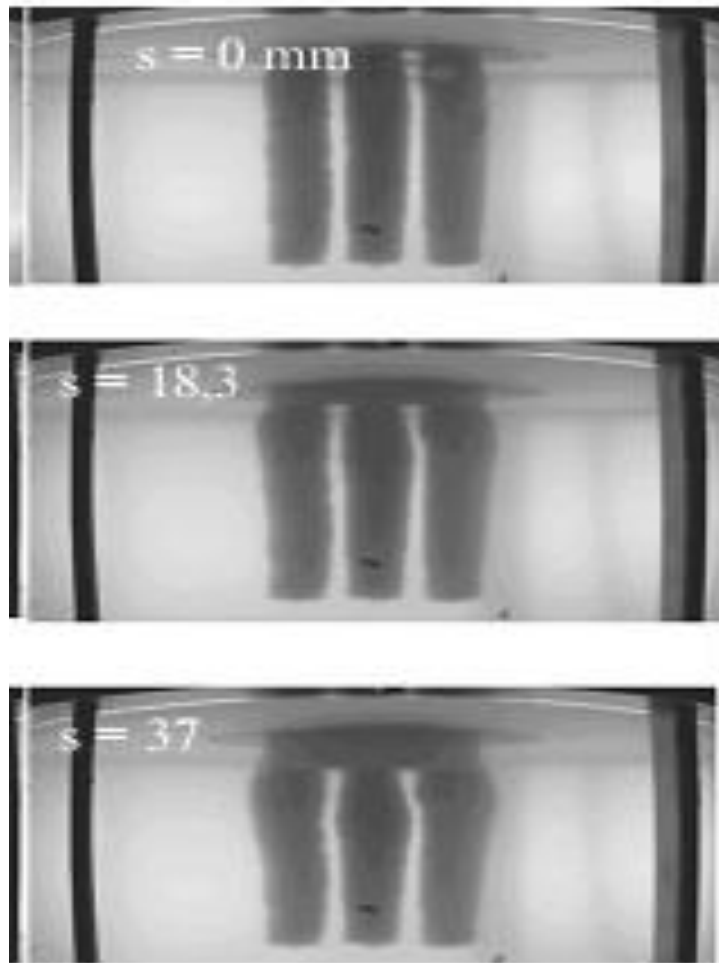


Figure 56: Bulging failure in sand columns in different steps of loading (Mckelvey et al, 2004)

The condition of applying a load on the column is very important to determine the stress, bulging and bearing capacity of the column. Subsequently, the load with area greater than the stone column diameter increases the bearing capacity and vertical and horizontal stresses and decreases the magnitude of bulging. Figure 57 illustrates the various types of loading.

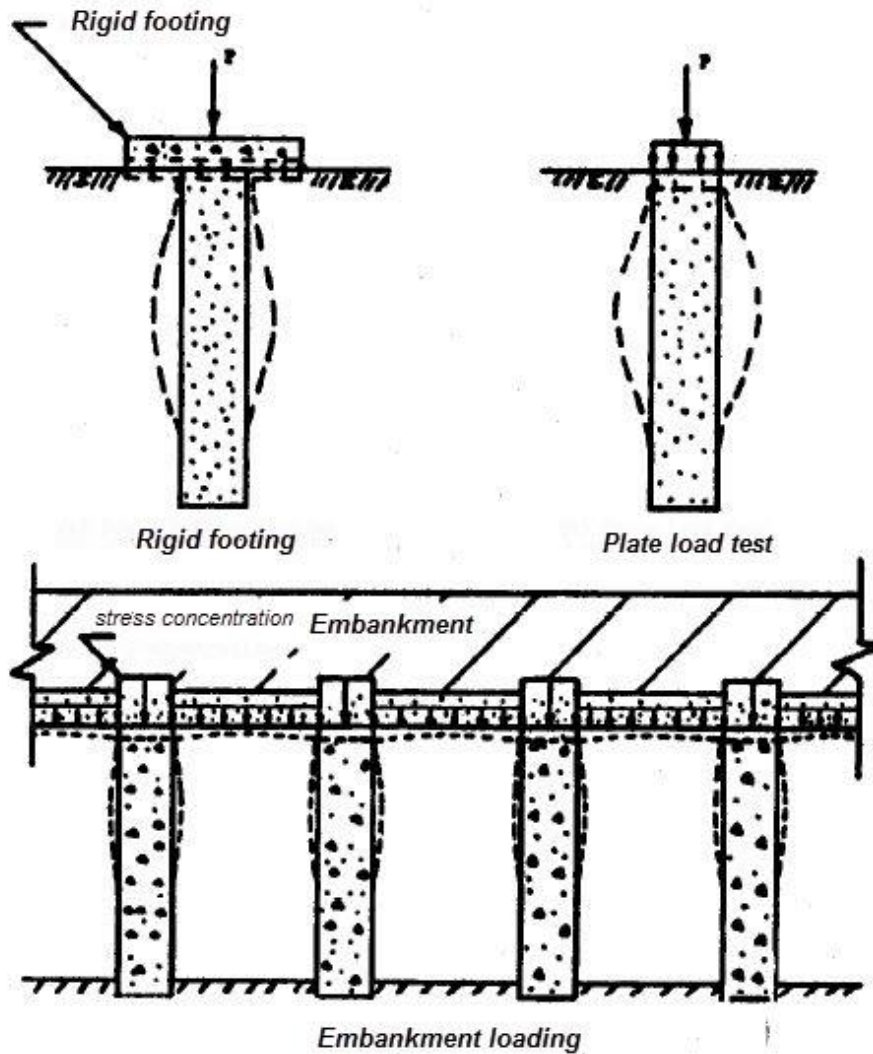


Figure 57: Bulging under various types of loading (Barksdale & Bachus, 1983).

5.3 Hoop Tension Force

Figure 58 depicts the formation of radial stress in stone column as a function of radial stress in surrounding soil and hoop tension of geosynthetic material.

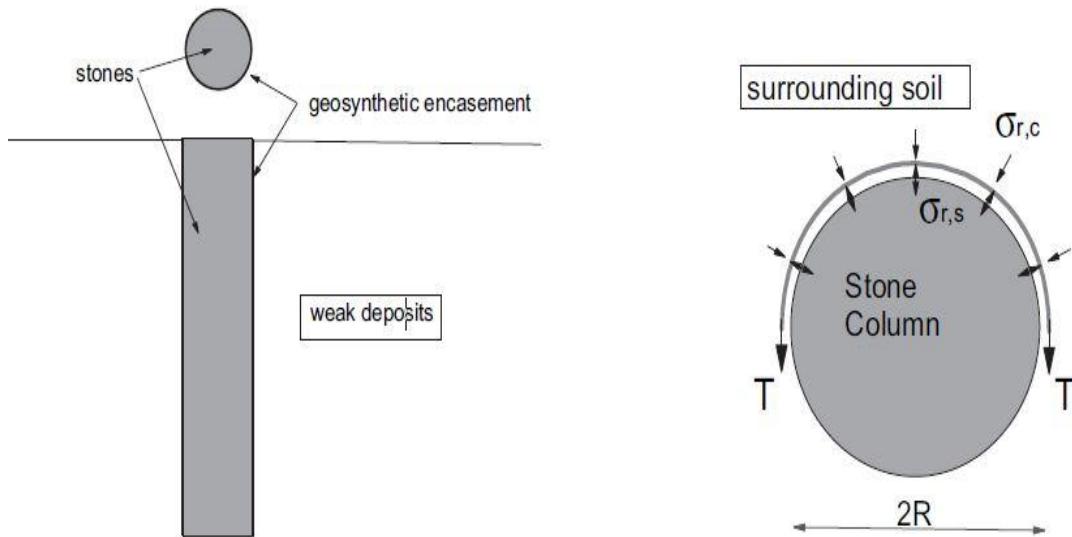


Figure 58: Hoop tension force around column

$$\sigma_{r,s} = \sigma_{r,c} + T/R \quad (25)$$

where;

T = Hoop tension of geosynthetic material

$\sigma_{r,c}$ = Stress in surrounding soil

$\sigma_{r,s}$ = Stress in stone column

R = Radius of stone column

5.4 Unit Cell Idealization of Sand Column in Different Models

In the present research, six models have been selected to study and characterize bulging, vertical settlement, and hoop tension. The different models studied are defined in Table 10.

Table 10: Various models of analysis

Model Name	Diameter of Sand Column (m)	Load Applied (kPa)	Loading Area	Geotextile Stiffness kN/m	Parameters Studied
A	1	40 60 80 100	-	-	Bulging
B	1 1.2 1.5	80	-	-	Bulging Settlement
C	1	80	Rigid footing 1D 2D 3D	-	Bulging Stress
D	1	40	1D 2D 3D 4D	-	Bulging
E	1	80	-	100 200 300 400	Bulging Settlement Hoop tension
F	0.8 1 1.2 1.5	80	-	200	Hoop tension

5.5 In-situ Soil Parameters

Soil properties of Tuzla area (Borehole 21) are used in this study because of the critical condition of material, which belong to alluvial deposits of the delta of River Pedios (Kanlidere). Sand column material was taken from the study of Ambily and Gandhi (2007). The sand column soil is modeled as drained whereas the subsoil layer is modeled in undrained condition. Because of the symmetry of the model, the right part of the model only has been considered in this study. Properties of sand and clay bed and material models are given in Table 11.

Ringtrac® mark geotextile was chosen for sand column encasement, which is suitable for soft soils. This kind of geotextile is subjected to radial support, preventing sand columns from enlarging. Recently, in some projects Ringtrac® was applied as encasement material, in encased column to heighten an embankment structure in Netherlands, and the New Airbus in Germany utilized 60000 encased sand columns using various kinds of Ringtrac®. In this research, four types of geotextile with various tensile strengths have been selected from Huesker Company. Table 12 gives the tensile strengths of different types of geotextiles used in this study.

Table 11: Properties of Sand and clay bed

Parameter	Symbol	Sand Column	Clay bed
Material model	Type	Mohr-Coulomb	Mohr-Coulomb
Loading	Condition	Drained	Undrained
Wet unit weight (kN/m ³)	γ_{wet}	18	19
Horizontal Permeability (m/day)	k_h	1	$8.64 \cdot 10^{-5}$
Vertical Permeability (m/day)	k_v	0.5	$8.64 \cdot 10^{-5}$
Young's modulus (kN/m ³)	E	2000	1000
Poisson's ratio	ν	0.3	0.2925
Cohesion (kN/m ²)	c	0	12
Friction angle (°)	ϕ	30	0
Dilatancy angle (°)	ψ	4	0

Table 12: Material properties of geotextile

Type Geotextile	Tensile strength (kN/m)
Ringtrac® 100	100
Ringtrac® 200	200
Ringtrac® 300	300
Ringtrac® 400	400

5.6 Mesh Analyses

The Plaxis software version 8.6.0 was used for numerical analyses of sand columns. Very fine mesh analyses have been selected for total area and refined line mesh analyses has been chosen for sand column to study bulging better. Figure 59 shows the deformed mesh of 1.2 m diameter of sand column after finishing the analyses.

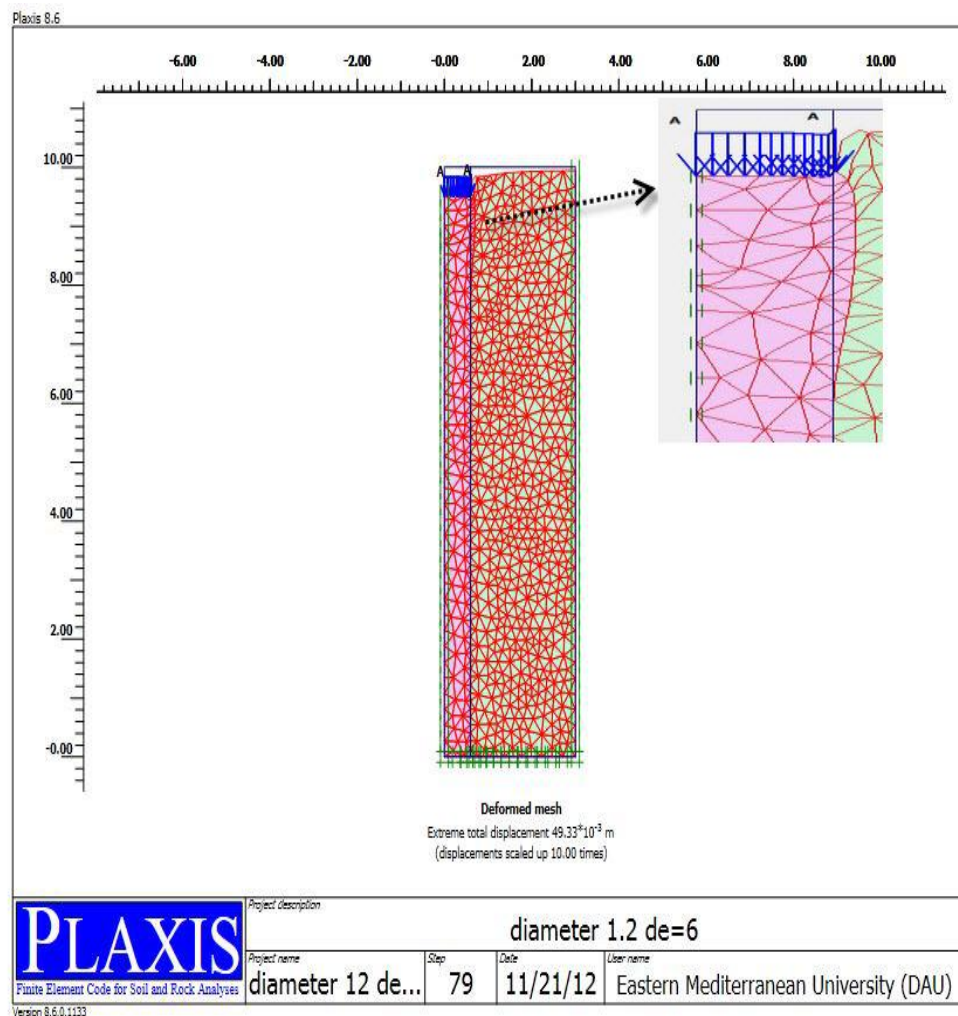


Figure 59: Fine mesh analysis

5.7 Results of Finite Element Analyses

5.7.1 Group A: Effect of Different Load Size on Bulging

Primarily, the sand column with a diameter of 1 m and different magnitudes of loading (40, 60, 80,100 kPa) was examined. Figure 60 shows the relationship between the amount of loading and bulging value along sand column length. As can be seen, at the same diameter of sand column, increasing the magnitude of load the value of bulging increased while the maximum bulging occurred at about the same depth of all sand columns. Therefore, it can be concluded that the spacing and the loaded areas are the important parameters influencing the depth of maximum bulging. In this study, the maximum bulging occurs at 1.06 times diameter of sand column. Bulging started from the top of the sand columns, increasing gradually and then reached to maximum value at a depth of 1.06 times the diameter of column. The bulging ceased approximately at a depth of 4D. As illustrated in Figure 60, the maximum bulging increased to 2.99, 5.60, 8.47, 14.23 mm under loads of 40, 60, 80, 100 kPa respectively.

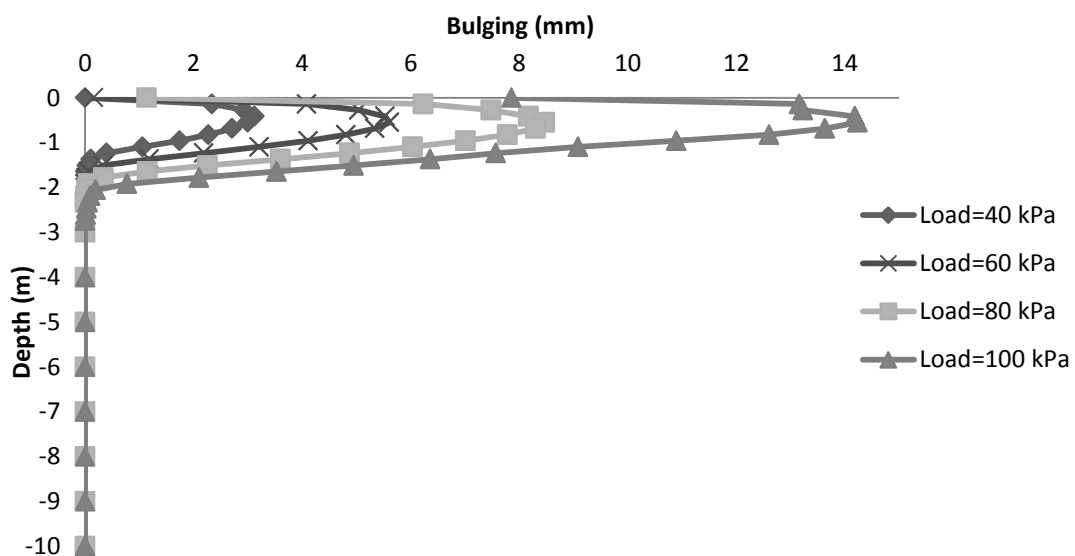


Figure 60: Bulging versus depth under different loads

5.7.2 Group B: Effect of Different Diameters of Sand Column on Bulging and Vertical Displacement

Sand columns of different diameters (1, 1.2, 1.5 m) under a given load were assumed. Figure 61 shows the effect of different diameters of sand column on bulging. It can be observed that keeping the load constant, the change of column diameter has influenced on bulging, By increasing the diameter of columns bulging increased and depth of the maximum bulging elevated from 1.06 to 1.3 D. Therefore, the maximum amount of bulging in column with a diameter of 1.5 m is 11.52 mm, and it is reduced by 26.47 % to 8.47 in column with 1m diameters. The maximum bulging occurred in column with 1.5 m diameter at a depth 1.5D, so, it has slightly increased in depth from 1.5 to 1.06 compared with the smaller diameter.

Vertical settlement between sand column and adjusting soil as a differential settlement above column were analyzed in Figure 62. The settlement amount in sand column is greater than surrounding soil due to load on the sand column. Diameter of columns has influence on amount of settlement, larger diameters having greater settlements than smaller diameters. It depicts in Figure 62 that, the settlement of sand columns increased from 41.32 to 53.3 mm from a column diameter of 1 to 1.5 m while this alteration is insignificant in surrounding soil from 3.24 to 8.9.

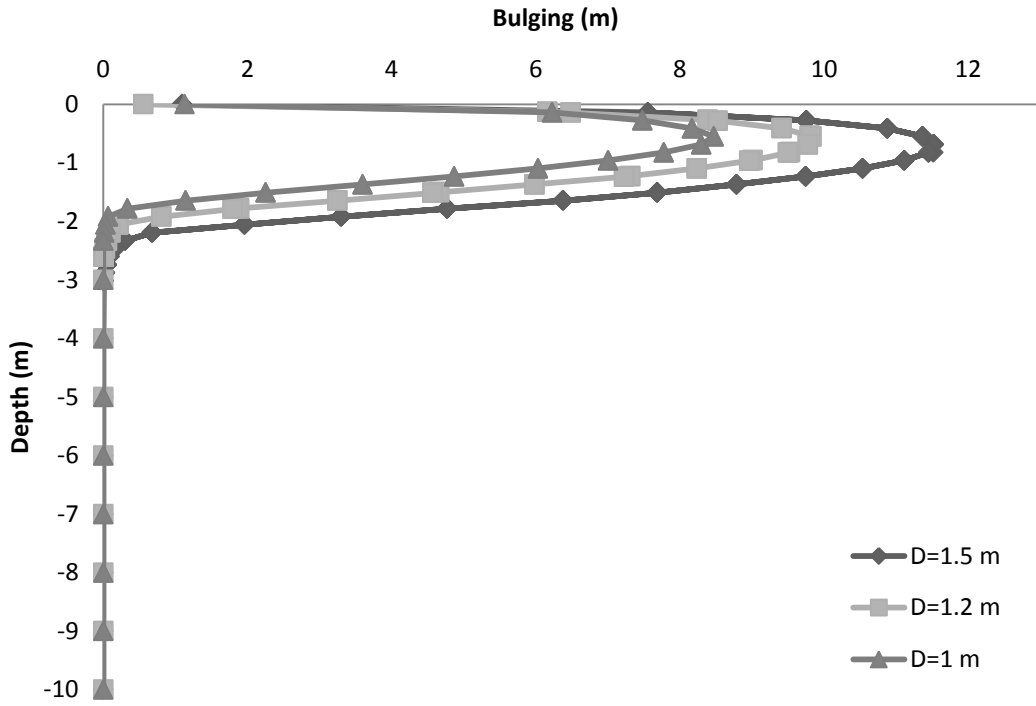


Figure 61: Bulging versus depth in for different diameters of sand column

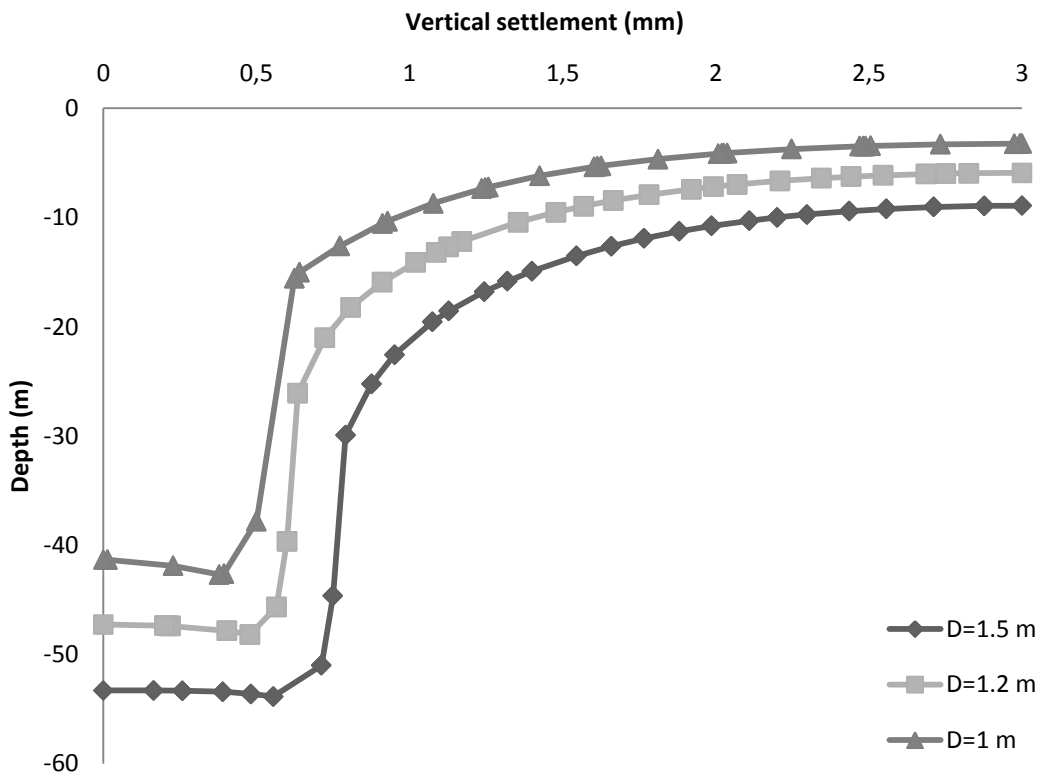


Figure 62: Vertical settlement versus depth in soil for different column diameters

5.7.3 Group C: Effect of Different Areas of Rigid Footing on Bulging

To distinguish a relationship between rigid footing and bulging, a rigid footing with different areas (1D, 2D, 3D) were used and the effect of area of rigid footing to change the bulging and stress were analyzed. It can be seen from the data in Figure 63 that with increasing the area of rigid footing the bearing capacity increases and causes less bulging while the depth of bulging increases. Strong evidence of decreased of bulging was observed in rigid footing with 3D compared to rigid footing with 1D. Footing with larger area improved horizontal and vertical stress in surrounding soils and increased bearing capacity. The stress result obtained from Figure 64 shows that, increasing area of rigid footing the amount of stress on the sand column reduced from 137 to 20 kPa. This is justified by the distribution of the stresses in the soil, increasing both the lateral and vertical stresses in the surrounding soil, hence less bulging. Finally, these results are justified with the findings of Barksdale & Bachus (1983).

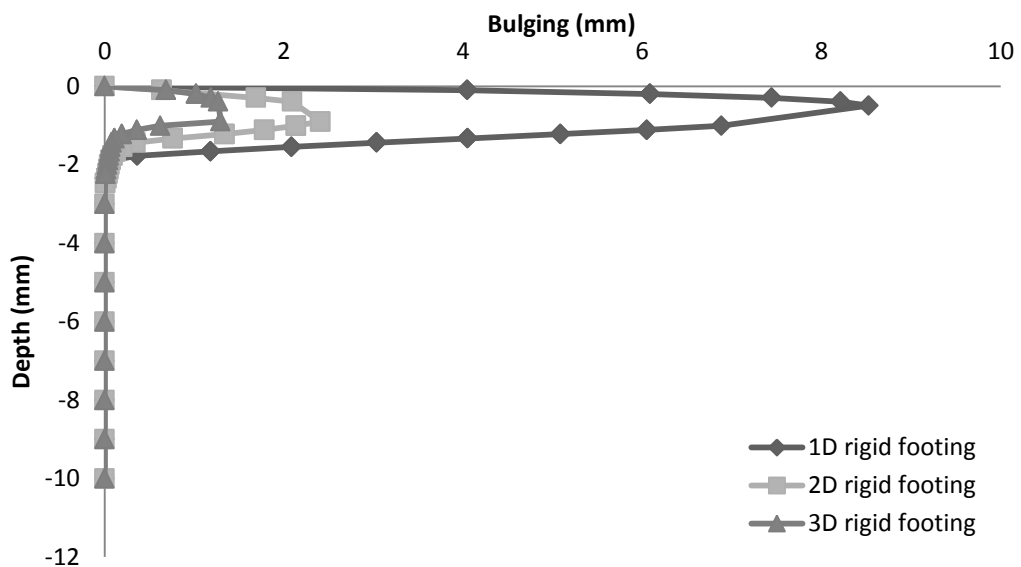


Figure 63: Bulging versus depth under different areas of rigid footing

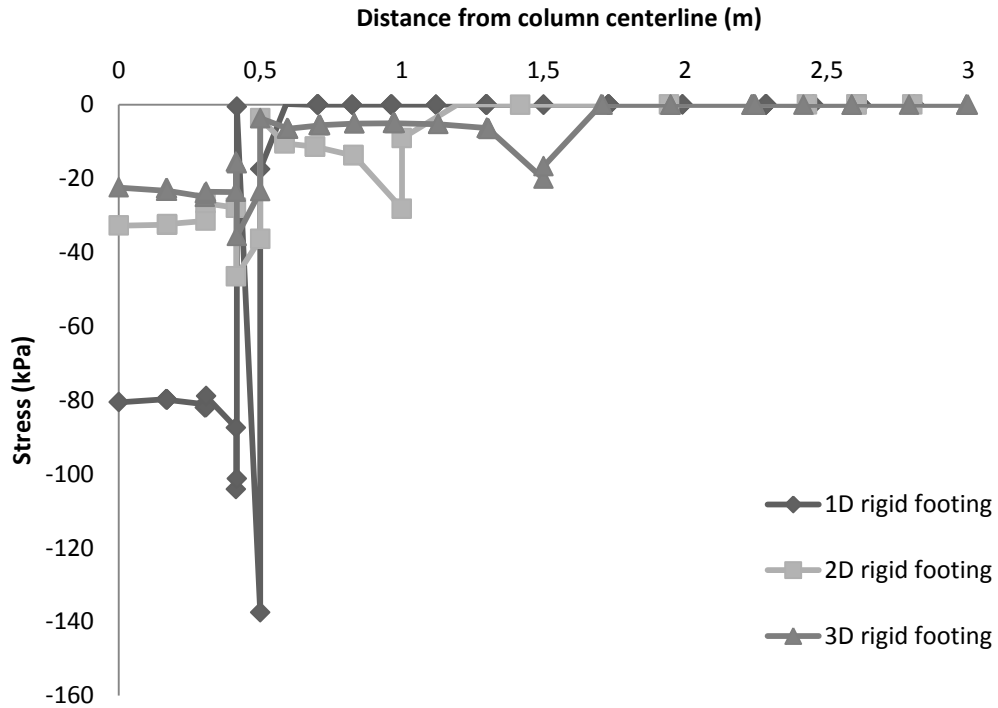


Figure 64: Distance from column centerline versus stress under different areas of rigid footing

5.7.4 Group D: Effect of Different Areas of Load on Bulging

In the unit cell idealization, the impact of different types of loading on columns is one of the important factors on settlement, bulging, and bearing capacity of soils. In this method, the sand column is subjected to 40 kPa load, which is kept constant while the loaded area is varied. Figure 65 depicts the relationship between different loaded areas of 1D, 2D, 3D, and 4D over sand columns and bulging. What is remarkable in this data is that by increasing loaded area from 1D to 4D the value of bulging increased but occurring at a deeper depth along the length of columns, when reached to the maximum value decreased gradually over a depth of 10 m. Therefore, the value of bulging increased with depth under loaded area of 1D to 4D.

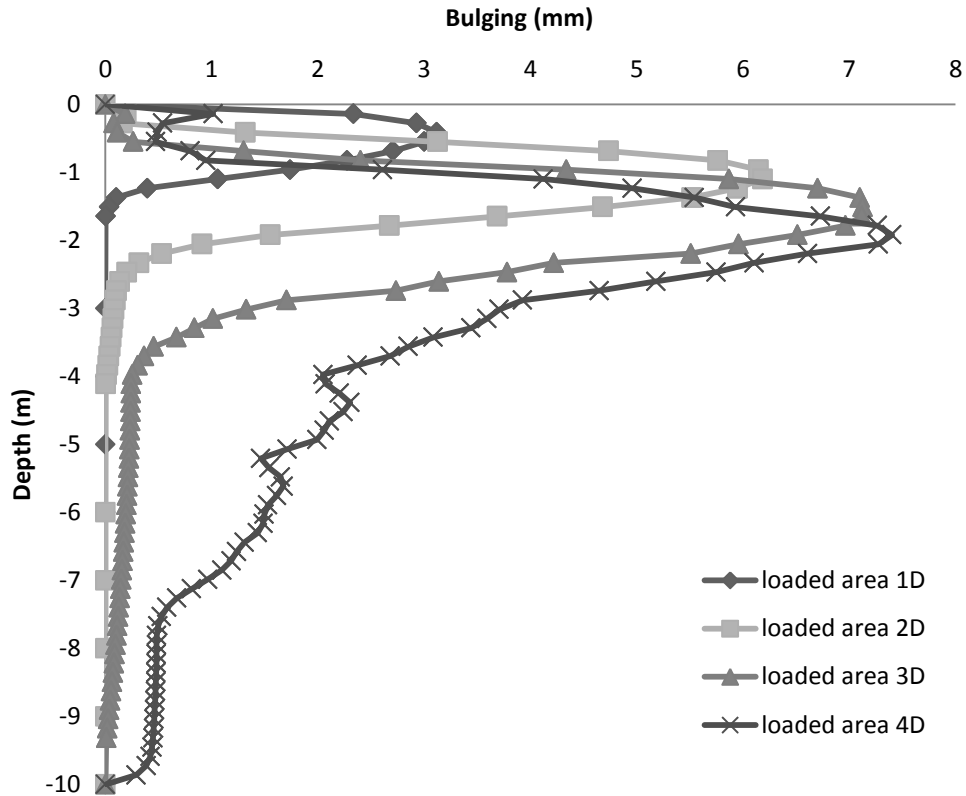


Figure 65: Bulging versus depth under of different areas of load

5.7.5 Group E: Effect of Different Stiffnesses of Geosynthetic Material

In order to assess the effect of geosynthetic properties on stone column, four kinds of geotextile of various stiffnesses (100, 200, 300, 400 kN/m) were selected to encase sand columns by using geogrid option in Plaxis software. The current study was designed to define the influence of geotextile on bulging value, hoop tension, and vertical settlement.

5.7.5.1 Influence of Stiffness on Bulging

From Figure 66 it can be seen that, with the increase in geotextile stiffness, amount of bulging reduced. It is worthy, of note that when geotextile of 400 kN/m stiffness was used, bulging reduced by 47% compare to the amount recorded on the conventional sand column.

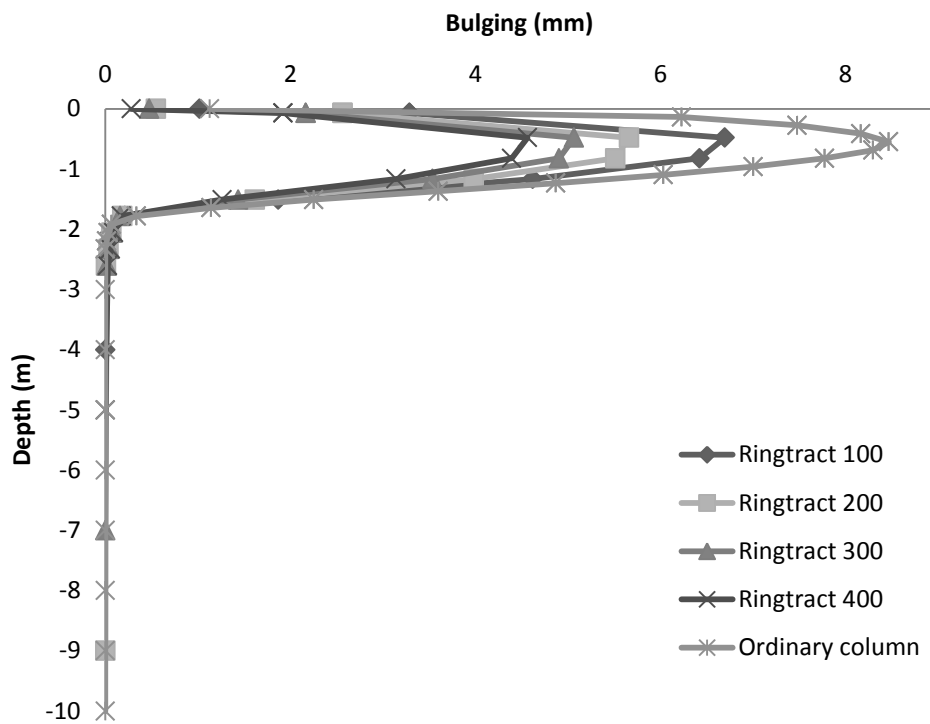


Figure 66: Bulging versus depth for different stiffnesses of geotextile

5.7.5.2 Effect of Stiffness on Hoop Tension

A hoop tension force is a property of the geotextile material. It creates a resistance against column displacement. Figure 67 shows the relationship between geotextile stiffness and hoop tension force. It can be seen that, by increasing geotextile stiffness the value of the hoop tension force increased. The hoop tension obtained are 1.33, 2.3, 3.09, and 3.7 kN/m for geotextile Ringtract 100, 200, 300, 400 respectively.

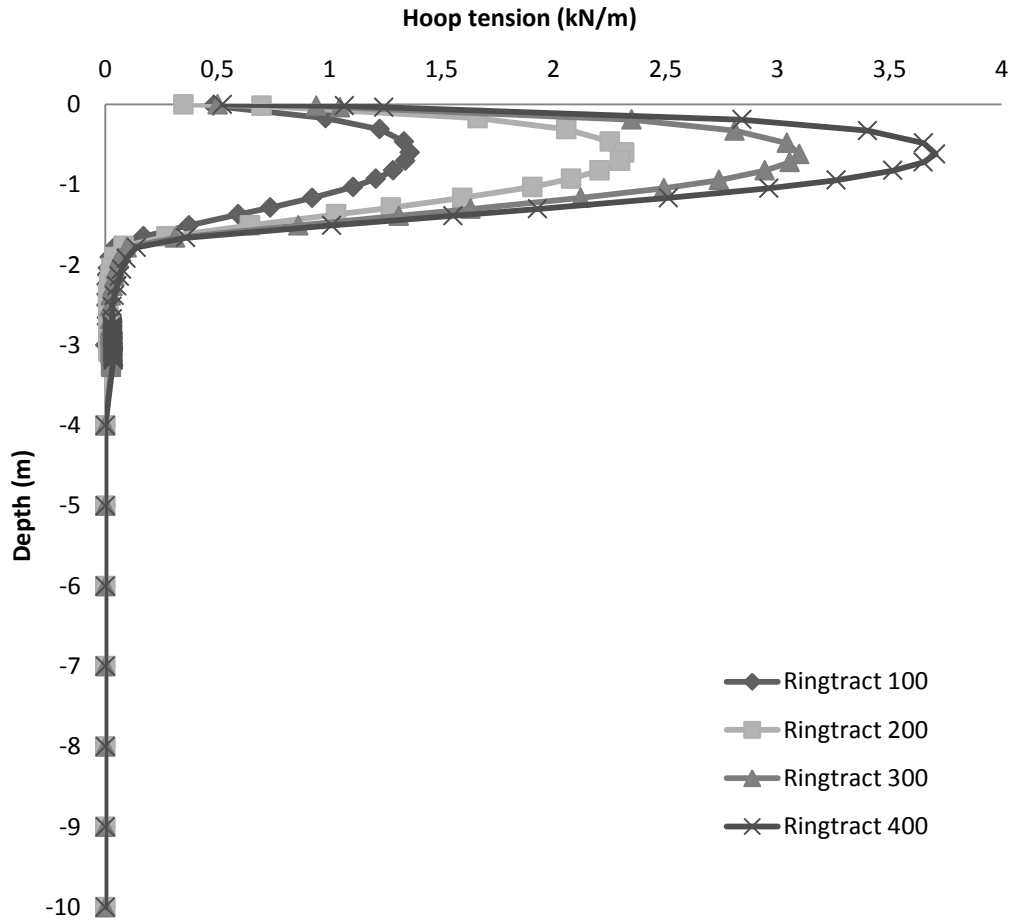


Figure 67: Hoop tension versus depth for different stiffnesses of geotextile

5.7.5.3 Influence of Stiffness on Vertical Displacement

Differential settlement at ground surface was investigated in Figure 68. Stiffness of geotextile has a marked influence on the amount of settlement when diameter is kept constant. Therefore, higher stiffness has lower settlement compared to conventional sand column. As represented in these figures, the settlement in sand columns reduced from 41.5 to 28 mm for geotextile stiffness of 400 kN/m. while this reduction is trivial in the surrounding soil.

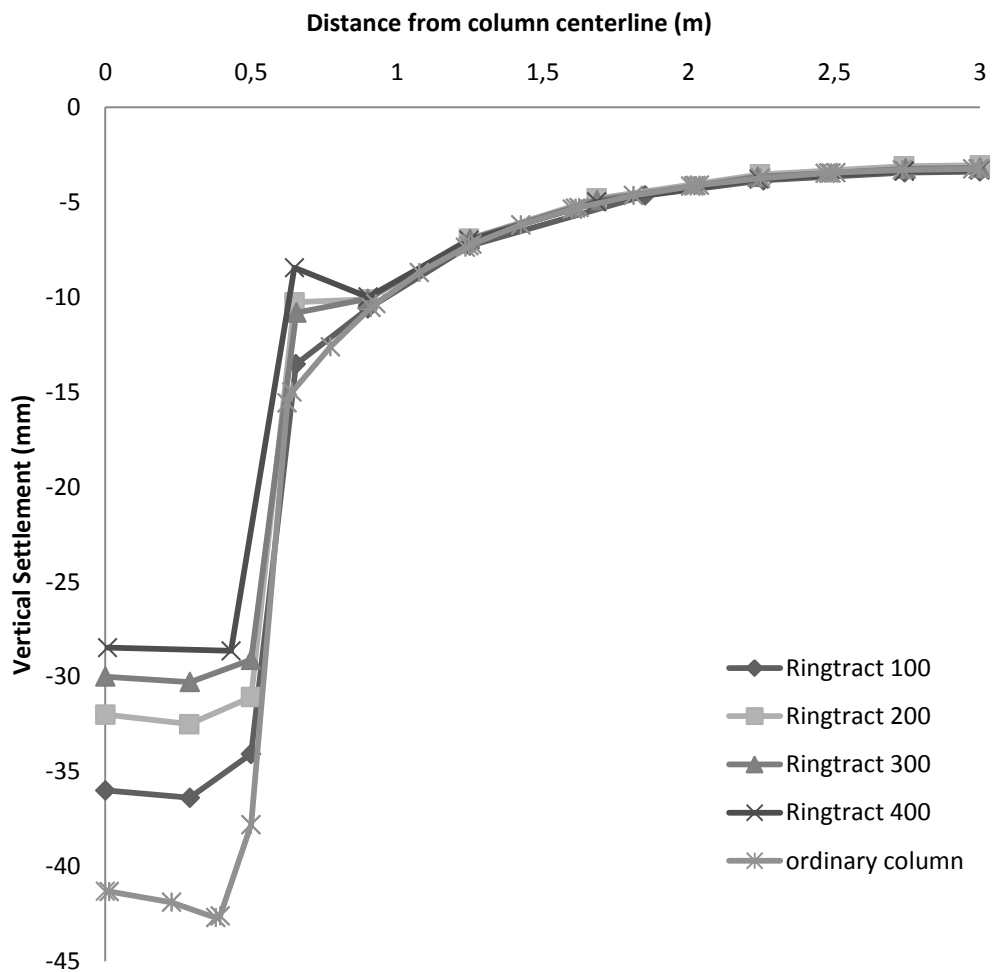


Figure 68 Effect of various stiffnesses of geotextile on vertical settlements at varying distances from the centerline

5.7.5.4 Influence of Stiffness on Maximum Bulging

Data in Figure 69 demonstrates the reduction of magnitude of bulging due to increasing stiffness of geotextile material under different magnitudes of applied load.

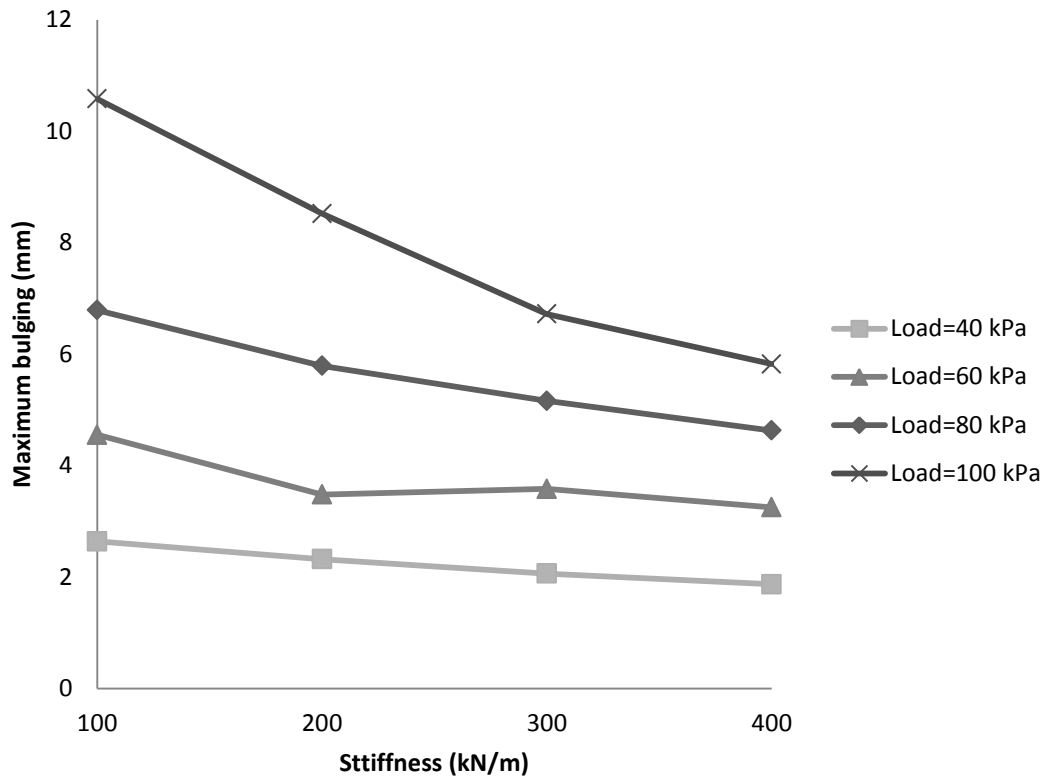


Figure 69: Maximum bulging versus geotextile stiffness under different magnitudes of load

5.7.6 Group F: Effect of Diameter on Hoop Tension Force

Figure 70 shows that increasing the diameter of the sand column has an important role in increasing the hoop tension of geosynthetic material. The amount of maximum hoop tension force increased with slightly increased depths corresponding to increased diameters.

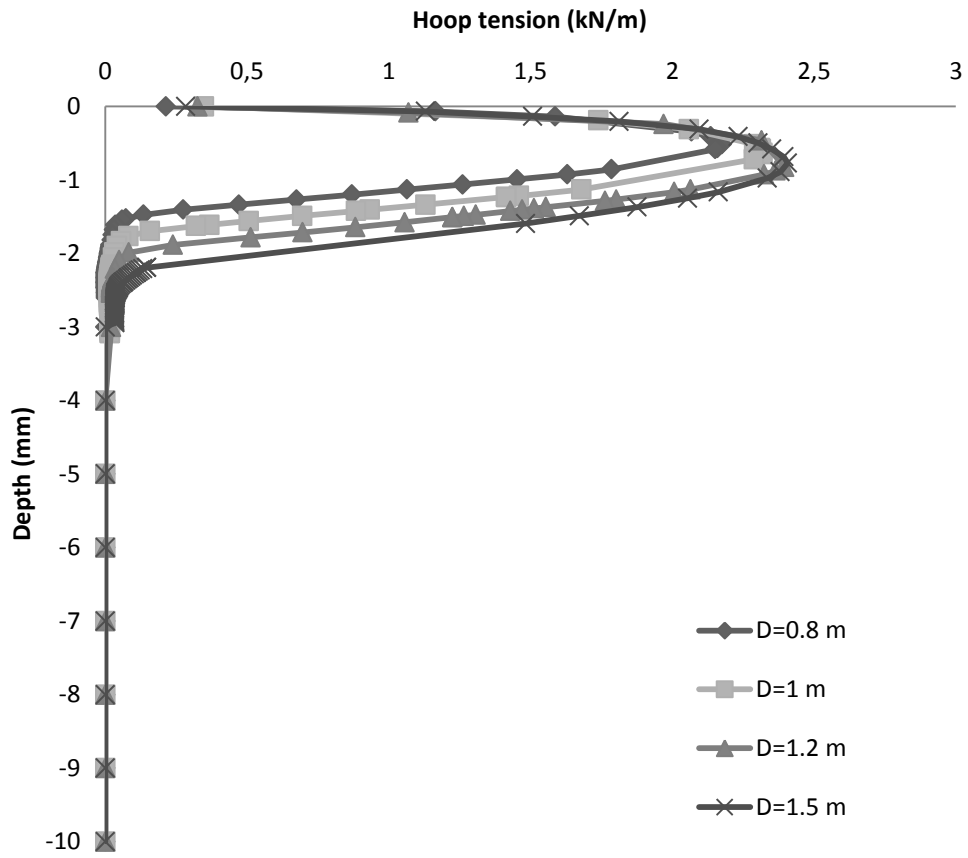


Figure 70: Hoop tension versus depth for different diameters of column

Chapter 6

Full-SCALE ANALYSIS OF STONE COLUMN

BENEATH AN EMBANKMENT STRUCTURE

6.1 Introduction

The present consideration is the mitigation of alluvial soils in the Tuzla region by utilizing stone columns as a new technology to reinforce the weak soil deposits in the region. Different types of structures can be constructed on these soils for different purposes such as buildings, highway embankment, etc. This research work provides a full-scale analysis of embankments improved by columns. A full-scale consideration can help to understand whether stone columns beneath an embankment construction in this area are beneficial or not.

6.2 Study Area

For full-scale evaluation, the data were retrieved from NovoSPT software for Borehole 36, which is from a location near the existing road. The model consists of three layers of different clay strata with high plasticity underlain by a firm stratum.

6.3 Materials and Parameters

The embankment fill properties are taken from the work of Abusharar et al. (2009), and the properties of stone column material from Ambily & Gandhi (2007)'s research. Table 13 shows the material properties of soil strata and Table 14 shows the material properties of stone and embankment fill.

Table 5: Properties of soil strata beneath the embankment

Depth (m)	Type	γ_{dry} (kN/m ³)	γ_{Sat} (kN/m ³)	E_s (kN/m ²)	Φ (°)	S_u (kPa)	k (cm/s)
0-5	CH	15.3	19.7	3100	---	40	10^{-7}
5-8.5	CL	15.2	19.6	2200	---	32	10^{-7}
8.5-15	CH	13.5	18.6	2100	0	31	10^{-7}

Table 6: Material properties of stone and embankment fill.

Parameter	Symbol	Gravel	Fill
Material model	Type	Mohr-Coulomb	Mohr-Coulomb
Loading	Condition	Drained	Drained
Wet unit weight (kN/m ³)	γ_{wet}	19.4	18
Horizontal Permeability (m/day)	k_h	6	1
Vertical Permiability (m/day)	k_v	6	0.5
Young's modulus (kN/m ²)	E	45000	20000
Poisson's ratio	ν	0.3	0.3
Cohesion (kN/m ²)	c	0	0
Friction angle (°)	ϕ	42	30
Dilatancy angle (°)	ψ	0	4

6.4 Numerical Procedure

For the determination of numerical simulation by Plaxis, Mohr-Coulomb model has been adopted for all materials. Drained condition was assumed for fill embankment and stone columns, and undrained condition was selected for the clay deposit. This research was accomplished on half of the model due to symmetry formation of the model. The plain strain consideration has been selected for full-scale simulation. The two sides of model boundary were assumed closed for consolidation. The water table was assumed at the ground level. Fine mesh considerations were used by selecting

mesh generation option in Plaxis software. In addition, 10 kPa load were applied on fill embankment as a traffic load.

Embankment fill was built in two equivalent stages, each layer being 2.5 m high. First stage was constructed in 5 days and was allowed for consolidating for 30 days. Second construction was built in 5 days and finally by utilizing minimum pore water pressure option allowed the consolidation end time was assessed.

FEM conception by Plaxis estimated the amount of settlements, excess pore water pressures in treated and untreated conditions. In numerical analysis, different points were selected to determine the settlements and excess pore water pressures. The position of these points can be seen in Figure 71.

Figure 72 represents mesh analyses for unreinforced condition.

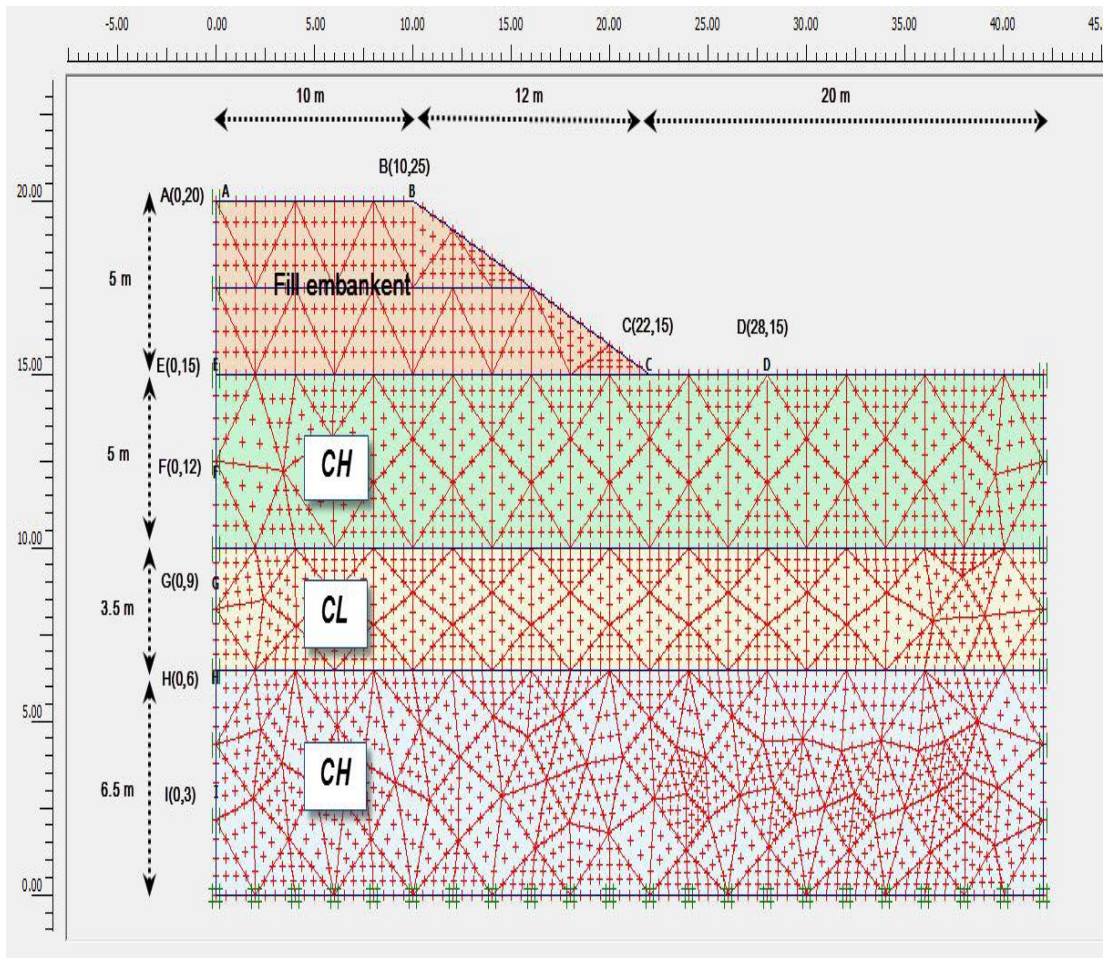


Figure 71: Point location in FEM analyses

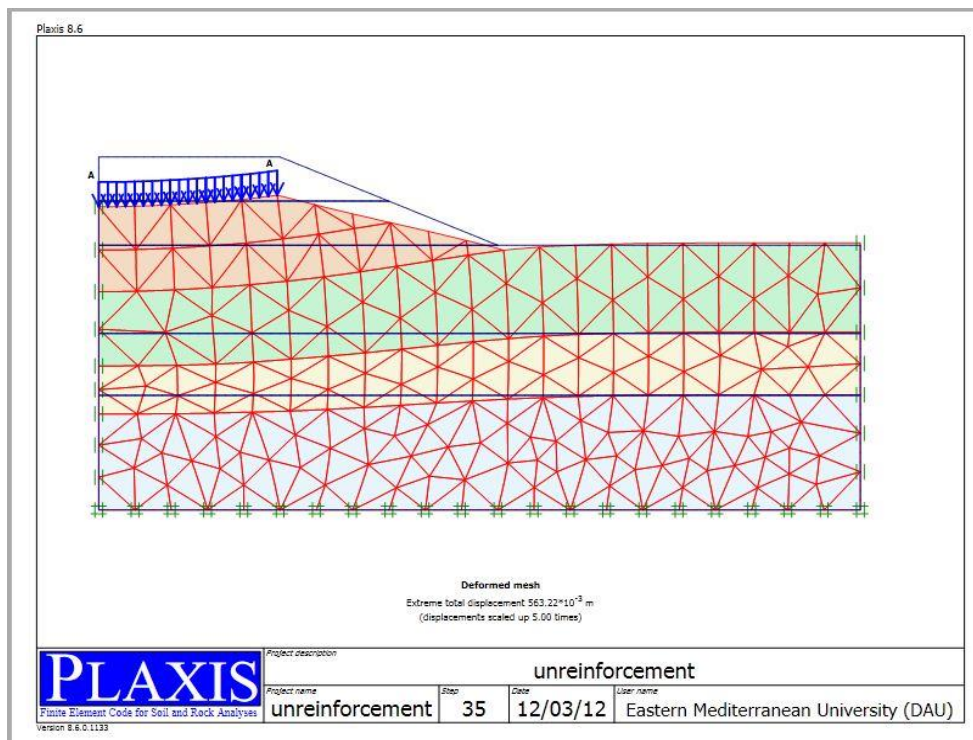


Figure 72: Mesh analyses of full-scale model

6.5 Results of Analyses

In order to assess the settlements and time relationships various depths were selected were selected in Plaxis for four different conditions as follows:

1. Unreinforced,
2. Stone column with 6 m height,
3. Stone column with 10 m height,
4. Stone column with 15 m height.

6.5.1 Settlement in Time

FEM analysis was used to predict the amount of settlements versus time at points A, B, and D. Four conditions of the model were analyzed in 8775 days, which is the consolidation end time of unreinforced case. Figures 73-75 present the results acquired from the settlement simulation. From this data, we can see that settlement amount is largest for unreinforced condition, reducing with increasing column heights of $h=6$, $h=10$ and $h=15$ m. Hence, the columns with 15 m height reduced the settlement by 71%. However, the detected difference in settlements between points A, B, and D show that the maximum settlement occurred at point A, the toe of the embankment, while the settlement at point D can be observed as a heave (swelling). Hence, at three points, the settlement is reduced when the height of columns increased.

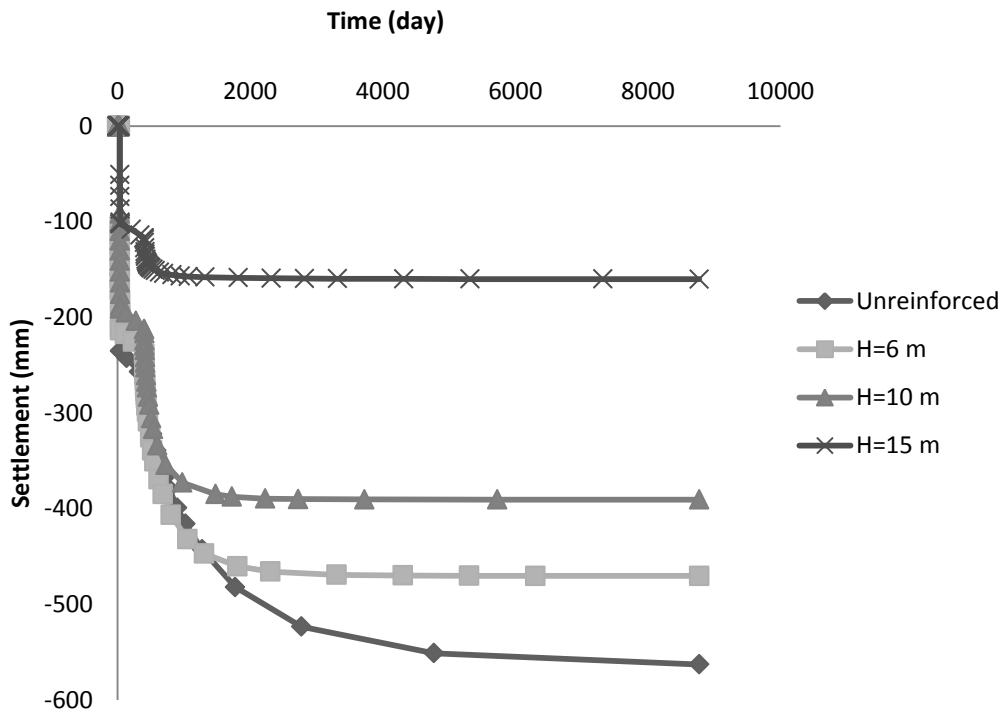


Figure 73: Settlement versus time at point A for different columns heights

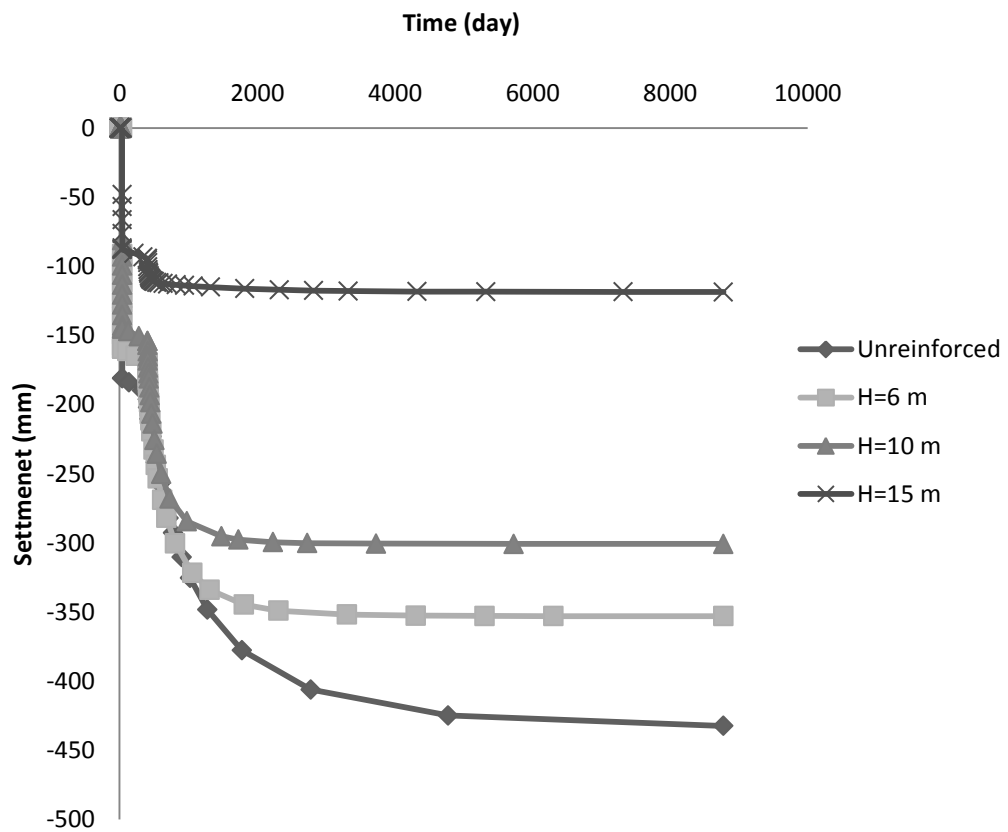


Figure 74: Settlement versus time at point B for different columns heights

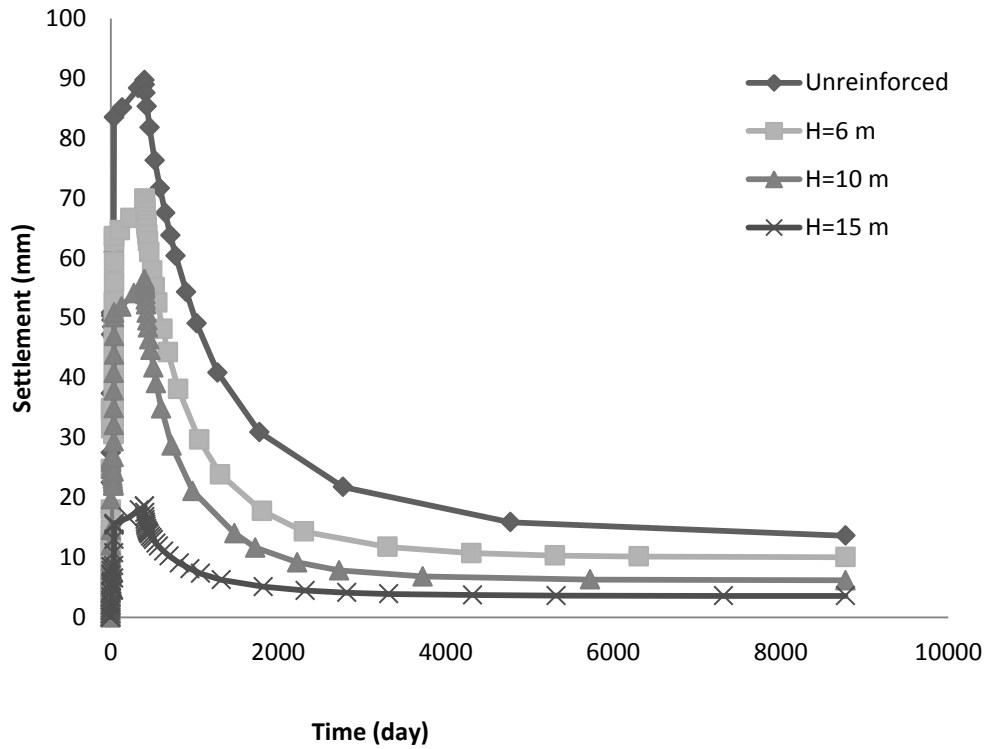


Figure 75: Settlement versus time at point D for different columns heights

6.5.2 Settlement versus Depth

FEM analysis was selected to calculate the amount of settlements versus depth at point E, C, and D. From the Figures 76-78 for point E and C, we can see that, by increasing the depth the amount of settlements gradually decreased until zero at depth 15 m below the ground surface, while at point D initially soil heaved and then settled. At all of points The stone column with height 15 m has substantial influence reducing settlement compared with smaller height of columns and untreated condition. This highest reduction of settlement by column with height 15 m is fixed end of column in firm strata while other heights of columns are floating column. In addition, it can be seen that maximum settlement at the ground surface decreased by increasing the distance from embankment centerline.

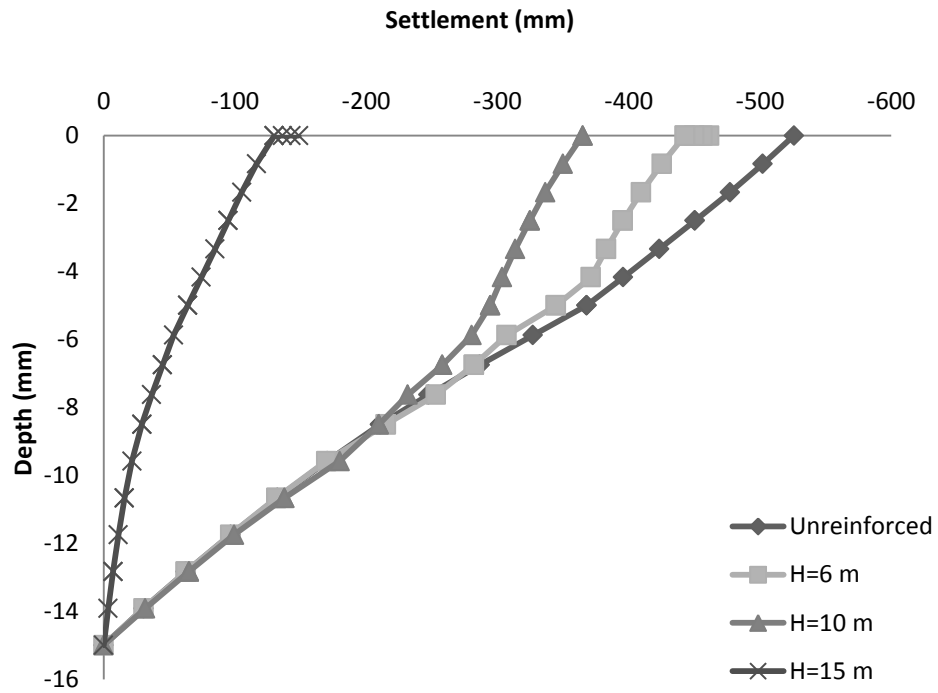


Figure 76: Settlement versus depth for different height of columns at point E

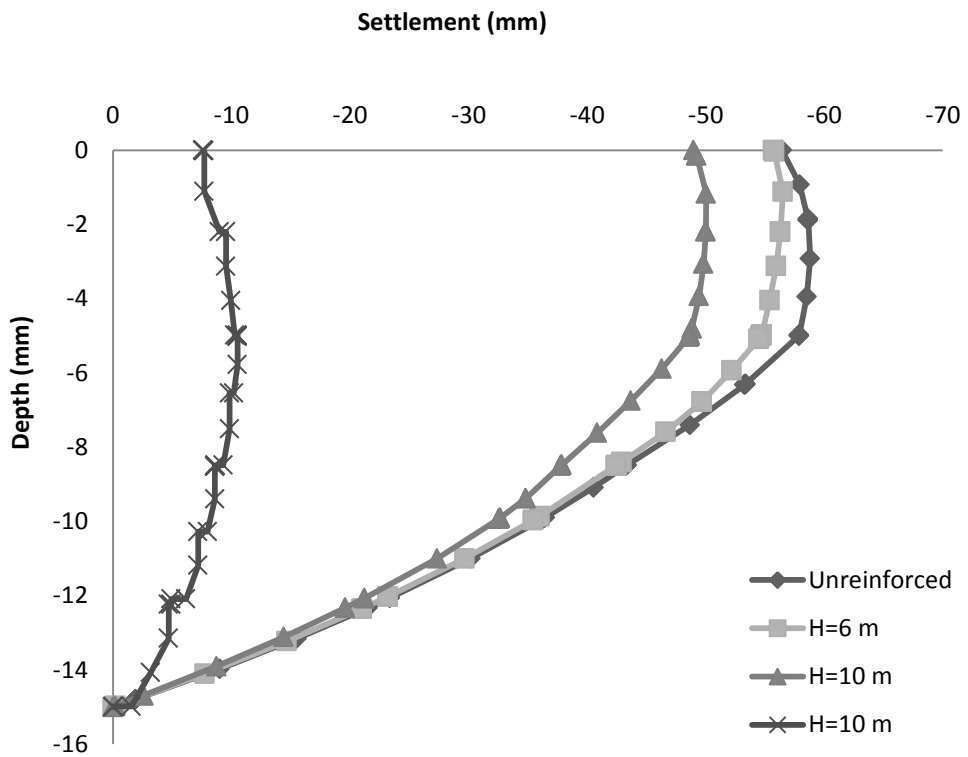


Figure 77: Settlement versus depth for different height of columns at point C

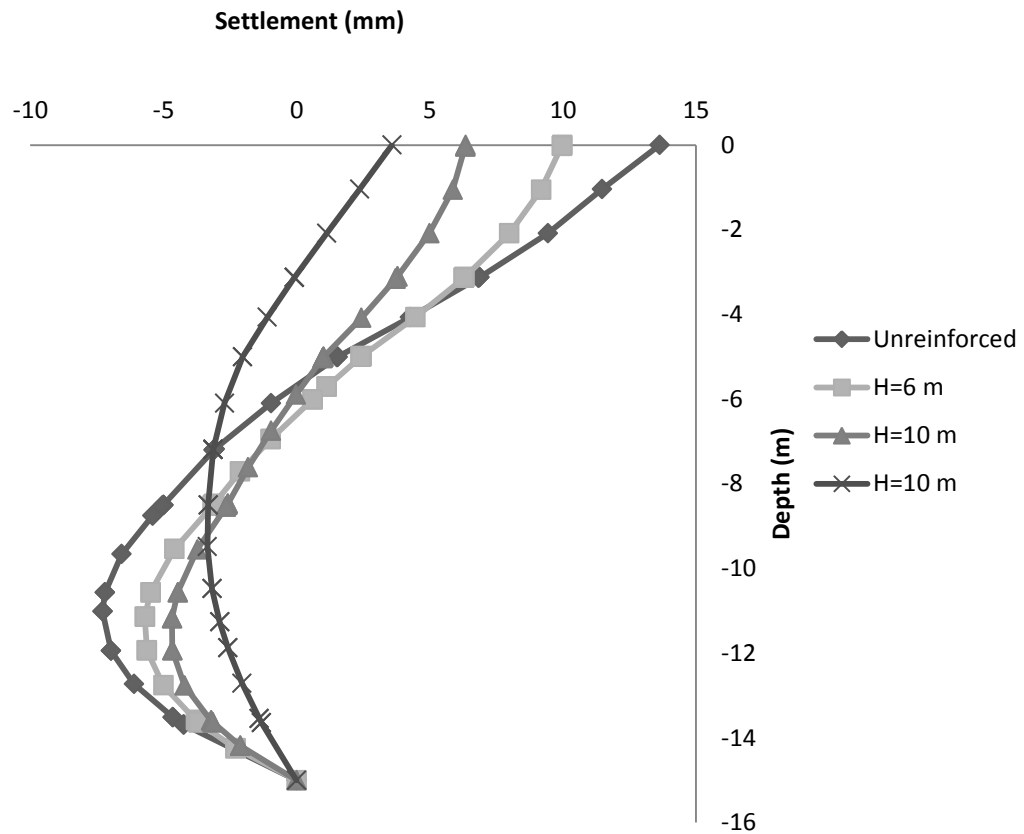


Figure 78: Settlement versus depth for different height of columns at point D

6.5.3 Lateral Settlement versus Depth

In order to assess the amount of lateral settlements versus depth, point C, and D were selected. As shown in Figures 79-80 initially the lateral settlements increased and then reduced with increased depth. Hence, as distance from embankment increased the amount of lateral settlement decreased. The marked reduction in settlement also can be seen in the presence of stone column with 15 m height.

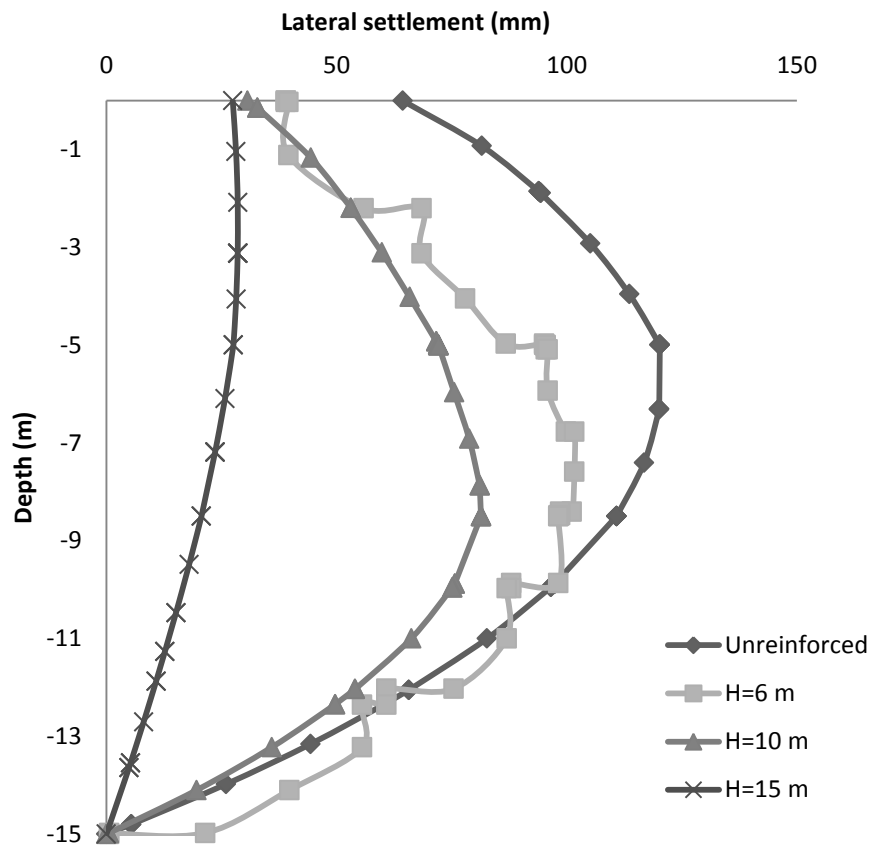


Figure 79: Lateral Settlement versus depth for different height of columns at point C

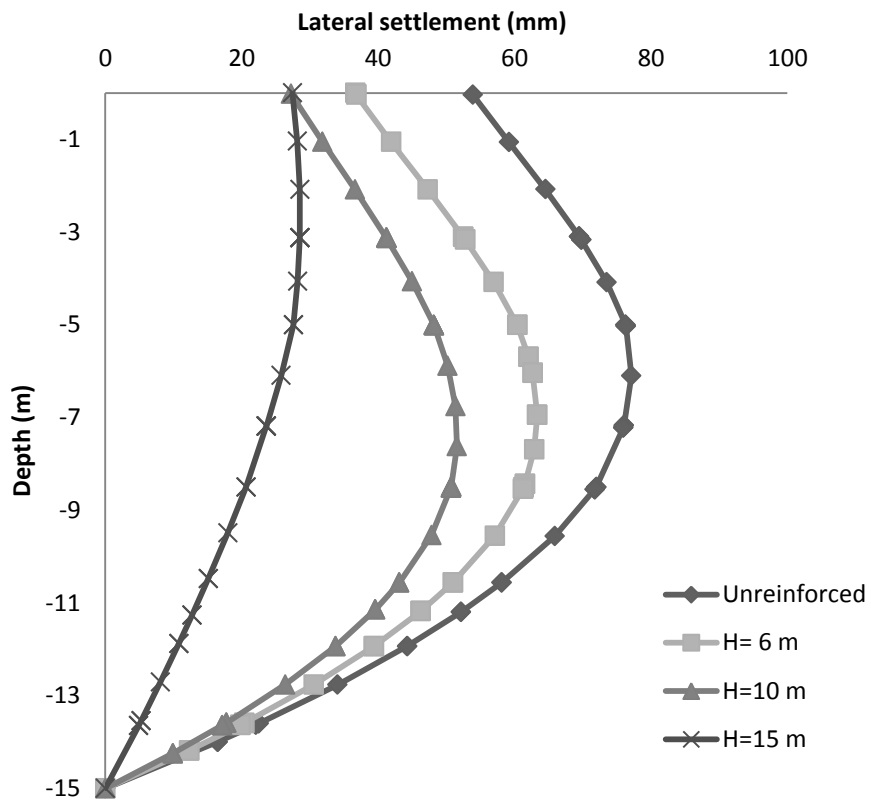


Figure 80: Lateral Settlement versus depth for different height of columns at point D

6.5.4 Settlement from Embankment Centerline

To distinguish the settlement differences between embankment centerline and end of the model, three sections, ground level, 2.5 m below the ground level, and 5.5 m below ground level, were calculated by numerical consideration in Plaxis. Figures 81-83 present the results acquired from settlement analyses between the end of the model and embankment middle line. It is manifested by these results that, largest value of settlement can be seen at ground level at centerline of embankment and gradually reduced toward end of the model while after 26 m distance from embankment centerline, it can be observed as a heave. Moreover, it is apparent from the data that very few differences were observed among columns with height 6 m, 10 m, and untreated section by increasing the distance from embankment centerline. Meanwhile, this change has not been observed elsewhere, but it is clearly in column with height 15 m due to significant effect on declining the settlement.

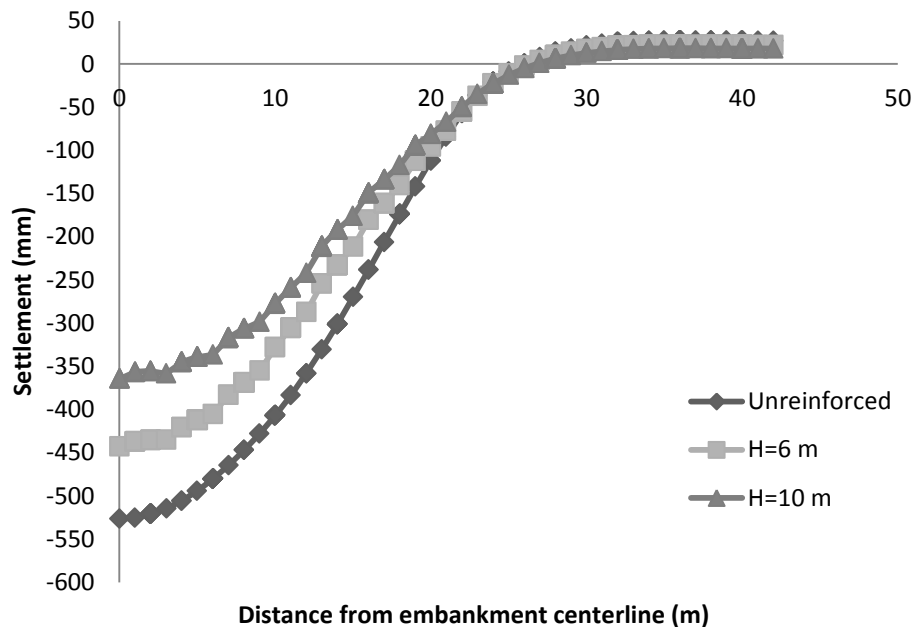


Figure 81: Settlements from embankment centerline

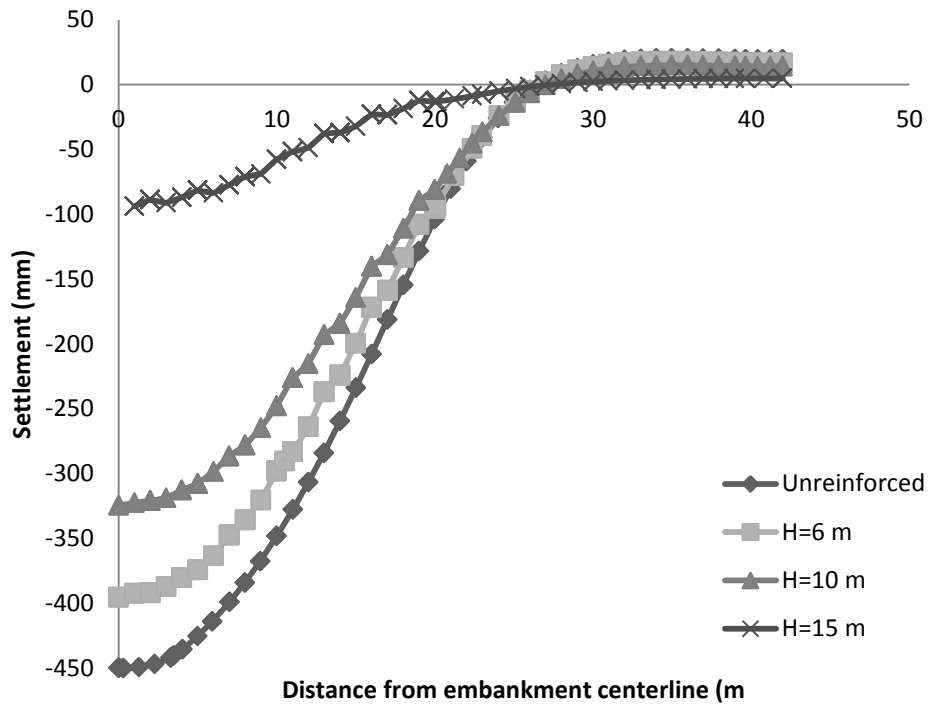


Figure 82: Settlements from embankment centerline

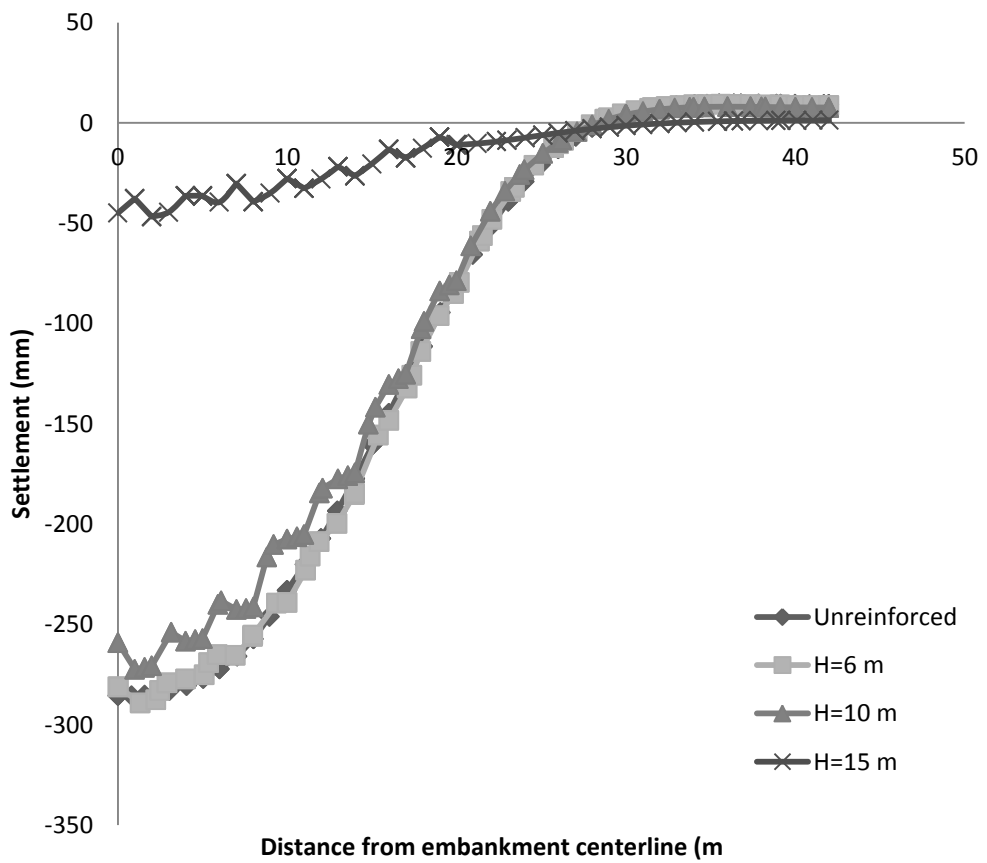


Figure 83: Settlements from embankment centerline

6.5.5 Consolidation End Time Analyses

It can be realized from Figure 84, the stone column with 15 m height speeds up the consolidation time in comparison to unreinforced condition from 8775 days (approximately 24 year) to 1875 days (5 years). Therefore, among different column heights, 15 m has a substantial influence on dissipation of excess pore water pressure and on reducing the consolidation time.

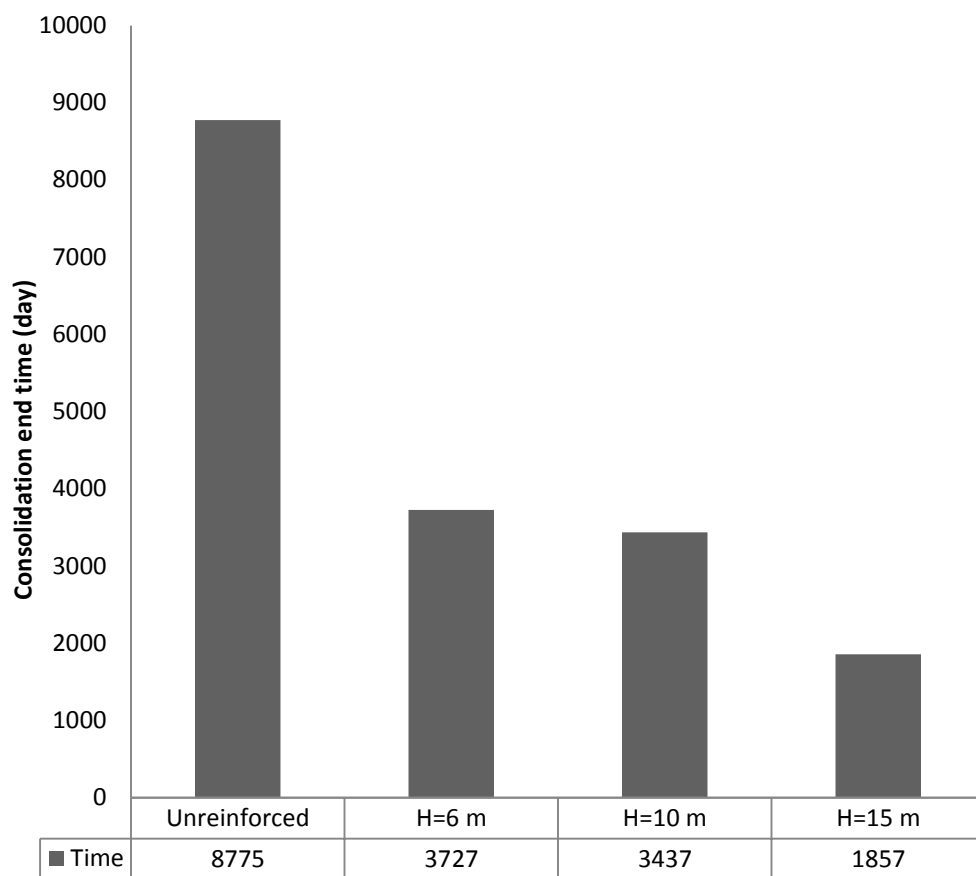


Figure 84: Consolidation end time

6.5.6 Pore Water Pressure Consideration

To realize the behavior of excess pore water pressure in time, points E, F, G, H, and I were selected. Figure 85-89 show that excess pore water pressures is attained at the maximum amount after the final stage of each step for embankment fill, then, it will be reduced progressively with time until it becomes zero at consolidation end time. The most remarkable result to emerge from data at point E to I, is that higher excess pore water pressures exist at lower layers compared to the ground level. It can be seen from point E that, there is no substantial modification in excess pore water pressure while these differences increase by increasing depth. Thus, in deeper layers stone column height plays an important role to decrease the amount of excess pore water pressure where at point I at depth 12 m below the ground level, just the column height of 15 m can reduce the excess pore pressure considerably in contrast to the other column heights.

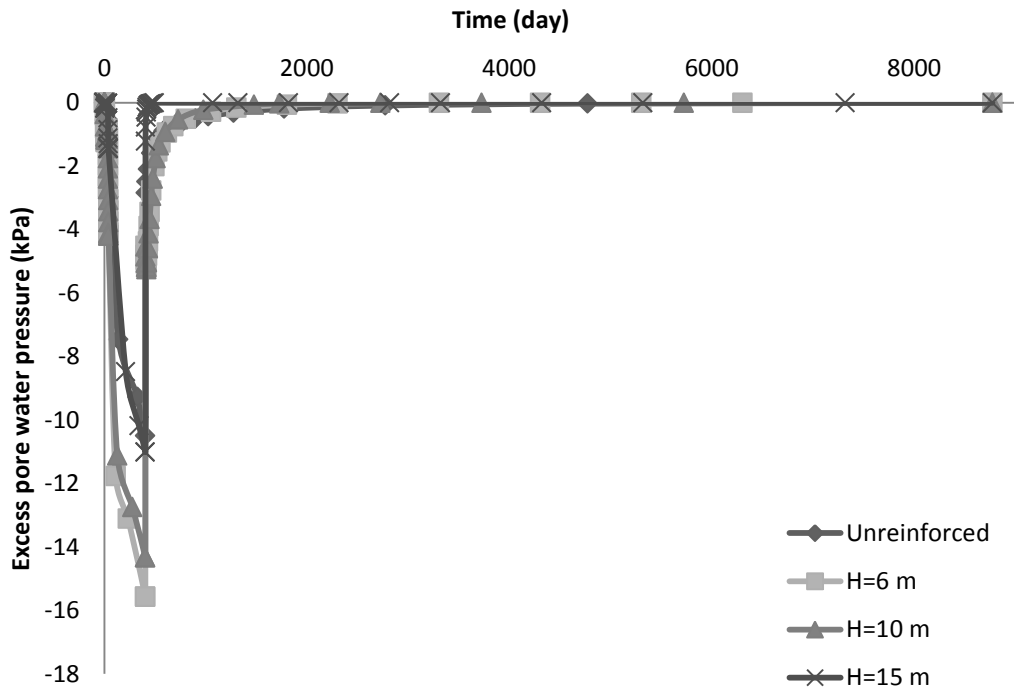


Figure 85: Excess pore water pressure versus time for different height of columns at point E

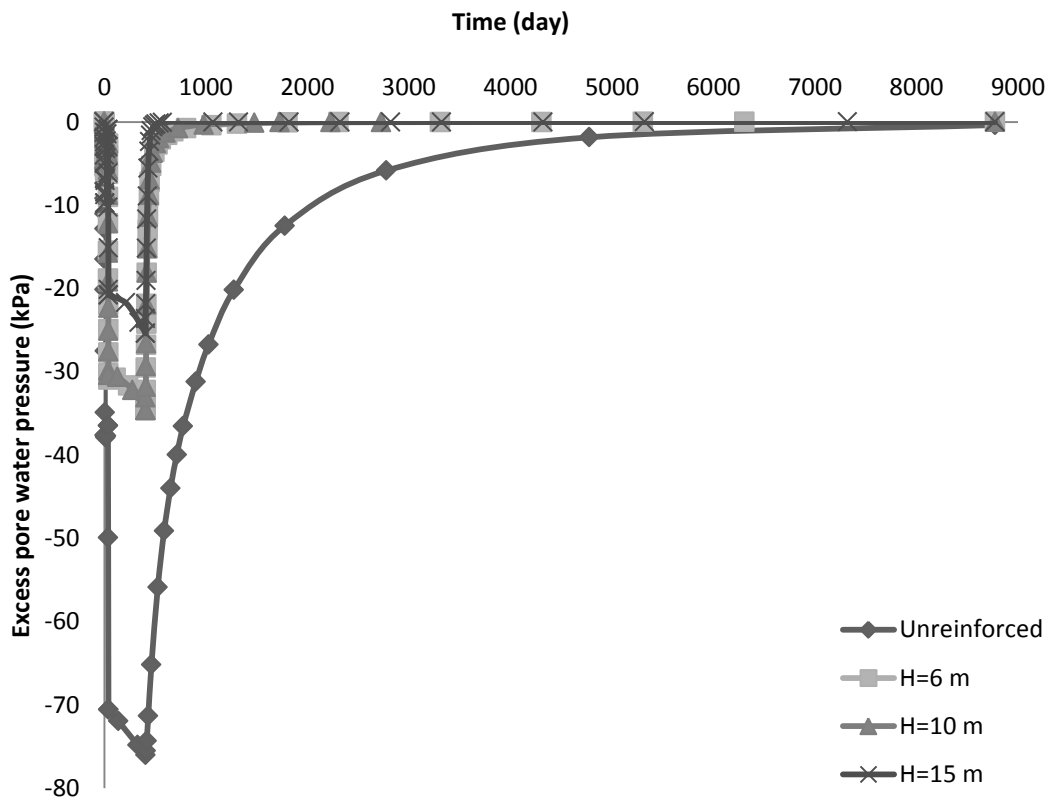


Figure 86: Excess pore water pressure versus time for different height of columns at point F

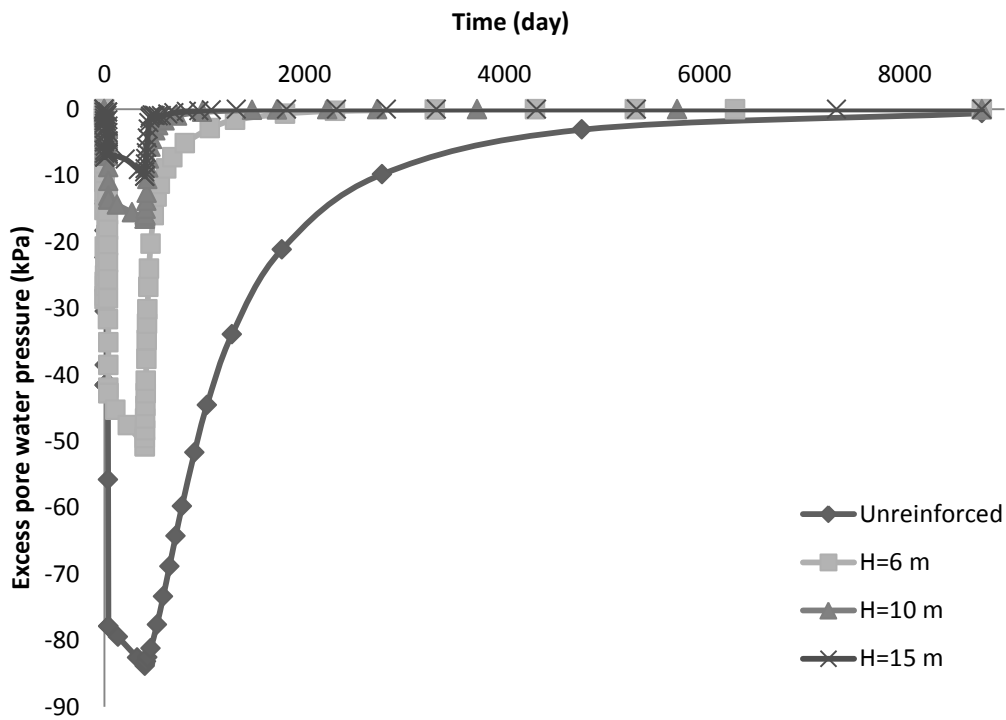


Figure 87: Excess pore water pressure versus time for different height of columns at point G

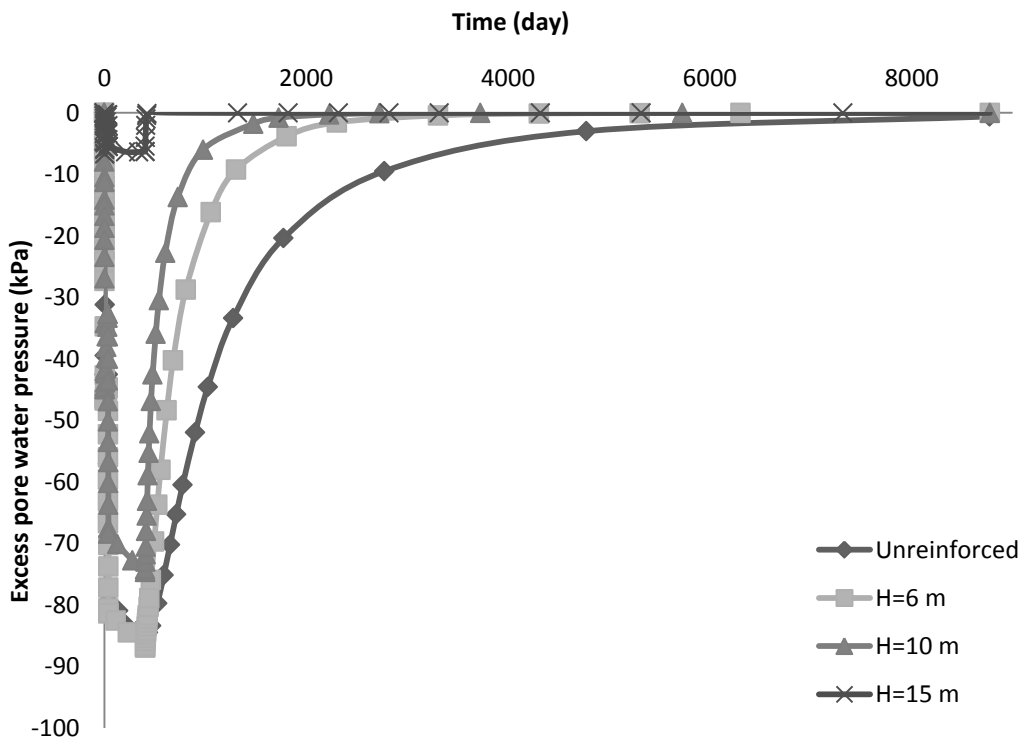


Figure 88: Excess pore water pressure versus time for of different height of columns at point H

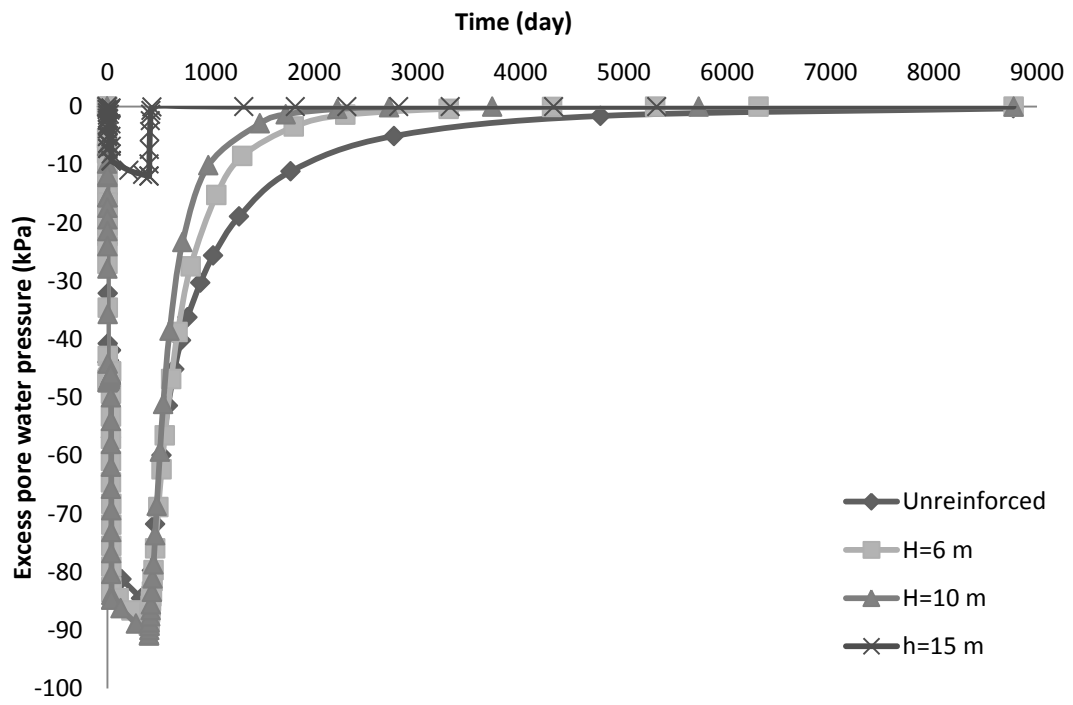


Figure 89: Excess pore water pressure versus time for of different height of columns at point I

Chapter 7

CONCLUSIONS

This dissertation has investigated on numerical simulation of the conventional and encased columns by Plaxis software version 8.6.0, and argued that stone column is the best method to control the excessive settlements of weak alluvial deposits in Tuzla region. This study was set out to represent the effect of columns in three conditions. Firstly, under an embankment fill in unit cell construction, secondly, bulging of conventional and encased column under different types of loading conditions, and finally, full-scale analyses of columns beneath an embankment fill.

The conclusions derived from this study are as follows:

1. Stone column has a remarkable influence on decreasing settlements and speeding up the consolidation time.
2. Stone column with larger diameter has more significant influence on the dissipation of excess pore water pressure and hence, reducing the consolidation time. Larger the column diameter, higher is the bearing capacity and lower is the settlement.
3. The maximum settlement occurs at ground level and reduces by increasing depth and increasing column diameter. The biggest reduction in settlement can be seen in upper layer, especially at ground surface, whereas, in lower

depths there is no significant difference in settlement between treated and untreated soil.

4. In the first and second construction periods, no significant reduction in settlement occurs in neither treated nor untreated section due to remaining excess pore water pressure in the system. However, this difference can be seen clearly in a larger amount after 2 years of embankment construction. Finally, a significant difference in settlement reduction between treated and untreated soil can be seen at the end of consolidation time, with an appreciable reduction occurring in the treated soil.
5. In unreinforced condition, the amount of settlements in soil is constant because of equal vertical strain theory. By using stone column, due to larger stress confining around it, the amount of vertical settlements increased in the vicinity of stone column, then suddenly decreased by increasing distance from column, remaining constant. Furthermore, by increasing the diameter of stone column the amount of settlements decreased. Therefore, higher differential settlements occur when column diameter becomes larger.
6. By increasing the area ratio, the maximum settlement reduced and increasing the area ratio the improvement factor increased.
7. Keeping the diameter constant, it was observed that increasing the magnitude of load the magnitude of bulging increased, while the maximum bulging occurred at the same depth for all sand columns. It was observed that the maximum bulging occurred at $1.06D$ of sand columns.
8. Keeping the load constant, the change of column diameter has influenced bulging. By increasing the diameter of columns, bulging increased and depth of the maximum bulging elevated from $1.06D$ to $1.3D$. The settlement

amount in sand column is greater than surrounding soil due to load on the sand column.

9. Increasing the area of rigid footing it was observed that the bearing capacity increased and less bulging occurred while the depth of bulging increased.
10. By Increasing in loading area, the value of bulging increased but occurring at a deeper depth. The magnitude of bulging increased with depth from 1D to 4D.
11. Using geotextile with higher stiffness, amount of bulging reduced, also value of the hoop tension force increased.
12. Stiffness of geotextile also has a marked influence on the amount of settlement. Therefore, higher stiffness has lower settlement compared to conventional sand column. Reduction of magnitude of bulging occurred due to increasing stiffness of geotextile material under different amounts of applied load.
13. Lateral settlements increased initially and then reduced with increasing depth and distance from the embankment.

REFERENCES

- Aboshi, H., Ichimoto, E., Harada , K., & Emoki , M. (1979). The Composer A Method to Improve the Characteristics of Soft Clays by Inclusion of Large Diameter Sand Columns. *Proceedings International of Conference on Soil Reinforcement*, Paris, p. 211-216.
- Abusharar, S. W., Zheng, J. J., & Chen, B. J. (2009). Finite element modeling of the consolidation behavior of multi-column supported road embankment. *Journal of Computers and Geotechnics, Elsevier, Vol, 36*, p. 676-685.
- Afkhami, A. (2009). NovoSPT User Manual. North Vancouver: Novo Tech Software.
- Ajayi, L., & Balogum, L. (1988). Penetration testing in tropical lateritic and. *Penetration Testing, ISOPT-1*, p.315-328.
- Ambily, A P; Gandhi, S R. (2007). Behavior of stone columns based on experimental and FEM analysis. *ASCE, Journal of Geotechnical and Geoenvironmental 133*, No. **4**, 405-415.
- Ballam, N P; Booker , I R. (1981). Analysis of rigid rafts supported by granular. *International Journal for Numerical and Analytical Methods in Geomechanics 5*, p. 379-403.

Ballam, N. P., Poulos, H. G., & Brown, P. T. (1977). Settlement Analysis of Soft Clays Reinforced with Granular Piles. *Proceeding of 5th S.E. Asian Conferences on Soil Engineering*, Bangkok, Thailand, (p. 81-92).

Bargado, D. T., Anderson, L. R., Muira, N., & Balasubramaniam, A. S. (1996). Soft ground improvement in lowland and other environments. *ASCE*, 427.

Barksdale, R. D., & Bachus, R. C. (1983). *Design and construction of stone columns*. Federal Highway Administration Report, RD-83/026.

Barkslade, R. D. (1981). *Site Improvement in Japan Using Sand Compaction Piles*. Atlanta: Georgia Institute of Technology.

Bea, W., Shin, B., & An, B. (2002). Behavior of foundation system improved with stone columns. *Proc. of the 12th international Offshore and Polar Engineering* Kitakyushu, Japan: Society of Offshore and Polar Engineering, p. 675-678.

Behpoor, L., & Gahramani, A. (1989). Correlation of SPT to Strength and Modulus of Elasticity of Cohesive Soils. *Proceedings of the 12th International Conference on Soil Mechanics and Foundation Engineering*, Rio de Janeiro, Brazil, p. 175-178.

Bowles, J. E. (1996). *Foundation Analysis and Design*. Singapore: McGraw-Hill Companies, Inc.

Choobbasti, A. J., Zahmatkesh, A., & Noorzad, R. (2011). Performance of stone columns in soft clay: Numerical Evaluation. *Geotechnical Geology Engineering, Springer, 29*, 675-684.

D'Appolonia, D. J., D'Appolonia, E. D., and Brissette, R. F. (1970). Closure: Settlement of Spread Footings on Sand. "Journal of the Soil Mechanics and Foundations Division", Vol 96, 754-762.

Das, B. (2011). *Principles of Foundation Engineering*. Stanford: Global Engineering.

Das, B. M. (2008). *Advanced Soil Mechanics*. New York: Taylor and Francis.

Deb, K. S. (2011). Laboratory model studies on unreinforced and geogrid-reinforced sand bed over stone column-improved soft clay. *Geotextiles and Geomembranes*, Vol. 26, p. 190-196.

Décourt, L. (1990). *The Standard Penetration Test*. Oslo: Norwegian Geotechnical Institute Publication.

Domingues, T. S., Borges, J. L., & Cardoso, A. L. (2007). Parametric Study of Stone Columns in Embankments on Soft Soils by Finite Element Method. *Applications of Computational Mechanics in Geotechnical Engineering*, Vol. 20, 281-291.

Elshazly, H., Hafez, D., & Mossaad, M. (2006). Back-calculating vibro-installation stresses in stone-column-reinforced soils. *Journal of Ground Improvement* 10, Vol. 9, p. 47-53.

Elsway, M., Lesny, K., & Richwien, W. (2010). Performance of geogrid-encased stone columns as a reinforcement of soft ground. *Numerical Methods in Geotechnical Engineering*, Vol. 26, p. 875-880.

Erhan., G. (2009). Assessment of Liquefaction/Cyclic Failure Potential of Tuzla Soils. *MS Thesis, Eastern Mediterranean University (North Cyprus)*.

Gibson, R. D., & Anderson , W. F. (1961). In-situ measurements of soil properties with pressuremeter. *Civil Engineering and Public Work Review*, vol.56, (p. 658).

Gniel, J., & Bouazza, A. (2009). Improvement of soft soils using geogrid encased stone columns. *Geotextiles and Geomembranes* 27 , 167-175.

Greenwod, D. A. (1970). Mechanical improvement of soils below ground surface. *Ground Engineering conference*. London, Institution of civil engineering.

Greenwood, D. A., & Kirsch, F. (1983). Specialist ground treatment by vibratory and dynamic methods. *International Conference on Advances in Piling and Ground Treatment for Foundation*, London, England, p. 17-45.

Hemsely., J. A. (1970). Design application of raft foundation, First edition. London: Tomas Telford LTD.

Hara, A., Ohta, T., Niwa, M., Tanaka, S., & Banno, T. (1974). Shear Modulus and Shear Strength of Cohesive Soils. *Soils and Foundation*, Vol. 14, 1-12.

Hettiarachchi, H., & Brown, T. (2009). Use of SPT Blow Counts to Estimate Shear. *Journal of Geotechnical and*, 6.

Huesker Compony .(1995), Retrieved on 2012 from <http://www.huesker.com>.

Keller Grundbau (2002). Die Tiefenrüttelverfahren. Firmenprospekt 10-02D

Issac, D. S., & Girish, M. S. (2009). Suitability of Different Materials for Stone Column Construction. *Journal of EJGE*, Vol.14.

Jacques, W. D., (1989) Ground Water Engineering Handbook.

Kirsch , F. (2008). Evaluation of ground improvement by groups of vibro stone columns. *Proceedings of the Second International Workshop on Geotechnics of Soft Soils*, Scotland, p. 241-248.

Lakayan, D. (2012) *A Comprehensive Soil Characteristics Study and Finite Element Modeling of Soil-structure Behavior in Tuzla Area*. MSc Thesis, Eastern Mediterranean University , (North Cyprus).

Lo, S. R., Zhang, R., & Mak, J. ((2010)). Geosynthetic-encased stone columns in soft clay: A numerical study. *Geotextiles and Geomembranes* **28**, 292–302.

Lothspeich, S. (1995, 2 1). 9 10, 2012 tarihinde Huesker: <http://www.huesker.com> adresinden alındı.

Malarvizhi, S. N., & Ilamparuth, K. (2006). Modeling of geogrid encased stone column. *Proceedings of the 2nd International Congress on Computational Mechanics International Congress on Computational Mechanics* . IIT Guwahati, India. p. 1489-1494.

Malarvizhi, S. N., & Ilamparuthi, K. (2004). Load versus settlement of clay-bed stabilized with stone and reinforced stone columns. Proceeding of the 3rd Asian Regional Conference on Geosynthetic. GEOASIA, Seoul, Korea: 322-329.

Malarvizhi, S. N., & Ilamparuthi, K. (2008). Numerical Analysis of Encapsulated Stone Columns. *The 12th International Conference of International Association for Computer Methods and Advances in Geomechanics (IACMAG)*,. Goa, India, p. 3719-3726.

Mckelvey, D., Sivakumar, V., Bell, A., & Graham, J. (2004). Modelling vibrated stone columns in soft clay. *Journal of Geotechnical Engineering* 157, No. 3, 137-149.

Murugesan, S., & Rajagopal, K. (2006). Geosynthetic-encased stone columns: numerical evaluation. *Geotextiles and Geomembranes Journal* 24, No. 6, 349-358.

Nixon, I. (1982). Standard penetration test: state of the art report. Amsterdam: Proceedings of the 2nd European Symposium on Penetration Testing.

Oliveira, P. V., & Lemos, L. L. (2011). Numerical analysis of an embankment on soft soils considering large displacements. *Computers and Geotechnics* 38, 88–93.

Priebe, H. J. (1976). Abschätzung des setzungsverhaltens eines durch stopfverdichtung verbesserten baugrundes Die., Germany, p. 160-162.

Priebe, H. J. (1995). Design of vibro replacement. *Ground Engineering Journal* 28, No.10, 31-37.

Robertson, P. K. (2006). *Guideto In-Situ Testing*. Signal Hill: Gregg Drilling & Testing, Inc.

Ruwan, R. (2008). *Geotechnical Engineering Calculations and Rules of Thumb*. Burlington: *Elsevier*.

Sanglerat, G. (1972). *The Penetration and Soil Exploration; Interpretation of Penetration Diagrams — Theory and Practice*. Amsterdam: Elsevier Publishing Co.

Sharma, R. S., Kumar, B. P., & Nagendra, G. (2004). Compressive load response of granular piles reinforced with geogrids. *Canadian Geotechnical Journal* 41, No. 1, 187-192.

Sirvikaya, O. (2009). Comparison of Artificial neural networks models with correlative works on undrained shear strength. *Eurasian Soil Science*, Vol. 49, 1487–1496.

Sowers, G. F. (1979). *Introductory Soil Mechanics and Foundations*. New York: Macmillan.

Stroud, M. A. (1974). The standard penetration test in insensitive clays and soft soil. *Proceedings of the 1st European Symposium on Penetration Testing*, vol. 2(2), 367-375.

Terzaghi, K., & Peck, R. (1967). *Soil Mechanics in Engineering Practice*. New York: John.

Van Impe, W., & De Beer, E. (1983). Improvement of settlement behavior of soft layers by means of stone columns. *8th European Conference on Soil Mechanics and Foundation Engineering: Improvement of Ground*, Helsinki, p. 309-312.

Vesic, A. C. (1972). Expansion of cavities in infinite soil mass. *Journal of the Soil Mechanic and Foundation Engineering Division ASCE Vol.93*, 27-43.

Zahmatkesh, A., & Choobbasti, A. (2010). Settlement evaluation of soft clay reinforced by stone columns, considering the effect of soil compaction . *International Journal of Research and Reviews in Applied Sciences* 3(2), 159-166.